

ISSN 0111-0136

copy 1



UNIVERSITY OF AUCKLAND
SCHOOL OF ENGINEERING

DEPARTMENT OF CIVIL ENGINEERING

REPORT No. 290

LIVE-BED SCOUR AT BRIDGE PIERS

**BY
R. K. W. Chee**

September, 1982

PRIVATE BAG, AUCKLAND, NEW ZEALAND





LIVE-BED SCOUR AT BRIDGE PIERS

ABSTRACT

R.K.W. CHEE

SCHOOL OF ENGINEERING
REPORT NO. 290

THE INSTITUTE OF ENGINEERING
REPORT NO. 290

REPORT NO. 290

A report submitted to the Road Research Unit of the National Roads Board

A report submitted to the Road Research
Unit of the National Roads Board

Supervised by

Supervised by
Professor A. J. Raudkivi

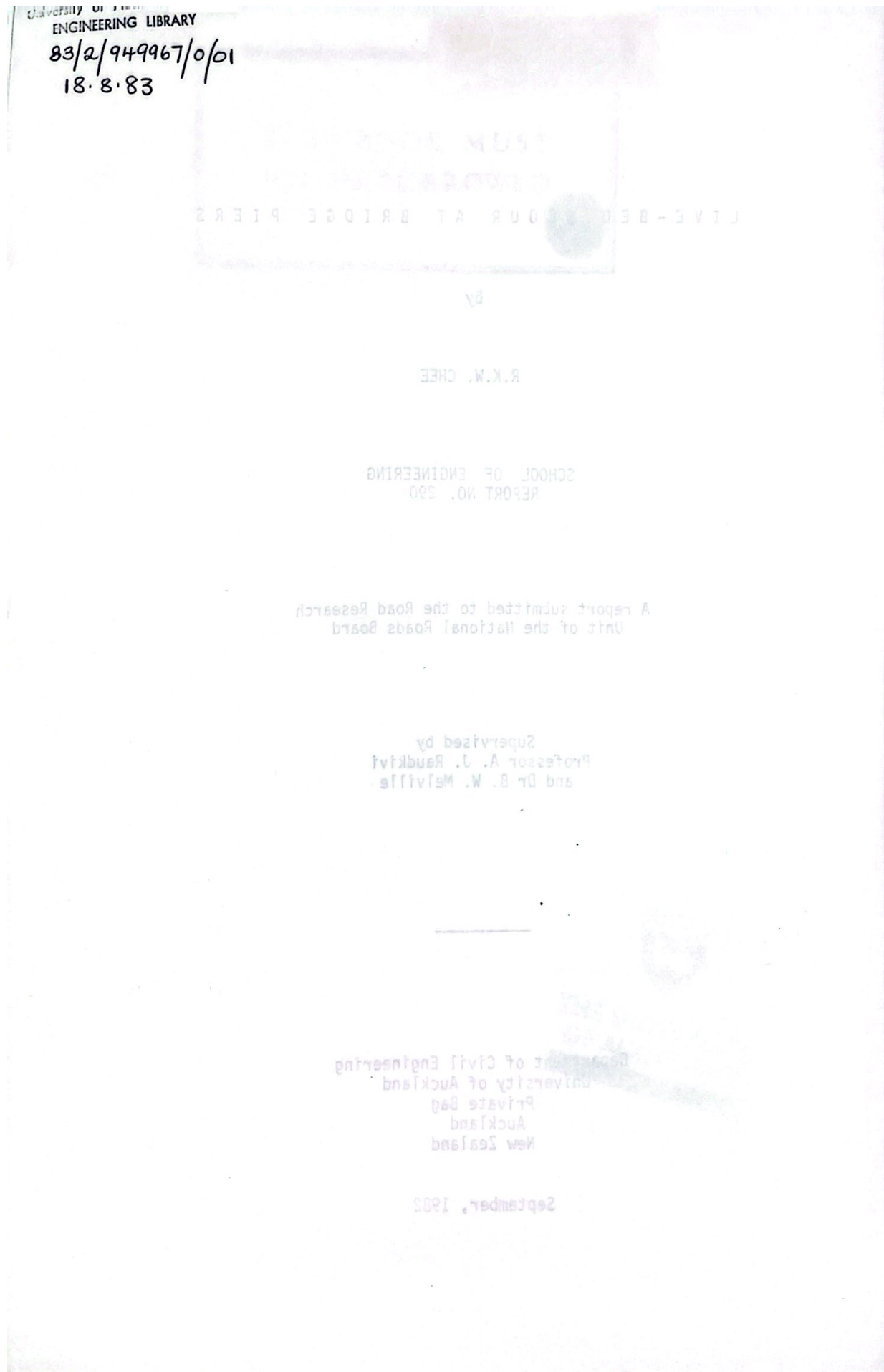
and Dr B. W. Melville) show two curves (one for the

and Dr. B. W. McTavish) which merge to form a single curve at about 1000 m.s.n.m. In the low central plateau, the surface water colour depth ($\frac{315}{315}$) max occurs at the maximum depth (the "midge period") and occurs at 1000 m.s.n.m.

and given as follows. The approach is based on the same logic for moderate b/d ratios (refer page 52) and will be discussed further for $b/d \geq 3$. The time for scour depth to reach equilibrium, t_{∞} , is very small for deep scour.

Department of Civil Engineering
University of Auckland
Private Bag
Auckland
New Zealand

September, 1982



(1)

ABSTRACT

The local live-bed scour at cylindrical piers in uniform cohesionless sediments was investigated in an experimental study. The primary aim of the study was to establish the trend of the relationship between local relative scour depth $\left(\frac{d_{se}}{D}\right)$ at a bridge pier and mean flow velocity, \bar{U} (or \bar{U}/\bar{U}_c).

Previous investigators have disagreed in their conclusions about the trend of the $\frac{d_{se}}{D}$ versus \bar{U} curve. A major contribution of this study is the establishment of the trend of this curve in the sediment-transporting regime, thereby identifying the variation in $\frac{d_{se}}{D}$ with increasing velocity from the clear-water regime into the sediment-transporting regime. As the velocity increases, $\frac{d_{se}}{D}$ increases almost linearly up to a first peak value around the threshold velocity, \bar{U}_c whereupon it decreases slightly with further increase in velocity until a minimum value is reached. Thereafter the scour depth increases again to a second peak value at about the transition flat-bed condition beyond which it appears to decrease again.

The influence of bed-forms on scour depth, d_{se} , was noted and the variation in scour depth ($d_{sem} - d_{ses}$) varies with the size of bed features reaching a maximum when the dunes are largest, that is, corresponding to the velocity of flow that produces the largest form drag, τ'' . This difference in scour depth, however, does not vanish at transition flat-bed conditions because of sediment avalanches from the slope into the scour hole.

The variation of $\frac{d_{se}}{D}$ versus \bar{U}/\bar{U}_c (normalised mean velocity) shows two curves (one for the ripple-forming and the other for the non-ripple-forming sediments) which merge to form a single curve at about $\bar{U}/\bar{U}_c = 3.5$ to 4.0. While for the former sediment, the maximum design scour depth $\left(\frac{d_{se}}{D}\right)_{max}$ occurs at the second peak beyond \bar{U}_c , for the latter sediment, $\left(\frac{d_{se}}{D}\right)_{max}$ occurs at \bar{U}_c .

Most of the live-bed scour data of previous researchers correspond reasonably with those of this study.

The influence of relative flow depth $\left(\frac{y_0}{D}\right)$ on d_{sem}/D for moderate D/d ratios (refer page 52 and Figure 2.12) becomes negligible for $y_0/D \geq 3$. The time for scour depth to reach equilibrium, t_{se} , is very short for high flows.

LIBRARY
83/2/94967/061
13-3-83

ABSTRACT

This paper presents a study on the effect of bridge piers on the scouring of river beds. The study was conducted on a river section where a bridge pier was located. The pier had a height of approximately 10 meters and a width of about 2 meters. The river bed was composed of sand and gravel. The study involved monitoring the scouring of the river bed around the pier over a period of one year. The results showed that the scouring was most pronounced near the pier, with a maximum depth of about 1.5 meters. The scouring was found to be influenced by the flow velocity, the size of the pier, and the characteristics of the river bed. The study also found that the scouring was more pronounced during the dry season than during the rainy season. The results of this study can be used to predict the scouring of river beds around bridge piers and to develop measures to mitigate the scouring.

(11)

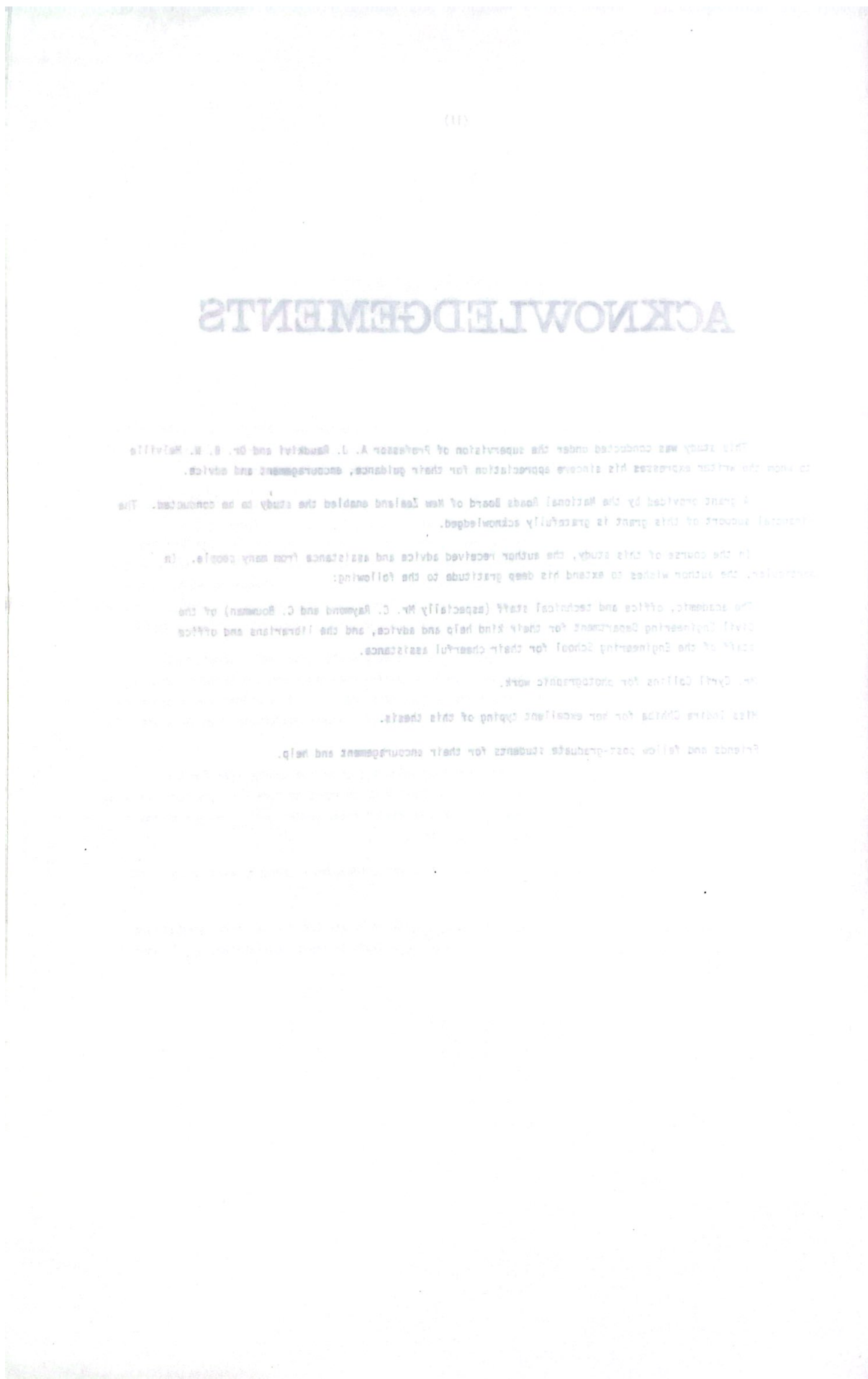
ACKNOWLEDGEMENTS

This study was conducted under the supervision of Professor A. J. Raudkivi and Dr. B. W. Melville to whom the writer expresses his sincere appreciation for their guidance, encouragement and advice.

A grant provided by the National Roads Board of New Zealand enabled the study to be conducted. The financial support of this grant is gratefully acknowledged.

In the course of this study, the author received advice and assistance from many people. In particular, the author wishes to extend his deep gratitude to the following:

The academic, office and technical staff (especially Mr. C. Raymond and C. Bouman) of the Civil Engineering Department for their kind help and advice, and the librarians and office staff of the Engineering School for their cheerful assistance.	11
Mr. Cyril Collins for photographic work.	12
2.1.4 - Influence of Flow Velocity	13
Miss Indira Chhiba for her excellent typing of this thesis.	14
Friends and fellow post-graduate students for their encouragement and help.	17
3.1 - The Flume	17
3.2 - Measurement Techniques	22
3.3 - Experimental Programmes	22
CHAPTER 4 - RESULTS AND DISCUSSION	27
4.1 - Introduction	27
4.2 - Geometry of Scour Hole	27
4.3 - The Influence of Mean Approach Velocity on Local Scour	27
4.4 - The Influence of Relative Particle Size (D/d_g) on Local Scour	58
4.5 - The Influence of Relative Flow Depth on Local Scour	59
4.6 - The Development of Local Scour	59
CHAPTER 5 - CONCLUSIONS	61
5.1 - Influence of Mean Flow Velocity on Relative Scour Depth	61
5.2 - Influence of Relative Particle Size (D/d_g) on Relative Scour Depth	62
5.3 - Influence of Relative Flow Depth on Relative Scour Depth	62
5.4 - Time Development of Local Scour	62
5.5 - Suggestions for Future Research	63
APPENDIX	68
REFERENCES	68
Appendix 1 - Summary of Experimental Results	71
Appendix 2 - Values of w_{∞} and \bar{w}_c (calculated)	72



(111)

CHAPTER 1

CONTENTS

	<u>PAGE</u>
The paper on failure of bridge pier foundations is one of major concern to the design engineers.	
The paper deals with bridge foundation failures in the scour holes created by flowing water around the piers.	
ABSTRACT	(1)
Bridge piers are supported by friction piles. If these piles are uncovered by the scour, the pier may fail.	
ACKNOWLEDGEMENTS	(11)
Scouring is the reduction in the friction between the piles and the surrounding soil. It is not	
surprise that, as British Report (1978) on bridge failures affirms, that of the 142 cases of failed	
piers were due to scour.	
CONTENTS	(111)
CHAPTER 1 INTRODUCTION	1
Object and Scope of this Investigation	2
Local Scour Literature Review	3
2.1 Parameters Influencing Local Scour	8
2.1.1 Influence of Bed Sediment Properties	8
2.1.2 Influence of Pier	11
2.1.3 Influence of Relative Flow Depth	12
2.1.4 Influence of Flow Velocity	13
2.2 Summary	16
CHAPTER 2 LOCAL SCOUR LITERATURE REVIEW	
2.1 Parameters Influencing Local Scour	8
2.1.1 Influence of Bed Sediment Properties	8
2.1.2 Influence of Pier	11
2.1.3 Influence of Relative Flow Depth	12
2.1.4 Influence of Flow Velocity	13
2.2 Summary	16
CHAPTER 3 EXPERIMENTAL SET-UP AND PROGRAMME	17
3.1 The Flume	17
3.2 Measurement Techniques	22
3.3 Experimental Programme	22
CHAPTER 4 RESULTS AND DISCUSSION	27
4.1 Introduction	27
4.2 Geometry of Scour Hole	27
4.3 The Influence of Mean Approach Velocity on Local Scour	27
4.4 The Influence of Relative Mean Particle Size (D/d) on Local Scour	58
4.5 The Influence of Relative Flow Depth on Local Scour	59
4.6 Time Development of Local Scour	59
CHAPTER 5 CONCLUSIONS	61
5.1 Influence of Mean Flow Velocity on Relative Scour Depth	61
5.2 Influence of Relative Particle Size (D/d_{50}) on Relative Scour Depth	62
5.3 Influence of Relative Flow Depth on Relative Scour Depth	62
5.4 Time Development of Local Scour	62
5.5 Suggestions for Future Research	63
BIBLIOGRAPHY	64
NOTATION	68
APPENDICES	70
Appendix 1 Summary of Experimental Results	71
Appendix 2 Values of u_{*c} and \bar{U}_c (calculated)	78

- 1 -

CHAPTER 2**CHAPTER 1****INTRODUCTION**

The problem of failure of bridge pier foundations is one of major concern to the design engineers.

One major cause of bridge foundation failures is the scour holes created by flowing water around the piers. Many bridge piers are supported by friction piles. If these piles are uncovered by the scour, the piers may settle or tilt owing to the reduction in the friction between the piles and the surrounding soil. It is not surprising, therefore, as Smith's report (1976) on bridge failures affirms, that of the 143 cases of failures studied, 66 were due to scour.

In order to produce a safe and economical design of bridge foundations, the engineer needs to make an accurate prediction of the maximum expected scour depth of the river bed around the piers. A good understanding of the mechanism of scour around a bridge pier is therefore essential.

The scour depth at a pier is generally influenced by three major factors:-

- (1) the river itself - its width, depth, course and regime,
- (2) the bed sediment - its size, shape and distribution, and
- (3) the structure of the pier itself - its geometry and orientation.

Three types of scour are, in general, recognised:-

- (1) general scour, which is due to the degradation of the river bed,
- (2) constriction scour, which is created by the constriction of the waterway when a structure is introduced into it, and
- (3) local scour, which is caused by local changes in the velocity distribution at obstructions such as spur dykes, bridge abutments and bridge piers. All three types of scour may occur together.

Local scour around bridge piers can be divided into two types:-

- (1) clear-water scour - where there is no general sediment transport, and,
- (2) scour with sediment-transport or live-bed scour - where sediment is continuously supplied into the scour hole.

As in many other fields of sediment transport, no entirely satisfactory theoretical or experimental results on live-bed scour around bridge piers, especially at high Froude Numbers, have been obtained. The reason for this is found in the complex nature of the processes involving water and sediment motion.

Most investigators in the field of local scour at bridge piers agree on the general shape of the curve which shows the variation of scour depth with mean flow velocity. Accordingly, scour depth increases with increase in mean velocity in the clear-water regime, reaches a maximum at around threshold velocity, and then decreases slightly to an approximately constant value at higher velocities (see Figure 2.4). Because of this trend, much research effort has been directed at determining the maximum scour condition, that is the scour at threshold of motion, while there have been relatively few investigations at higher flows and the data that have been obtained show wide scatter. More experimental data are required to adequately define the relationship between scour depth and flow velocity in the live-bed regime.

(i) Clear-water scour

(ii) Scour with continuous sediment transport

(iii) Development of scour depth to equilibrium (if & constant)

- 2 -

Object and Scope of Investigation

CHAPTER

This study was primarily concerned with the collection of experimental data on local scour around bridge piers under live-bed conditions. Experiments were conducted, in which pier size, mean sediment size and flow velocity were systematically varied. Cylindrical piers were used throughout.

To ensure linkage of the scour depth versus mean velocity curves from clear-water to live-bed conditions, some data were also collected in the clear-water regime for three series of experiments, thus establishing the trend of these curves for both regimes.

A review of the existing literature on physical model studies of scour at bridge piers was made and a summary of the findings is presented in the literature review and background discussion (Chapter 2). A description of the equipment and the experimental procedures used in this study is given in Chapter 3. This is followed by the presentation and discussion of the results obtained from the laboratory experiments (Chapter 4). Finally, the conclusions drawn are presented in Chapter 5, followed by suggestions for further work.

- 3 -

CHAPTER 2

LOCAL SCOUR

LITERATURE SURVEY

Many publications dealing with local scour at bridge piers founded in non-cohesive bed materials are to be found in the technical literature. In this chapter, a critical review of papers relating to this subject is presented with particular importance being given to those papers dealing with live-bed scour experiments.

When the fluid flow enlarges the flow cross-section by erosion of its boundaries, scour is said to occur.

Local scour is defined as the erosion at an obstruction, e.g. pier, abutment, etc. and is due to the local flow pattern created by the obstruction. Figure 2.1 shows a typical scour hole.

The type of local scour may be classified by considering the difference in the amount of sediment transport into and out of the scour hole per unit time:-

$$q_s = q'_s - q''_s$$

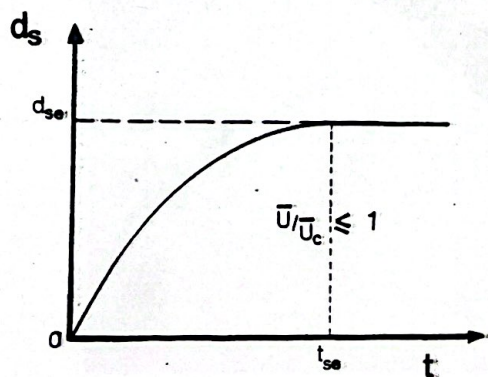
where: q'_s = the rate of local erosion in volume per unit time,
 q''_s = the capacity of the flow to transport sediment out of the scour hole in volume per unit time,
 q'''_s = the rate at which sediment is fed into the scour hole in volume per unit time.

The three cases of scour that arise are as follows:

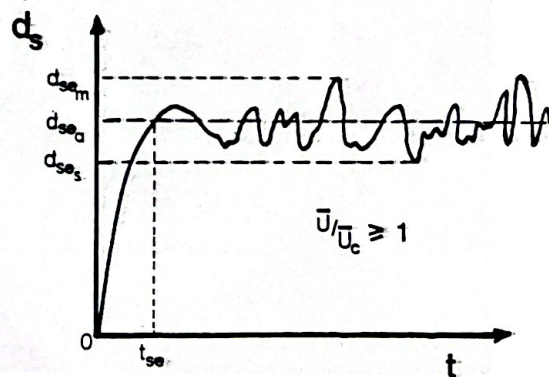
- (a) No scour (i.e. $q'_s = 0$),
- (b) Clear-water scour (i.e. $q'_s = q''_s$ for $0 < t < t_{se}$, $q''_s = 0$),
- (c) Scour, with continuous movement of sediment (i.e. $q'_s > q''_s > 0$, and at equilibrium, $q'_s = q''_s$).

The clear-water scour begins when q'_s is slightly greater than zero. This is the case where material is removed from the scour hole but not replaced, i.e. no sediment supply to the hole.

The condition of maximum scour is reached when the flow entering the hole is no longer capable of removing the bed sediment from the hole. The equilibrium scour depth (d_{se}) is approached asymptotically as shown in Figure 2.2 (i).

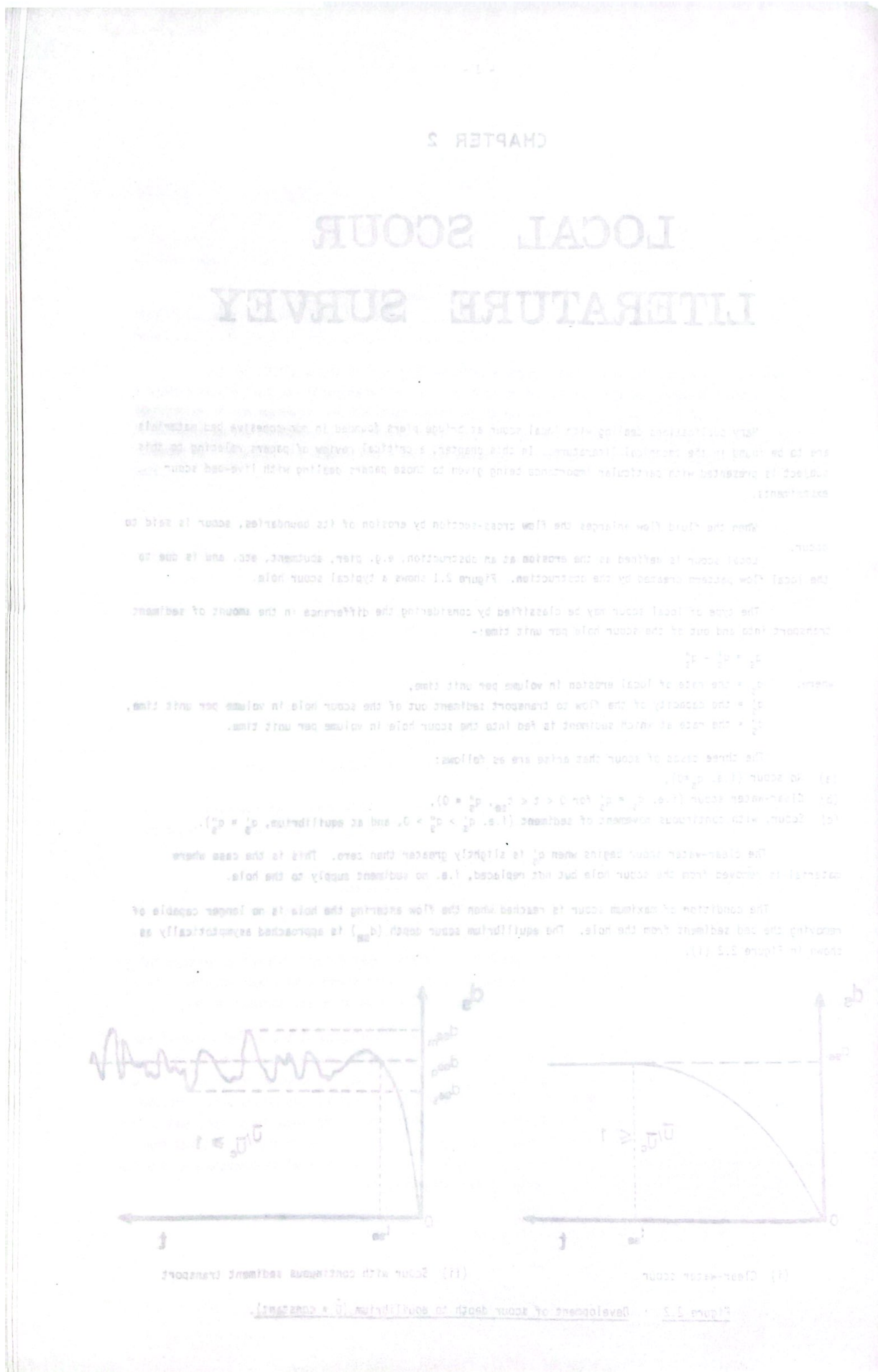


(i) Clear-water scour



(ii) Scour with continuous sediment transport

Figure 2.2 : Development of scour depth to equilibrium ($U = \text{constant}$).



- 4 -

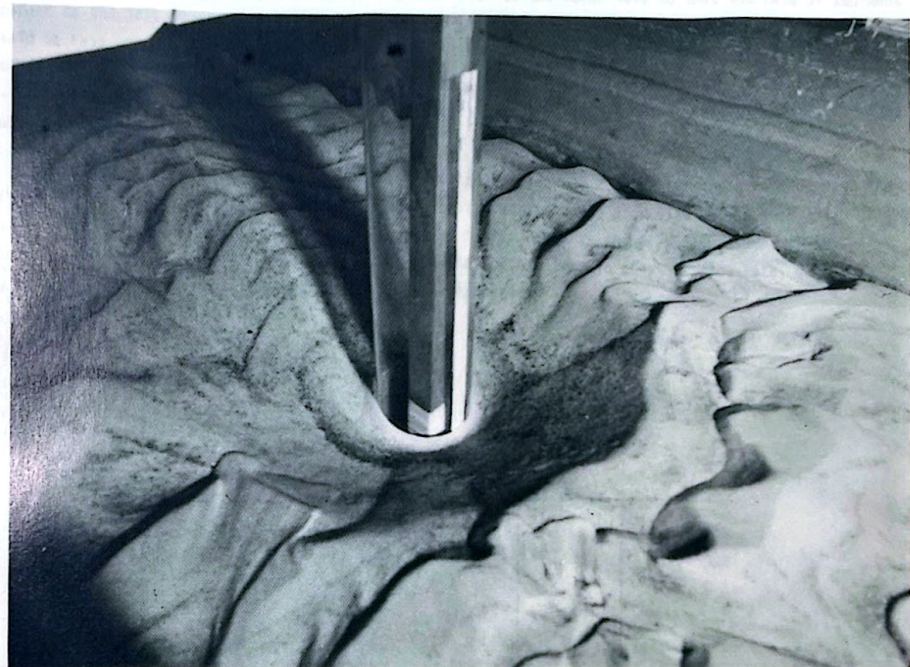
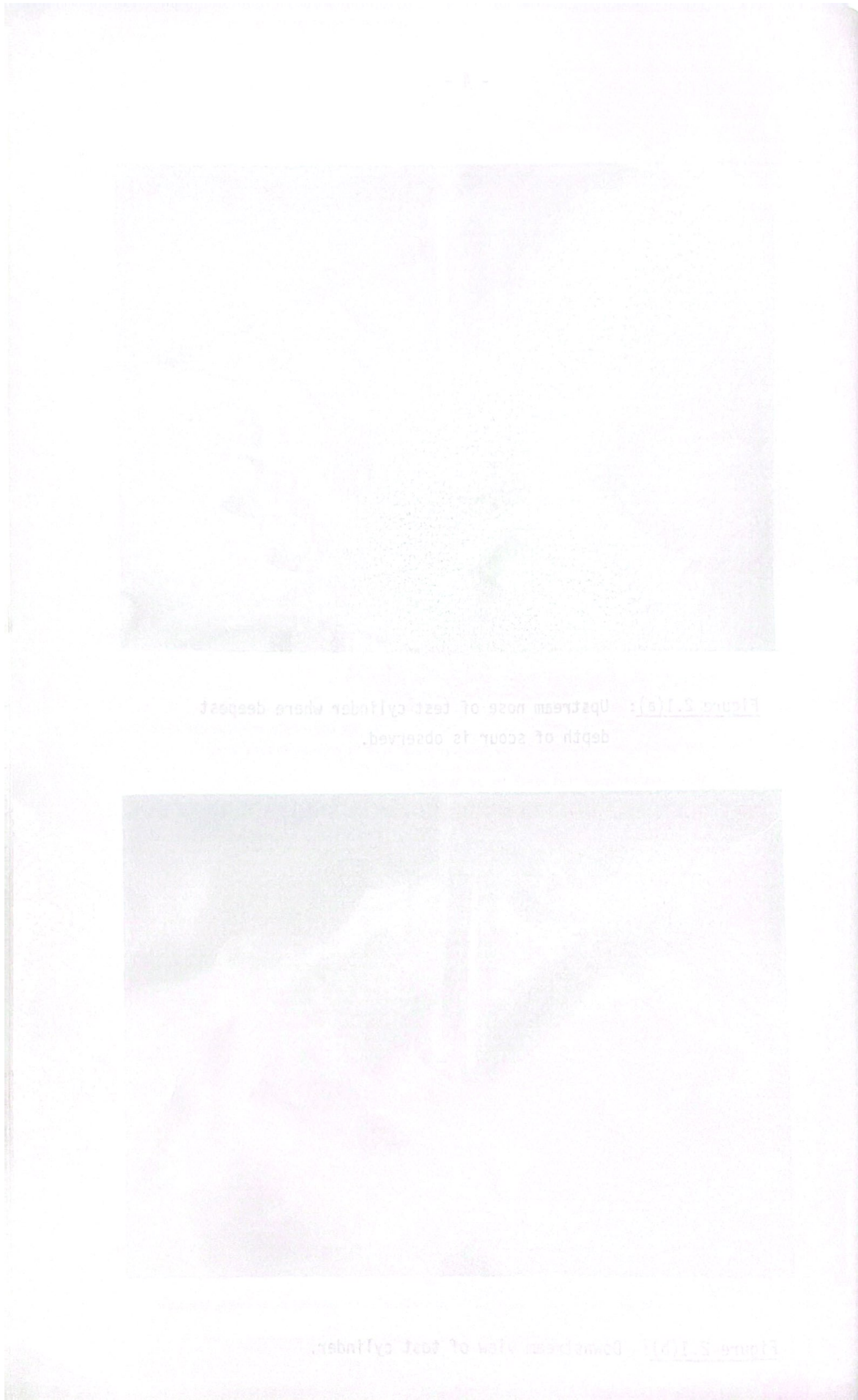


Figure 2.1(a): Upstream nose of test cylinder where deepest depth of scour is observed.



Figure 2.1(b): Downstream view of test cylinder.



- 5 -

If q'_s is greater than q''_s , a live-bed local scour is formed, but if smaller, deposition occurs. When sediment is continuously supplied by the approach flow to the scour hole so that the rate of sediment transport to the hole equals the rate of local erosion (i.e. $q'_s = q''_s$), then $q_s = 0$ and an equilibrium state is said to have been reached. The scour depth oscillates non-periodically with time, t , about a time-average value, d_{se} , at equilibrium (see Figure 2.2 (ii)). The oscillations are due to the passage of bed-forms past the pier^a. The definition of the maximum (d_{se}^a) and the minimum or smallest (d_{se}^m) recorded values of scour depth at equilibrium conditions is shown in Figure 2.2 (ii).

The time development of local scour is depicted in Figure 2.2. The time required to reach the equilibrium scour depth, t_{se} , is dependent on the velocity, sediment and pier size but is much less for the live-bed than for clear-water scour. The definition of t_{se} is given as shown in Figure 2.3. Note that t_{se} starts after $t = T$, where T is the time taken for flow to reach a certain constant flow-rate, Q' (i.e. $\bar{U} = \text{constant}$ for uniform cross-sectional area of channel).

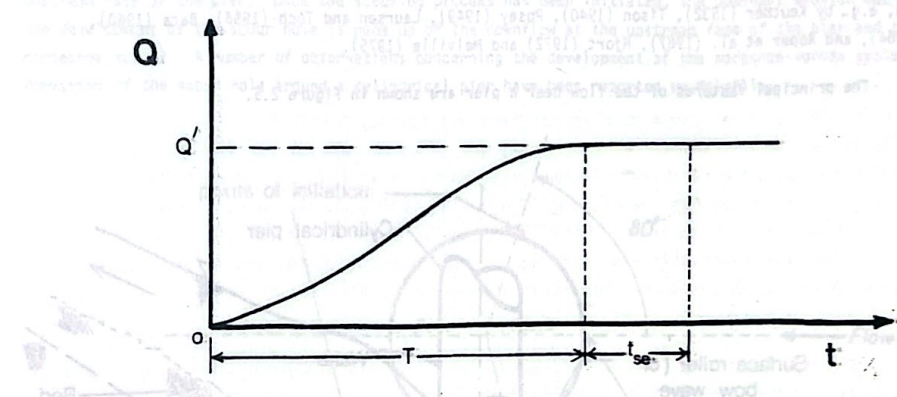


Figure 2.3 : Definition of t_{se} .

Chabert and Engeldinger (1956) found that the scour depth varies with the mean flow velocity in the manner shown in Figure 2.4.

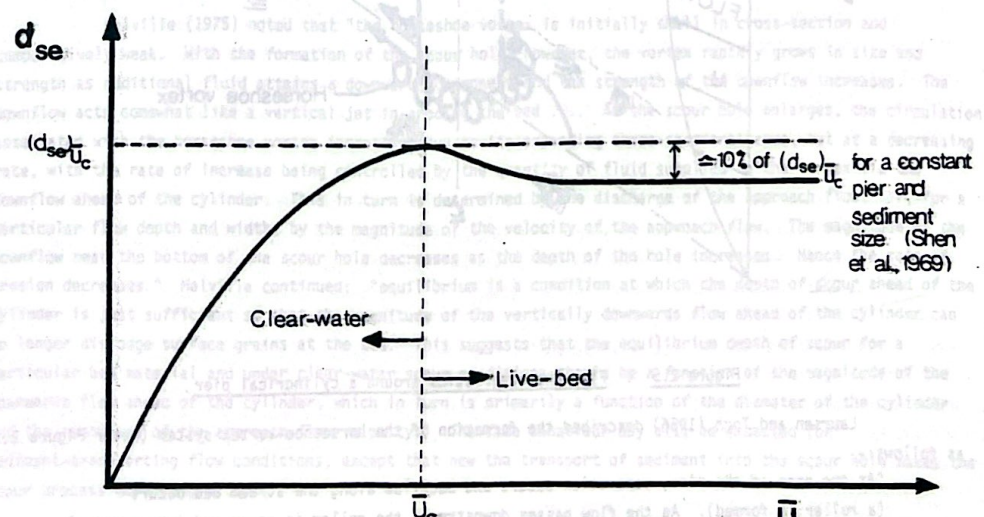


Figure 2.4 : Variation of scour depth with velocity. Typical results by Chabert, J. and Engeldinger, P. (1956).

- 6 -

The equilibrium scour depths for scour with continuous sediment transport were estimated by Shen et al. (1969) to be approximately 90 percent of the maximum equilibrium clear-water scour depth i.e. $0.90(d_{sc})_c$ (see Figure 2.4). This, however, is an estimate and the exact trend of the curve for $\bar{U}/\bar{U}_c > 1.0$ has not been adequately defined.

The chief characteristics of the flow field about a cylinder in flow are the downflow and the system of vortices which develop. The vortices are:-

- (i) the horseshoe vortex,
- (ii) the cast-off vortices, and if the cylinder is completely submerged,
- (iii) the trailing vortex.

The vortices (i) and (ii) are one of the causes of erosion around bridge piers, and the form of these has been discussed, e.g., by Keutner (1932), Tison (1940), Posey (1949), Laursen and Toch (1956), Bata (1960), Neill (1964), and Roper et al. (1967), Hjort (1972) and Melville (1975).

The principal features of the flow near a pier are shown in Figure 2.5.

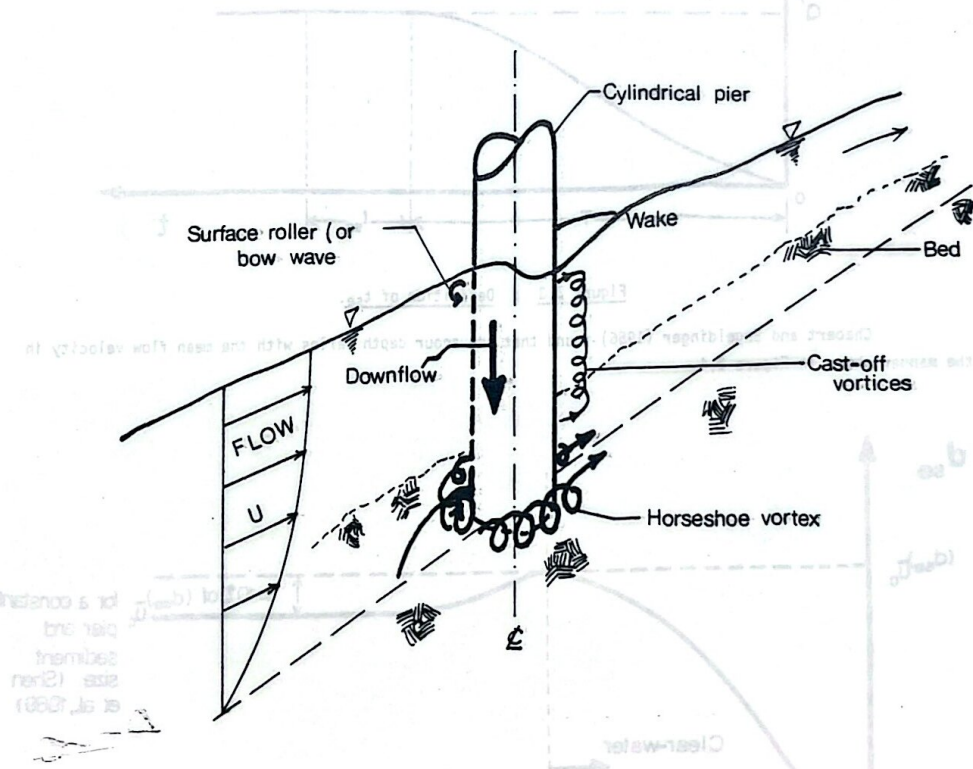


Figure 2.5 : Flow characteristics around a cylindrical pier.

Laursen and Toch (1956) described the formation of the horseshoe-vortex system (refer Figure 2.5) as follows:-

"At the nose of the pier, separation occurs and backflow along the stream bed occurs (a roller is formed). As the flow passes downstream, the roller is converted into a spiral roller around the sides of the pier."

The vortex system forms as a result of a concentration of the vorticity already present in the approach flow. This concentration is caused by the pressure field which is induced by a blunt-nosed pier.

- 7 -

The cast-off vortices are formed by the rolling up of the boundary layer separating from the pier surface (refer Figure 2.5). The action of the cast-off vortices is somewhat like that of a vacuum cleaner in lifting-up of bed material. The bed material is then transported downstream by the flow.

The rate with which the horseshoe and cast-off vortices remove the bed material around the pier is largely determined by the flow velocity and the shape and geometry of the pier.

Melville (1975) observed, for a cylinder protruding from a flat bed, that the maximum velocity occurs near the cylinder at approximately $\pm 80^\circ$ from the stagnation point (see Figure 2.6). These high local velocities create large bed shear stresses and initiate the local scour process around the pier. Scouring then continues very rapidly on the upstream edges of these two small holes until they extend around the upstream face of the pier. Once the scouring process has been initiated, the dominant erosion mechanism for the development of the scour hole is made up of the downflow at the upstream face of the pier and the horseshoe vortex. A number of observations concerning the development of the horseshoe-vortex system with the formation of the scour hole around a cylindrical pier have been reported by Melville.

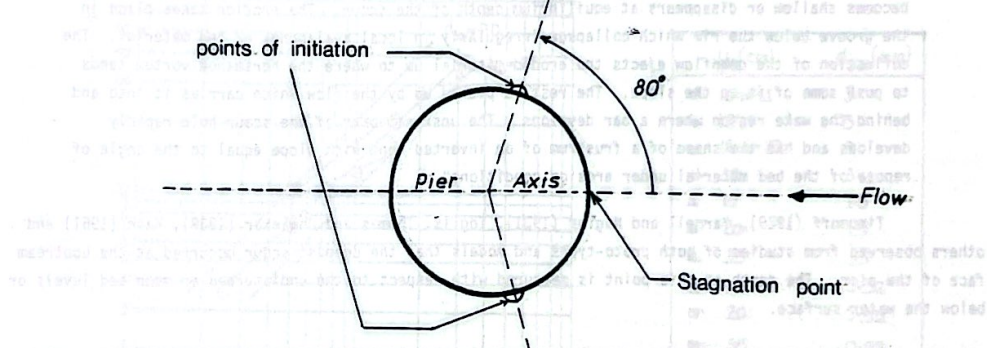


Figure 2.6 : Position of initiation of scour hole.

Melville (1975) noted that "the horseshoe-vortex is initially small in cross-section and comparatively weak. With the formation of the scour hole, however, the vortex rapidly grows in size and strength as additional fluid attains a downwards component and the strength of the downflow increases. The downflow acts somewhat like a vertical jet in eroding the bed As the scour hole enlarges, the circulation associated with the horseshoe vortex increases, due to its expanding cross-sectional area, but at a decreasing rate, with the rate of increase being controlled by the quantity of fluid supplied to the vortex via the downflow ahead of the cylinder. This in turn is determined by the discharge of the approach flow; or, for a particular flow depth and width, by the magnitude of the velocity of the approach flow. The magnitude of the downflow near the bottom of the scour hole decreases as the depth of the hole increases. Hence the rate of erosion decreases." Melville continued: "equilibrium is a condition at which the depth of scour ahead of the cylinder is just sufficient so that the magnitude of the vertically downwards flow ahead of the cylinder can no longer dislodge surface grains at the bed. This suggests that the equilibrium depth of scour for a particular bed material and under clear-water scour conditions should be a function of the magnitude of the downwards flow ahead of the cylinder, which in turn is primarily a function of the diameter of the cylinder and the magnitude of the approach flow velocity." The same behaviour may also be expected for sediment-transporting flow conditions, except that now the transport of sediment into the scour hole makes the scour process more complex.

Since the approach flow on the surface is higher than near the bed the stagnation pressures at the face of the pier show a gradient which drives the flow downwards at a mean velocity, v . Experimental data obtained by Ettema (1980) showed that the strength of the downflow in front of the pier reaches a maximum just below the bed level when a scour hole is present; thereafter it gradually decreases as the hole deepens. He

- 8 -

stated that "the depth of scour at which the strength of the downflow impinging on the base of the scour reaches a peak value is dependent on the approach flow to the scour hole, and the relative size parameter D/d ." The stagnation pressure in the front of the pier not only causes the downflow but also leads to sideways acceleration of the flow past the pier.

Raudkivi and Sutherland (1981) described the development of scour hole as follows:

"Scour hole development commences at the sides of the cylinder with the holes rapidly propagating upstream around the perimeter of the cylinder to meet on the centreline. The eroded material is transported downstream by the flow. Soon after the commencement of scouring, a shallow hole, concentric with the cylinder, is formed around most of the perimeter of the cylinder (about $\pm 120^\circ$) but not in the wake region. The downflow acts like a vertical jet eroding a groove in front of the pier. The eroded material is carried around the pier by the combined action of accelerating flow and the spiral motion of the horseshoe vortex. The downflow is turned in the groove by 180° and the upward flow is deflected by the horseshoe vortex in the upstream direction, up the slope of the scour hole. At this turning point, the tip of the groove is often very sharp and the face is almost vertical. The groove becomes shallow or disappears at equilibrium depth of the scour. The erosion takes place in the groove below the rim which collapses irregularly in local avalanches of bed material. The deflection of the downflow ejects the eroded material up to where the horseshoe vortex tends to push some of it up the slope. The rest is picked up by the flow which carries it into and behind the wake region where a bar develops. The upstream part of the scour hole rapidly develops and has the shape of a frustum of an inverted cone with slope equal to the angle of repose of the bed material under erosion conditions".

Timonoff (1929), Yarnell and Nagler (1931), Inglis, Thomas and Joglekar (1939), Kain (1961) and others observed from studies of both proto-types and models that the deepest scour occurred at the upstream face of the pier. The depth at this point is measured with respect to the undisturbed or mean bed levels or below the water surface.

For blunt-nosed piers, the general consensus is that in the clear-water regime, the scour holes produced around them have the form of an inverted cone with the slope of the sides approximately equal to the natural angle of repose of the bed sediment. Jain and Fischer (1980) observed, for high flow velocity rates, that "a dynamic equilibrium exists between scour hole and streamflow which is not apparent when the flow is stopped; the flow field near the base of the pier is strong enough to support the sides of the scour hole at angles greater than the angle of repose of the sediment. In fact, the scour hole can, at times, be nearly vertical. The wall periodically collapses and dumps sediment into the hole, either as a dune encroaches upon the pier, or the fluid forces supporting it become unstable."

2.1 PARAMETERS INFLUENCING LOCAL SCOUR

2.1.1 Influence of Bed Sediment Properties

Schwartz (1929), Bata (1960), Laursen (1962), Tarapore (1962) and Bonasoundas (1973) found, from their live-bed experiments, that the particle size, d had little or no effect on the maximum depth of the scour hole. Model studies by Inglis (1949) and investigations by Ahmad (1962), Chitale (1962) and

- 9 -

Thomas (1972) did not show any significant influence of grain size on the depth of scour for bed sediments in the fine to coarse sand range in either the clear-water or sediment-transporting regimes. Shen et al. (1966a) concluded that up to a median diameter of approximately 0.50 mm, scour depths were independent of the particle size. Other researchers, like Knezevic (1960), Arunachalam (1965), Bata (1960), Blenck (1965), and Yaroslavtzier (1968), did not include the bed material size in the formulation of their relationships for prediction of the local scour depths.

The results of Chabert and Engeldinger (1956) (see Figure 2.7) show a small influence of grain size. In the range of velocities near that of threshold, the 0.26 mm, 0.52 mm and 1.50 mm sediments indicate an increasing trend of maximum equilibrium scour depth with increase in sediment size. However, the 3 mm sediment produced smaller d_{se}/D values than the 1.5 mm sediment for flows around the critical velocity.

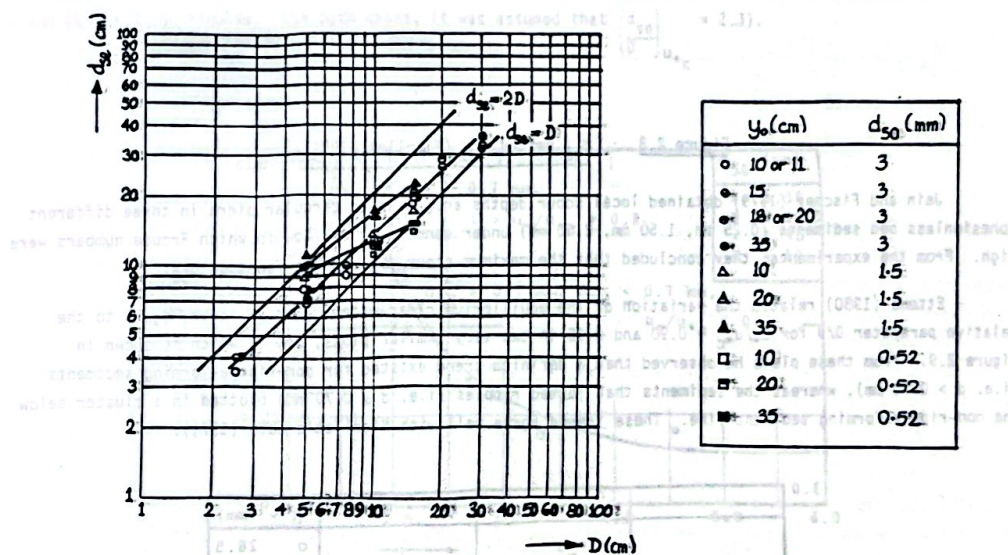


Figure 2.7 : Influence of d_{50} , D and y_0 on d_{50m} . Data from Chabert and Engeldinger (1956) (replotted by Shen et al., 1977).

Nicollet (1971) concluded from experimental tests that the scour depth was influenced by the size of particles, d_{50} (see Figure 2.8). He noted that for a constant depth of flow, scour depth increased with sediment size up to $d_{50} = 2$ mm, after which a decrease was observed with further increase in particle size. This trend agrees with the data of Chabert and Engeldinger (1956), Hancu (1971), Leclerc (1971) and partly also with Ettema (1976, 1980). Ettema (1980) explained the variations in d_{se} with d_{50} in terms of

- (i) the differences between ripple-forming sediments and sediments which do not form ripples,
- (ii) the grain-size distribution of the sediment,
- (iii) the similarity of the temporal development of local scour, relative flow depth to pier diameter and
- (iv) the relative size of the pier to the bed sediment.

- 10 -

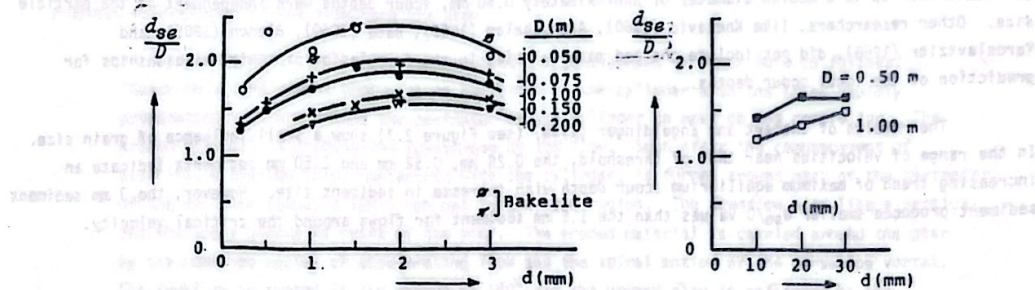


Figure 2.8 : d_{se} versus d_{50} (Nicollet, 1971).

Jain and Fischer (1979) obtained local scour depths around solid circular piers in three different cohesionless bed sediments (0.25 mm, 1.50 mm, 2.50 mm) under conditions of flow in which Froude numbers were high. From the experiments, they concluded that the maximum scour depth was a function d_{50} .

Ettema (1980) related the variation of the equilibrium clear-water depth of scour, d_{se}/D to the relative parameter D/d for $u_*/u_{*c} = 0.90$ and 0.95 in two very similar plots, one of which is shown in Figure 2.9. From these plots he observed that a definite trend existed for non-ripple-forming sediments (i.e. $d > 0.70$ mm), whereas the sediments that formed ripples (i.e. $d < 0.70$ mm) plotted in a cluster below the non-ripple-forming sediment line. These trends agree well with Nicollet's data (1971).

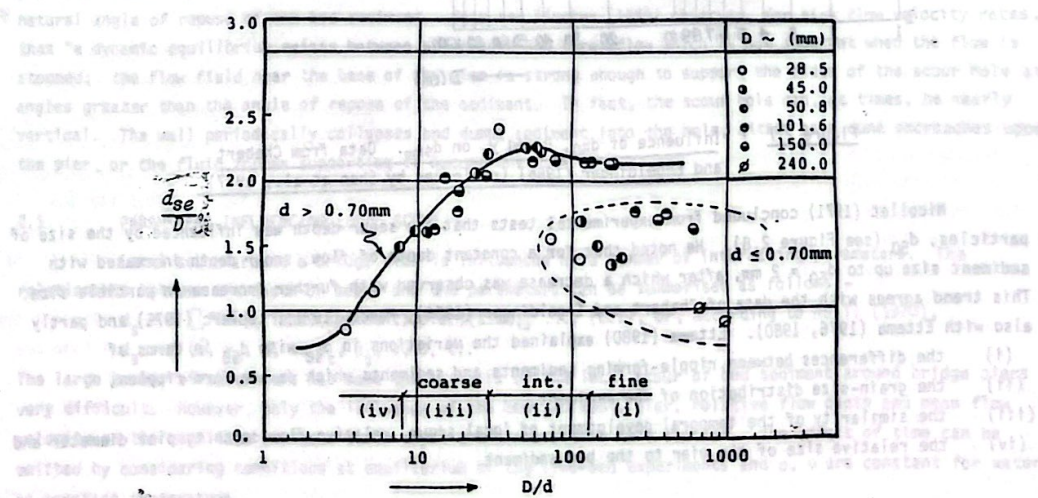


Figure 2.9 : Equilibrium scour depth versus D/d for $u_*/u_{*c} = 0.90$.

Ettema (1976, 1980) also formalised the earlier observation by Nicollet and Ramette (1971) that the grading of a bed sediment has a pronounced influence upon the development and final (or equilibrium) depth of

- 11 -

local scour. Ettema (1980) plotted his results as d_{se}/D versus σ_g/d_{50} (based upon experimental data obtained with a 101.6 mm diameter pier for $u_*/u_{*c} = 0.95$ and flow depth = 600 mm). For application, d_{se}/D was normalised with (d_{se}/D) for uniform sediment. The ratio K_g was presented versus the geometric standard deviation, σ_g , of the sediment (refer Figure 2.10). Figure 2.10 shows that equilibrium scour depths decrease with increasing non-uniformity of bed sediment and Ettema concluded that this trend was due to armouring of the bed within the scour hole. The equilibrium scour depth for a non-uniform sediment was defined by equation (2.2).

$$\frac{d_{se}}{D}(\sigma) = K_g \frac{d_{se}}{D}(\sigma_g = 1.0, d_{50} \geq 0.70 \text{ mm}) \quad \dots \dots \dots \quad (2.2)$$

where $\frac{d_{se}}{D}(\sigma)$ is the relative equilibrium depth for a non-uniform sediment and $\frac{d_{se}}{D}(\sigma_g = 1.0, d_{50} > 0.70 \text{ mm})$

is the value for a uniform sediment or the maximum clear-water scour depth for both the sediments which do, and do not form, ripples. (In both cases, it was assumed that $\left[\frac{d_{se}}{D}\right]_{u_{*c}} = 2.3$).

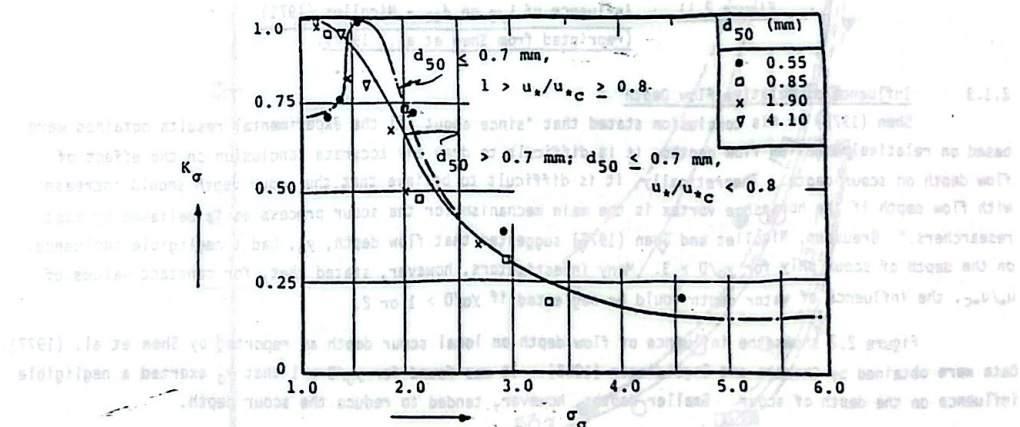


Figure 2.10 : Equilibrium scour depth coefficient K_g versus geometric standard deviation of particle size distribution, when $u_*/u_{*c} \leq 1.0$ (Ettema, 1980).

2.1.2 Influence of Pier

The extent of the secondary flow around a bridge pier has been found to be influenced by the size and form of the pier. This has been well substantiated by data from a variety of experimental and field investigations. Tarapore (1962), Larras (1963) and Breusers (1965) concluded that the maximum depth of scour was dependent only on the effective pier size. Further, Knezevic (1960) concluded from his experiments that the magnitude of maximum scour was a function of the size and shape of the pier. Laursen (1958, 1962) showed, from the results of an experimental study that the pier width and its geometry had an influence on the magnitude of the maximum depth of live-bed scour. In addition, White (1975), using a coarse sand ($d_{50} = 0.9$, $d_{90} = 3.4 \text{ mm}$) and various pier shapes and sizes found, in a series of experimental runs at high Froude numbers ($Fr = 0.8$ to 1.2), that scour depth increased with effective pier width which was affected by the approach angle of flow.

Chabert and Engeldinger (1956) reported from model study data that the scour depth was dependent on the pier width (see Figure 2.7). An increase in scour depth with D^α , in which $\alpha < 1$, can be seen from Figure 2.7. They also noted an influence due to variation of pier shape and angle of attack. The majority of their experiments were conducted in the sediment-transport regime.

- 12 -

Nicollet (1971) performed experimental studies in both the clear-water and sediment-transporting regimes using piers of different aspect ratios ($L/D = 1, 2$ and 3 with $D = 0.1 \text{ m}$). He found that d_{se} was only slightly influenced by the aspect ratio (see Figure 2.11).

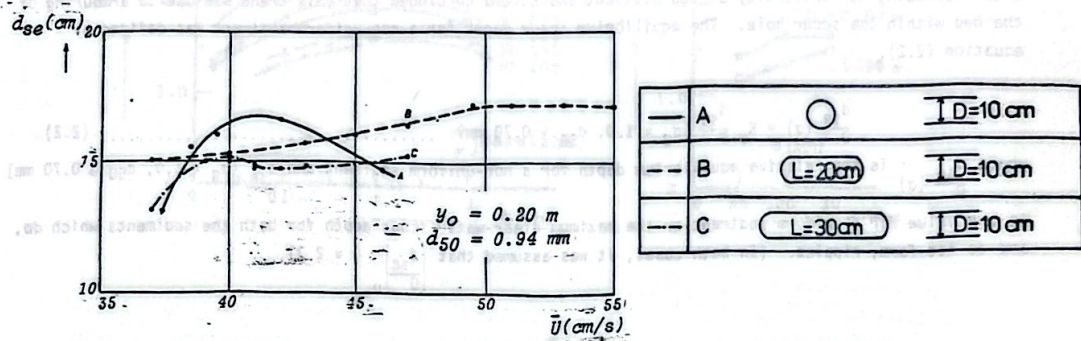


Figure 2.11 : Influence of L/D on d_{se} - Nicollet (1971)
(reprinted from Shen et al., 1977).

2.1.3 Influence of Relative Flow Depth

Shen (1973) in his conclusion stated that "since about all the experimental results obtained were based on relatively shallow flow depths, it is difficult to draw any accurate conclusion on the effect of flow depth on scour depth. Theoretically, it is difficult to believe that the scour depth should increase with flow depth if the horseshoe vortex is the main mechanism for the scour process as is believed by most researchers." Breusers, Nicollet and Shen (1977) suggested that flow depth, y_0 , had a negligible influence on the depth of scour only for $y_0/D > 3$. Many investigators, however, stated that, for constant values of u_* / u_{*c} , the influence of water depth could be neglected if $y_0/D > 1$ or 2.

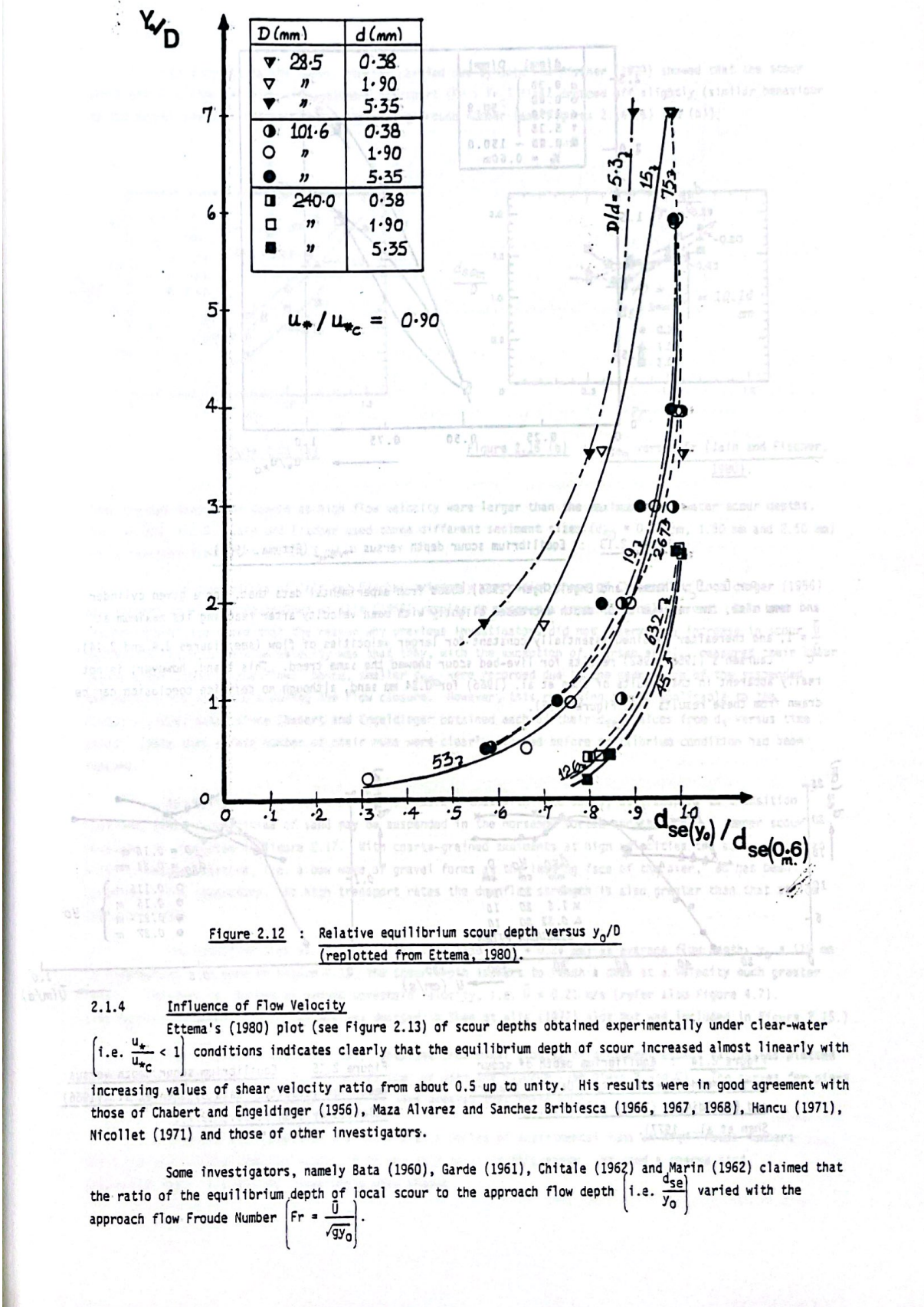
Figure 2.7 shows the influence of flow depth on local scour depth as reported by Shen et al. (1977). Data were obtained by Chabert and Engeldinger (1956). It was found for $y_0/D > 1$ that y_0 exerted a negligible influence on the depth of scour. Smaller depths, however, tended to reduce the scour depth.

Ettema (1980) studied the influence of flow depth on local scour for constant u_* / u_{*c} ($= 0.90$) and concluded that "for a shallow flow, the reduction in the equilibrium depth of scour increases with bed particle size for the same values of the parameters u_* / u_{*c} and y_0/D . That is, when u_* / u_{*c} is constant, the equilibrium depth of local scour at a pier decreases more rapidly with decreasing flow depth for lesser values of relative size parameter, D/d (see Figure 2.12)". He stated that in the case of the 0.38 mm sediment, the development of local scour around each of the pier sizes was independent of the flow depth for $y_0/D > 3$ and was almost independent of flow depth for $y_0/D > 1$. However, the results with $D = 240 \text{ mm}$ pier may be influenced also by the size of the flume used.

Laursen and Toch (1956) stated that the scour depth in the continuous bed-load movement case is dependent on the flow depth. The maximum scour depth was found to increase with increasing relative flow depth y_0/D .

Figure 2.7 shows the influence of flow depth on local scour depth as reported by Shen et al. (1977). Data were obtained by Chabert and Engeldinger (1956). It was found for $y_0/D > 1$ that y_0 exerted a negligible influence on the depth of scour. Smaller depths, however, tended to reduce the scour depth.

- 13 -

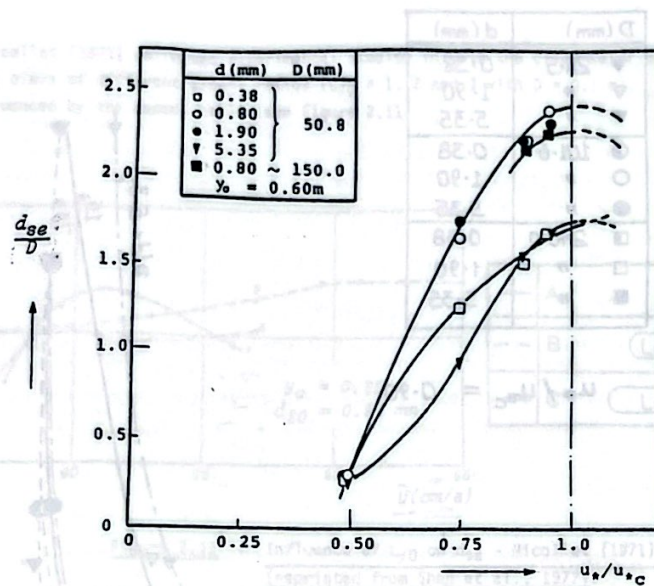


2.1.4 Influence of Flow Velocity

Ettema's (1980) plot (see Figure 2.13) of scour depths obtained experimentally under clear-water (i.e. $\frac{u_*}{u_{*c}} < 1$) conditions indicates clearly that the equilibrium depth of scour increased almost linearly with increasing values of shear velocity ratio from about 0.5 up to unity. His results were in good agreement with those of Chabert and Engeldinger (1956), Maza Alvarez and Sanchez Bribiesca (1966, 1967, 1968), Hancu (1971), Nicollet (1971) and those of other investigators.

Some investigators, namely Bata (1960), Garde (1961), Chitale (1962) and Marin (1962) claimed that the ratio of the equilibrium depth of local scour to the approach flow depth (i.e. $\frac{d_{se}}{y_0}$) varied with the approach flow Froude Number ($Fr = \frac{U}{\sqrt{gy_0}}$).

- 14 -

Figure 2.13 : Equilibrium scour depth versus u^*/u_{*c} (Ettema, 1980).

For $\bar{U} > \bar{U}_c$, Chabert and Engeldinger (1956) found from experimental data that, for a given cylinder and sand size, the maximum scour depth decreased slightly with mean velocity after reaching its maximum at $\bar{U} = 1$, and thereafter remained essentially constant for larger velocities of flow (see Figures 2.4 and 2.14). Laursen's (1958, 1962) results for live-bed scour showed the same trend. This trend, however, is not really apparent in the results of Shen et al. (1966) for 0.24 mm sand, although no definite conclusion can be drawn from these results (see Figure 2.15).

Data were obtained by Chabert and Engeldinger (1956). It was found for $y_0/D > 1$ that y_0 exerted a negligible influence on the depth of scour. For smaller values, however, tended to reduce the scour depth.

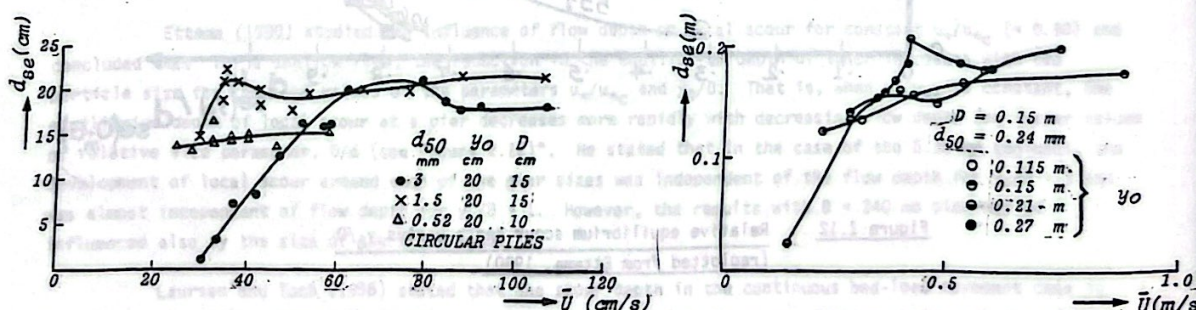


Figure 2.14 : Equilibrium depth of scour

Figure 2.15 : Equilibrium scour depth versus

mean flow velocity. Data of Chabert and Engeldinger (1956) and Shen et al., 1977, replotted by Shen et al., 1977.

mean flow velocity. Data of Shen et al. (1966) replotted by Shen et al., 1977.

- 15 -

CHAPTER 3

In contrast to the above, studies carried out by Jain and Fischer (1979) showed that the scour depth around a circular pier with sediment transport ($Fr > Fr_c$) first dropped off slightly (similar behaviour to the above) and then increased with increasing Froude number (see Figures 2.16 (a) and (b)).

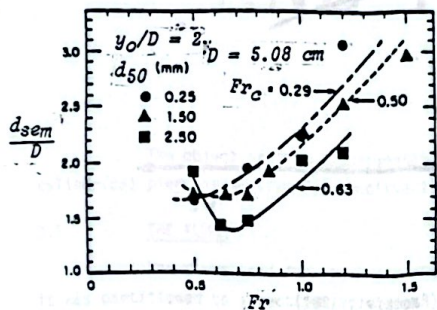
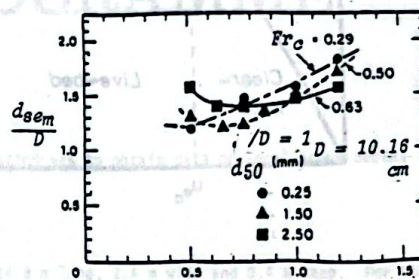


Figure 2.16 (a)

Figure 2.16 (b) : $d_{se\bar{m}}$ versus Fr (Jain and Fischer, 1980).

They claimed that scour depths at high flow velocity were larger than the maximum clear-water scour depths, i.e. at $\bar{U}/\bar{U}_c = 1.0$. Jain and Fischer used three different sediment sizes ($d_{50} = 0.25 \text{ mm}, 1.50 \text{ mm} \text{ and } 2.50 \text{ mm}$) and a constant flow depth of 101.6 mm.

The conclusions of Jain and Fischer evidently contradict those of Chabert and Engeldinger (1956) and Laursen et al., although Shen et al's (1966) results do suggest a somewhat similar trend. Jain and Fischer (1979) explained that the reason why previous investigators did not observe any increase in scour depth with increase in flow velocity was that they, with the exception of Laursen et al., measured their scour depths after stopping the flow; hence, smaller $d_{se\bar{m}}$ were recorded due to the deposition of the suspended sediment in the scour hole during the flow closure. However, this reasoning is not applicable to the Chatou's (1956) data, since Chabert and Engeldinger obtained each of their $d_{se\bar{m}}$ values from d_s versus time plots. (Note that a fair number of their runs were clearly stopped before equilibrium condition had been reached.)

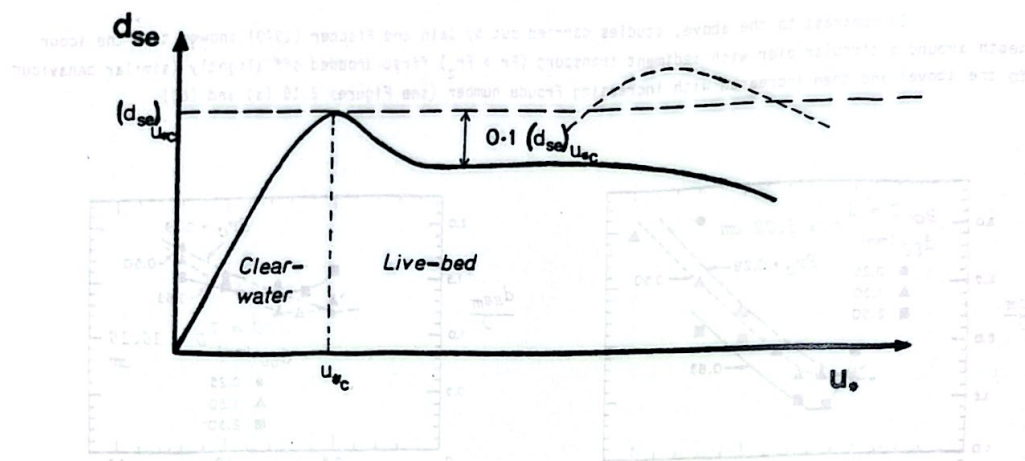
Raudkivi (1981) stated that "it is feasible that with fine sands, at transport as transition flat-bed, greater quantities of sand may be suspended in the horseshoe vortex and that then a deeper scour develops, as indicated in Figure 2.17. With coarse-grained sediments at high velocities the scour depth can actually become negative, i.e. a bow wave of gravel forms at the leading face of the pier," as has been observed in the laboratory. At high transport rates the downflow strength is also greater than that at low transport rates.

The result of Shen et al. (1966) for fine sand ($d_{50} = 0.24 \text{ mm}$) at average flow depth, $y_0 = 115 \text{ mm}$ is interesting. As seen in Figure 2.15, the scour depth appears to reach a peak at a velocity much greater than \bar{U}_c . No peak is obvious at around threshold velocity, i.e. $\bar{U} = 0.21 \text{ m/s}$ (refer also Figure 4.7). (The additional point at $\bar{U} = 1.08 \text{ m/s}$ was omitted in Shen et alia (1977) plot but was included in Figure 2.15.)

The results of Nicollet (1971) obtained from model studies of different aspect ratios, as plotted in Figure 2.11, indicate a similar trend to that of Jain and Fischer (see piers B and C). The curves for piers B and C show that the scour depths at $\bar{U} > \bar{U}_c$ were greater than those at \bar{U}_c .

White (1975) found from the results of a series of experimental runs at high Froude Numbers ($Fr = 0.8 \text{ to } 1.2$) that the influence of Fr was only small in this range. He used a coarse sand ($d_{50} = 0.9, d_{90} = 3.4 \text{ mm}$) and three basic pier shapes.

- 16 -

Figure 2.17 : d_{se} versus u_* (Raudkivi, 1981)

2.2 SUMMARY

The local scour process about cylindrical piers in granular beds is not fully understood. Much experimental data has been produced and many empirical formulae proposed, each one pertinent to the conditions of the particular experiments on which it was based but a complete description of the local scour is not yet available. Particularly, the live-bed scour process is as yet ill-defined.

A comparison of laboratory data from different sources indicates a wide scatter. The reasons for this are probably included in the following:-

- (1) The experimental techniques, for example, the measuring of the maximum scour depths. For live-bed experiments, some investigators measured the depths of scour only after stopping the flow so that inaccuracy in measurement occurred due to the deposition of the suspended particles in the scour hole. Jain and Fischer (1979) stated that the difference between the measured and actual depths of scour increases with flow velocity and becomes significant at velocities greater than those at threshold condition.
- (2) The variation of flow around a pier is extremely complex even without the added complications from erodible boundaries.
- (3) The time-development of scour in the clear-water regime. The importance of this aspect was frequently overlooked, and it is clear in some cases that equilibrium scour depths had not been reached.
- (4) The variation of grain-size distribution of bed sediment, the effect of which has been often neglected in the study of local scour. Ettema (1976) asserted that within the range of so-called "uniformity", noticeable variation in erosion is observable.
- (5) The effect of different turbulence intensity and local flow patterns on the strength of erosion of the flow in the scour hole.

- 17 -

CHAPTER 3

EXPERIMENTAL SET-UP AND PROGRAMME

The object of this experimental investigation was to obtain data on local scour depths around cylindrical piers under live-bed conditions.

3.1 THE FLUME

The flume used for scour experiments is 14.8 m long, 2.4 m wide and 0.4 m deep. For these tests it was partitioned to a rectangular channel of 0.6 m in width along one side. The discharge end of the channel led into the centre of the end tank which contained the collecting and weighing tank for sediment (refer Figures 3.1 and 3.2).

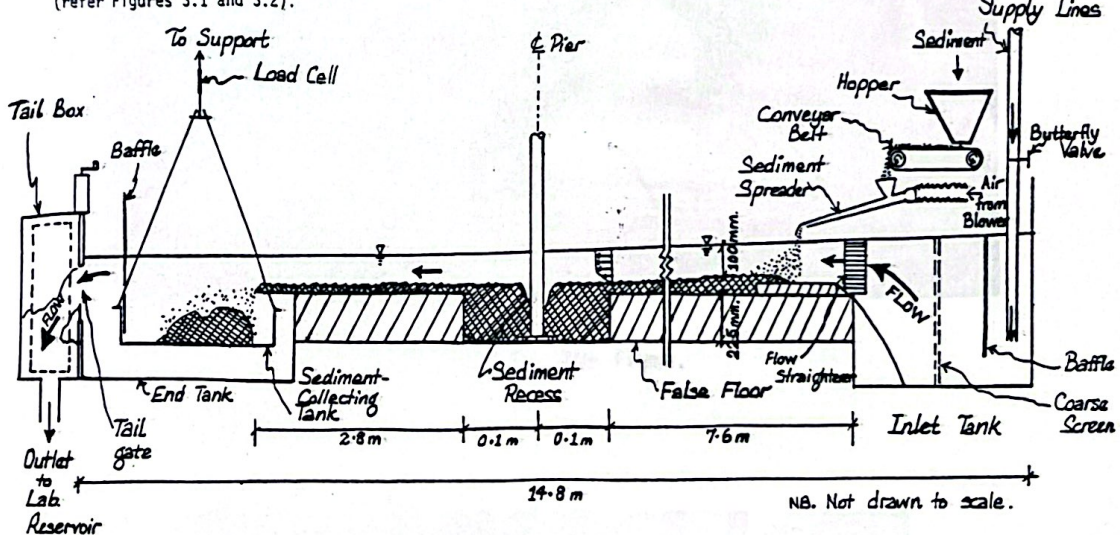


Figure 3.1 : Longitudinal section of Flume

The channel contains a 2m-long sediment recess in which the piers were inserted as shown in Figure 3.1. For the rest of it the depth was reduced to 0.225 m by insertion of a false floor, which was covered by the same sediment as that used in the recess (refer Figure 3.1).

For most of the experiments, the flume was kept horizontal and the stream bed was allowed to adjust itself over a period of time to the equilibrium bed slope for each particular run (see Section 3.3). For the runs at very high flow-rates, the flume was tilted to a slope of 1:100. In these experiments, the bed was again allowed to adjust to an equilibrium slope.

Water was supplied to the flume from the laboratory constant-head tank via two 152.5 mm diameter pipelines. The flow rate was measured with orifice plates ($M = 0.5$, $D = 4.262$) in the supply lines and was controlled by butterfly valves at the outlets to the flume.

The level of eddying of the water in the inlet tank of the flume was effectively reduced by a

CHAPTER

maximum of 2,321 and six small board-mounted yokes were used with each of the four sets of ballasts and incandescent lamps.

the following sections we will see how it can be associated with a value and be used to compute the function

- 18 -



Figure 3.2: The flume.

the change in the water level in the collecting tanks. This was done by connecting the tanks to the flume and measuring the time taken for the water level to change from one point to another. The time taken for the water level to change from one point to another was measured by a stop watch. A straight line graph was plotted with the height of water level in the tanks against time taken for the water level to change from one point to another. The slope of the straight line graph was calculated and hence a constant rate of discharge was obtained.



Figure 3.3: Outlet end of flume showing tail-gate (adjustable weir).



- 19 -

coarse screen and a baffle, Figure 3.1. From the tank the water passed first through a flow-straightener before entering the channel.

At the downstream end of the flume, an adjustable weir was used to control the water levels within the channel (see Figure 3.3).

For experiments with sediment movement, the condition of uniform flow was maintained by the addition of dry sediment at the upstream end of the channel. Dry sediment was fed into a hopper (refer Figures 3.4 and 3.5). Holes drilled through the bottom plate of the hopper allowed the sediment to fall through it on to a conveyor belt driven by a variable-speed motor. In addition to the motor control, the rate of sediment input could be adjusted by varying the narrow gap between the conveyor belt and the bottom of the hopper. The sediment from the belt was deposited into a fan-shaped sediment spreader by way of a "rectangular funnel" (see Figures 3.4 and 3.5). An air-blower (see Figures 3.1 and 3.4) was used to force the sediment through the spreader. The fan-shaped spreader had a downstream lip which deflected the grains driven by air vertically downwards so that these shot through the surface to the bottom of the flume. This overcame the problem of floating dry grains. In this way the sediment was evenly distributed over the whole width of the channel.

The sediment-supply apparatus was directly calibrated by collecting and measuring the quantity of sediment transported at different belt-hopper spacings and different motor speeds. The sediment supply rates were measured in g/min (dry).

It was important to maintain a sediment equilibrium, uniform flow condition and also to ensure that flow depth remained constant throughout the experiment. The sediment discharge rate was measured by means of a collecting tank (2.29 m long, 0.87 m wide and 0.210 m deep) (refer Figure 3.6) suspended from a load-cell (see Figures 3.1 and 3.7) and positioned at the downstream end of the channel.

A set of wooden baffles (see Figure 3.6) assisted with the settling out of most of the suspended sediment in the collecting tank. Nevertheless, some loss of sediment did occur and the purpose of the collecting tank was to determine whether the rate of sediment discharge from the channel was steady or not. The flow-rate and rate of sediment supply were maintained constant throughout each experimental run so that a record of constant rate of sediment discharge indicated the equilibrium stage.

The load-cell consisted of a piece of 1 mm thick EN25 stainless steel plate with a central portion of dimensions 10 mm by 70 mm (see Figure 3.7). In the centre of this portion, four identical strain gauges were mounted with two on each side of the plate. Any change in strain due to a change of load in the collecting tank was detected by a strain-indicator which was calibrated to read 1 μ s (micro-strain) for every 1 N (Newton) force. The rate of sediment collected in the tank over a duration of time was readily determined from the slope of the graph of sediment weight (in N) versus time (in second). A straight line graph indicated a steady rate of sediment accumulation in the tank and hence a constant rate of sediment discharging from the channel.

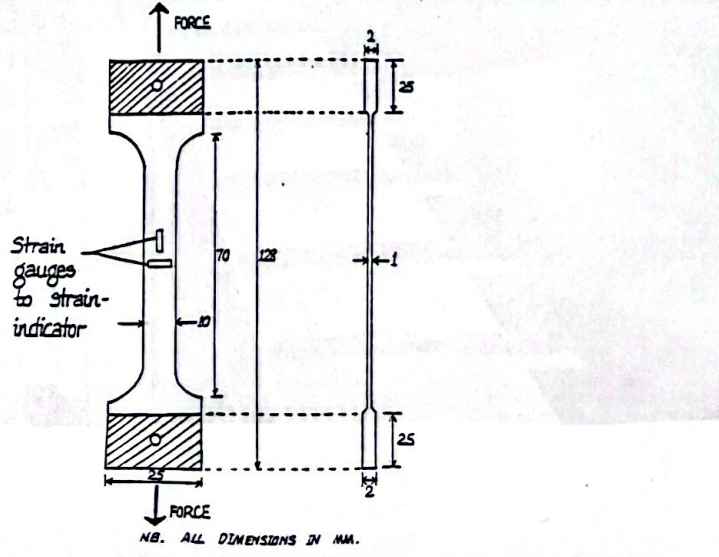
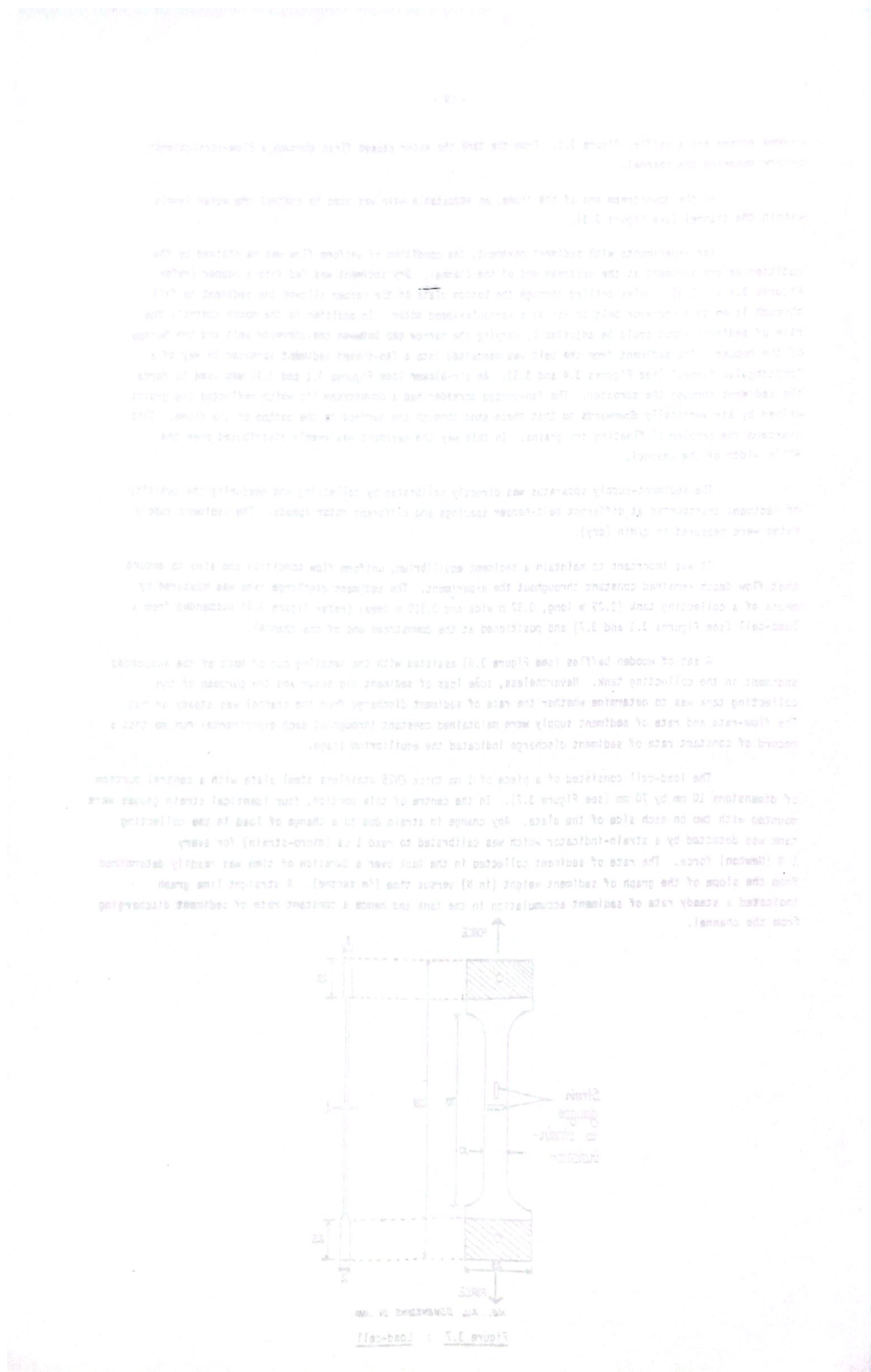


Figure 3.7 : Load-cell

Figure 3.4: Sediment-supply apparatus showing the hopper and air-blower.

Figure 3.5: Sediment-supply apparatus showing the hopper and sediment spreader.



- 20 -

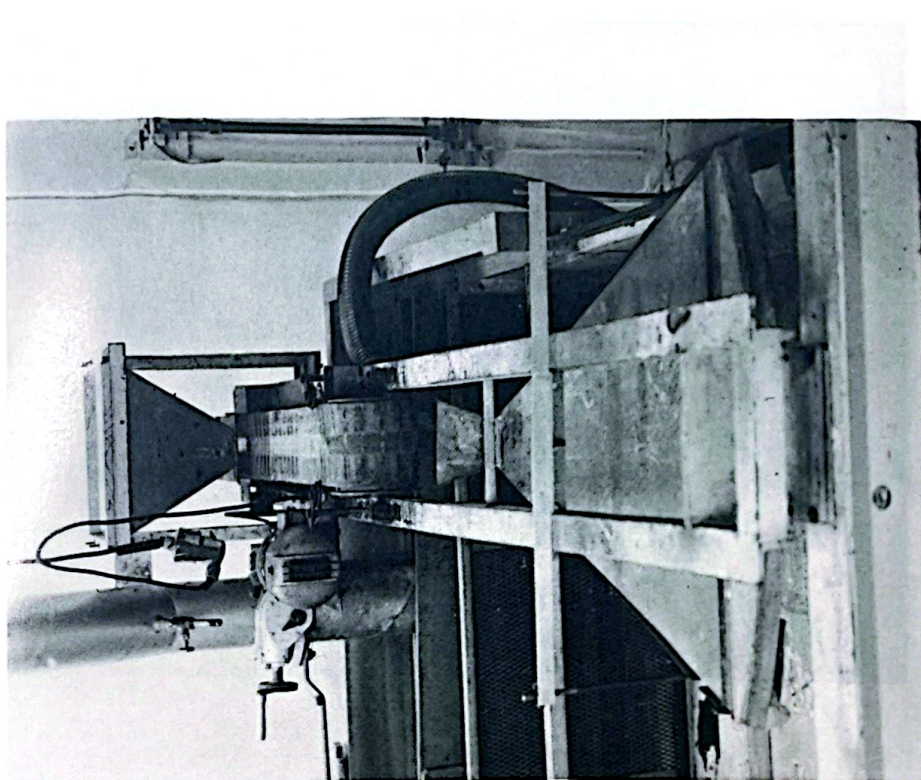


Figure 3.5: Sediment-supply apparatus showing the hopper and sediment spreader.

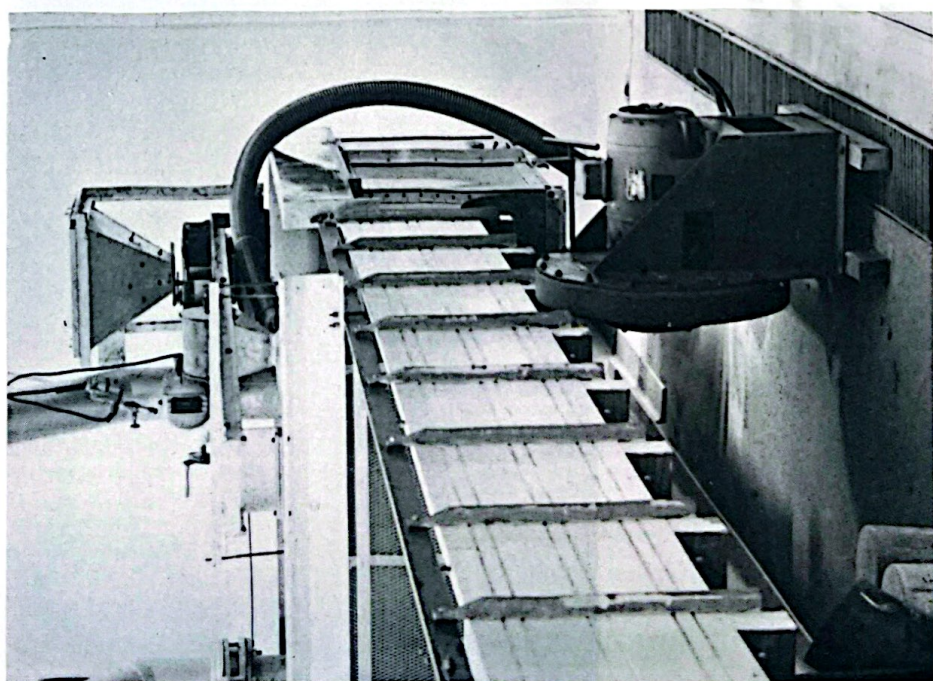


Figure 3.4: Sediment-supply apparatus showing the hopper and air-blower.



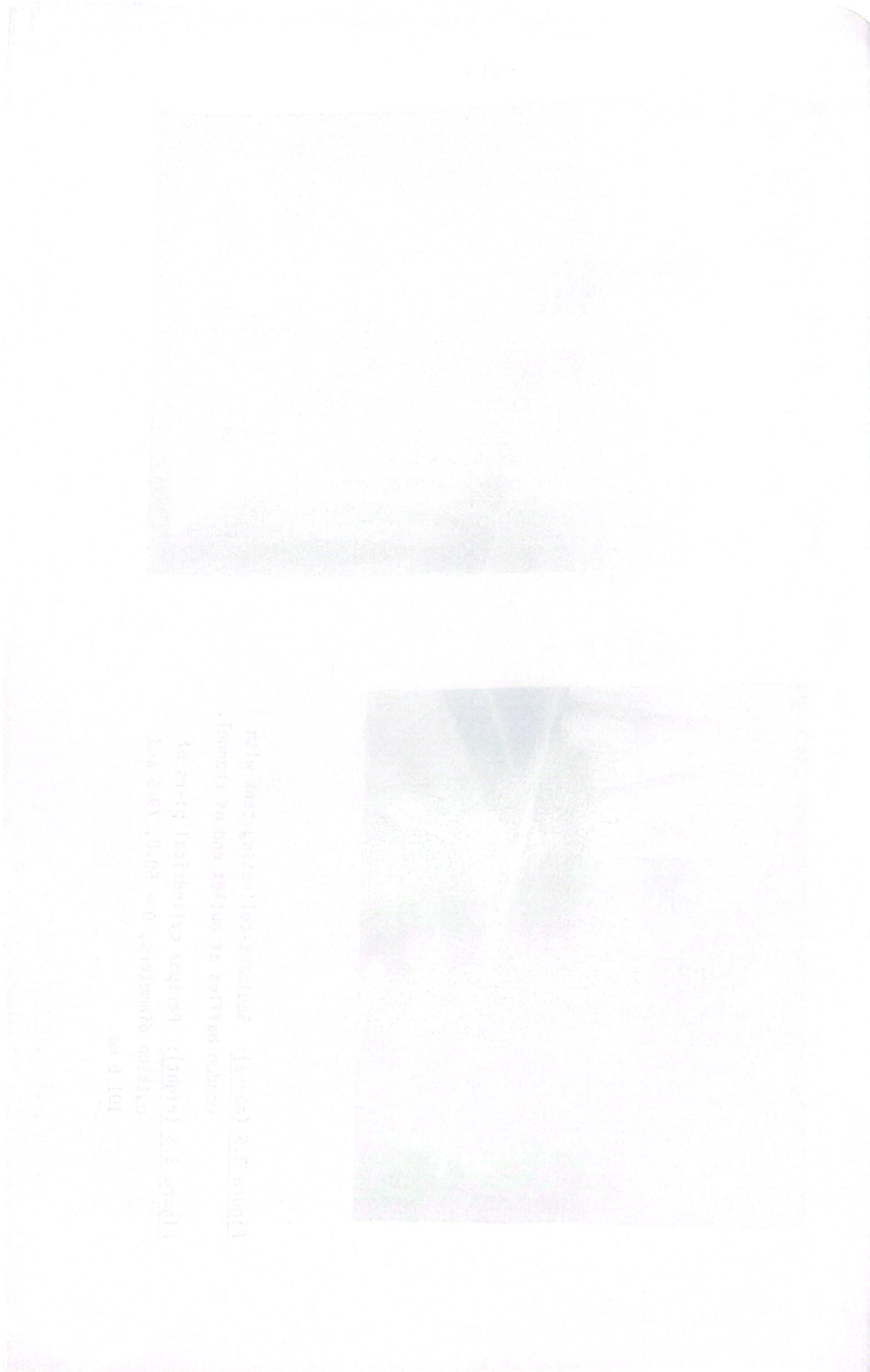
- 21 -



Figure 3.6 (above): Sediment-collecting tank with wooden baffles at outlet end of channel.



Figure 3.6 (above): Sediment-collecting tank with wooden baffles at outlet end of channel.
Figure 3.8 (right): Perspex cylindrical piers of outside diameters, $D = 50.8$; 79.5 and 101.6 mm.



- 22 -

3.2 MEASUREMENT TECHNIQUES

Uniform flow conditions were maintained throughout each run. Approach flow depths were kept constant at 100 ($\pm 1-3$ mm) and these were measured by averaging the depths of ten to twenty crests and troughs below the surface of the water at three locations, namely at the vicinity of the pier, and at about 3 m and 5 m upstream of the pier. A steel ruler was used for these measurements. These depths were checked against permanent elevation marks on the channel walls.

Velocity profiles for some experiments (low flow velocities) were measured on the centre-line of the approach flow by a standard pitot tube situated about 1.0 m upstream of the pier. A reasonably straight logarithmic profile was obtained. The mean velocity, \bar{U} calculated from each of these graphs was checked against that derived from the orifice plate reading. For high flow rates, measurements of velocity profiles on the approach bed became difficult due to the high sediment transport rates and rapid passage of bed-forms at the measurement point, and values of u_* obtained from these velocity profiles show large scatter (see Appendix 1 for values of u_* obtained).

Scour depth observations were made using a "periscope" inside the hollow cylindrical piers. The piers were made of perspex and each had a round P.V.C. or metallic base sealed to one end of it to ensure water-tightness (refer Figure 3.8). With the aid of a strong light it was possible with this periscope to observe the base of the scour hole through the wall of the pier and its location relative to a millimeter scale glued vertically on to the inside wall of the leading edge of the pier. In this way, the deepest depth of the scour hole, d_s , around the pier at any particular instant could be read to 0.5 mm accuracy.

3.3 EXPERIMENTAL PROGRAMME

Four series of experiments, with four different sized non-cohesive, uniform bed-sediments ($d_{50} = 0.24, 0.38, 0.80$, and 1.40 mm) were carried out. In each of these series, three different sizes of piers (outside diameters = 50.8, 79.5 and 101.6 mm) were used. For each pier size tested, the mean flow velocity was systematically varied. All the experimental runs, with the exception of a few clear-water runs, were performed in the sediment-transporting regime. The flow depth was kept constant at 0.100 mm for all experiments. A summary of the experimental programme is shown in Table 3.1 (for further details, see Appendix 1). All the experiments were carried out in a 0.6 m-wide channel which formed part of a larger flume.

Series	1			2			3			4		
d_{50} (mm)	0.24			0.38			0.80			1.40		
D (mm)	50.8	79.5	101.6	50.8	79.5	101.6	50.8	79.5	101.6	50.8	79.5	101.6
Ranging from 0.17 to 1.40m/s												

Table 3.1 : Summary of experimental programme

The four uniform cohesionless bed sediments selected for tests have properties as given in Table 3.2. The particle size distribution for each of these sediments is shown in Figure 3.9.

The degree of uniformity of the particle size distribution of a sediment is defined by the value of its standard deviation, σ , the most commonly used being the geometric standard deviation, σ_g , where

(1) Water temperature was maintained. General laboratory temperature variation was limited to $\pm 2^\circ\text{C}$ during each run.

STANDARD DEVIATION (%)

- 23 -

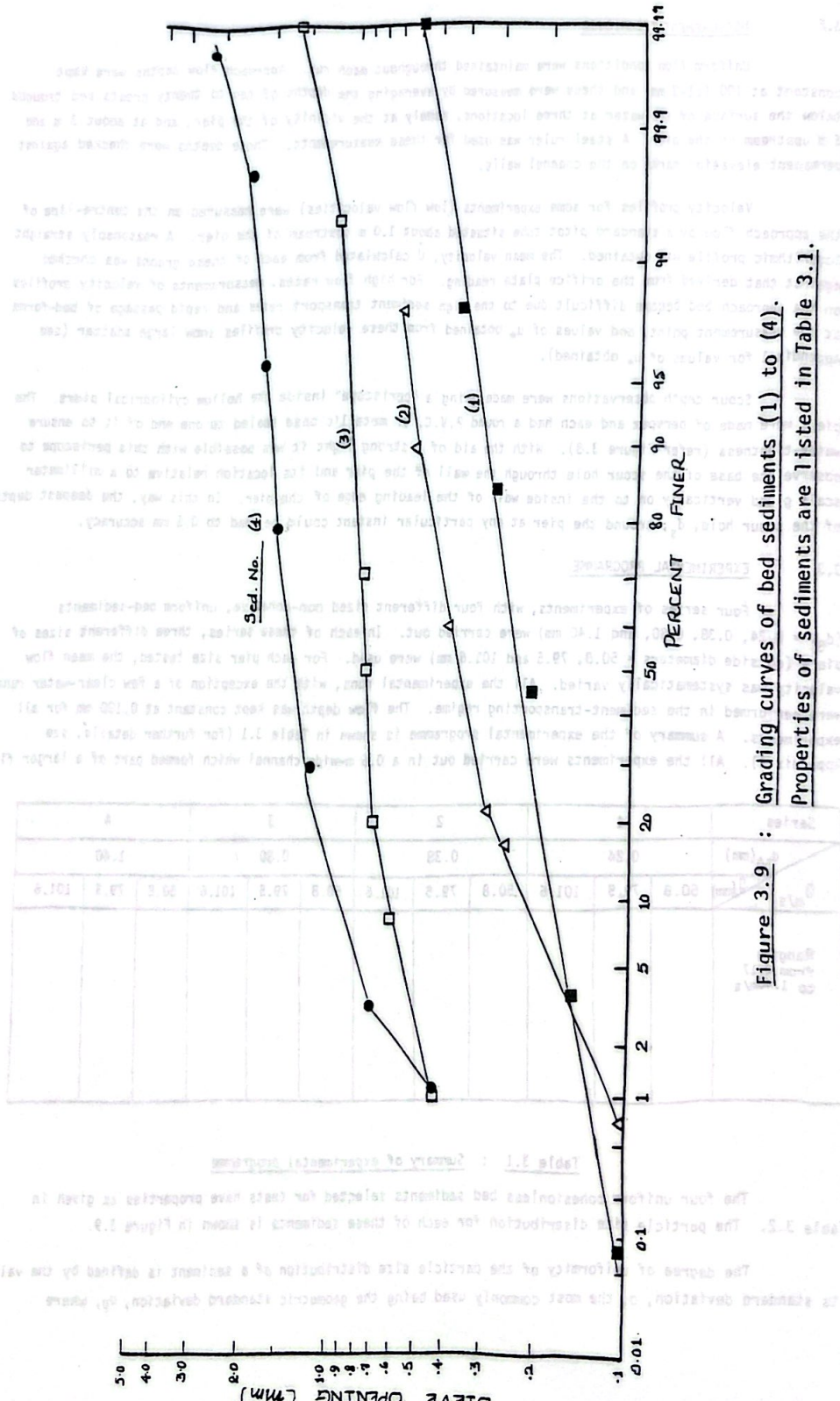


Figure 3.9 :
Grading curves of bed sediments (1) to (4).
Properties of sediments are listed in Table 3.1.

- 24 -

$\sigma_g = \left(\frac{d_{84.1}}{d_{15.9}} \right)^{k_1} = \frac{d_{84.1}}{d_{50}} = \frac{d_{50}}{d_{15.9}}$ of a log-normal plot of grain size. This is given in Table 3.2 for each of the sediments used. Also given in Table 3.2 are the inclusive graphic standard deviations, σ_I , where $\sigma_I = \left(\frac{d_{84.1}}{d_{15.9}} \right)^{0.250} \left(\frac{d_{95}}{d_5} \right)^{0.152}$. Since the value of σ_g for each of the four sediments used in the experiments is less than 1.3, they can be considered uniform bed sediments. The sediments used were well rounded and may be assumed to have shape factor, S.F. = 1.0 (S.F. = c/\sqrt{ab} where a, b, c are lengths of mutually perpendicular axes of a particle, c being the shortest.) All sediments had specific gravities, S_s of 2.65 ± 0.01 . The Shields function was employed in the calculation of the critical shear velocity, u_{*c} , for the d_{50} particle size of each sediment. The angles of static particle repose, α , were determined by tilting a large beaker containing sand in water until the particles on the sand surface just started to move.

Bed Sediment Number	d_{50} (mm)	S_s	u_{*c} ($\times 10^{-2} \text{ ms}^{-1}$)	σ_g	σ_I	S.F.	α
1	0.24	2.65	1.25	1.25	1.16	1.0	32
2	0.38	2.65	1.43	1.22	1.20	1.0	33
3	0.80	2.65	2.03	1.29	1.27	1.0	36
4	1.40	2.65	2.79	1.30	1.31	1.0	38

Table 3.2 : Properties of sediments used in experiments

Small amounts of pumice was present in both the 0.38 mm and 1.4 mm sands. The latter also contained a very small amount of very fine gravels (refer Figure 3.9).

At the commencement of each experimental run, the flume was slowly flooded to approximately the depth required, care being taken not to disturb the sediment bed. The butterfly valves in the supply lines were then adjusted to the required flowrate and the tail-gate adjusted to give a flow depth of 100 mm ($\pm 1-3$ mm) just upstream of the pier. For the runs with live-bed conditions, it was necessary to maintain a sediment supply at the inlet end of the channel. Both the tail-gate and the sediment supply rate were regulated till no appreciable changes in flow conditions took place. This steady state was indicated by:

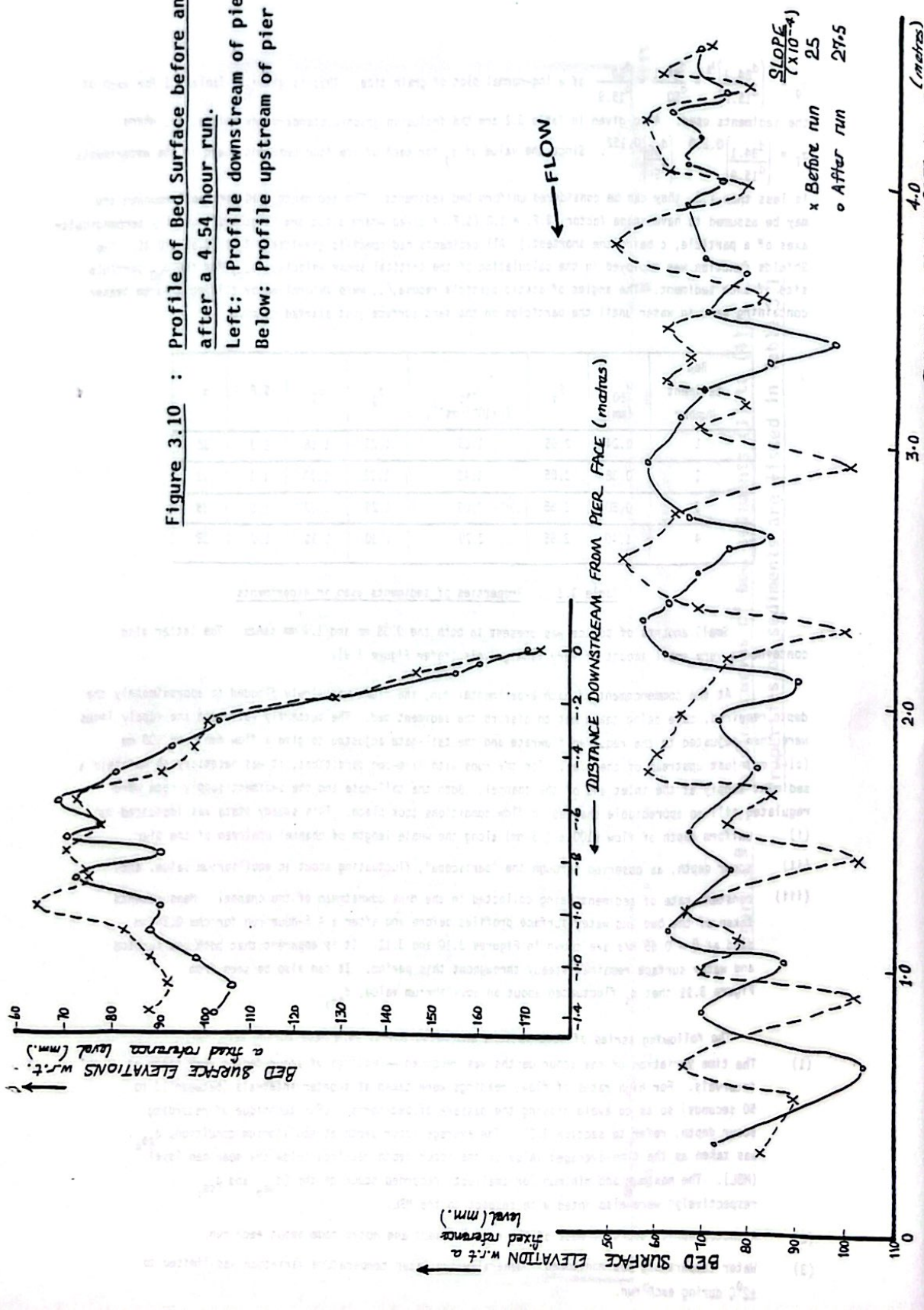
- (i) uniform depth of flow ($100 \pm 1-3$ mm) along the whole length of channel upstream of the pier,
- (ii) scour depth, as observed through the "periscope", fluctuating about an equilibrium value, and,
- (iii) constant rate of sediment being collected in the tank downstream of the channel. Measurements taken of the bed and water-surface profiles before and after a 4.5-hour run for the 0.24 mm sand at $U = 0.65 \text{ m/s}$ are shown in Figures 3.10 and 3.11. It is apparent that both bed surface and water surface remained steady throughout this period. It can also be seen from Figure 3.11 that d_s fluctuated about an equilibrium value, d_{sea} .

The following series of observations and measurements were made during each run:

- (1) The time variation of the scour depths was recorded — readings of scour depths were taken at intervals. For high rates of flow, readings were taken at shorter intervals (between 10 to 50 seconds) so as to avoid missing the passage of bed-forms. (For technique of recording scour depth, refer to section 3.2). The average scour depth at equilibrium condition, d_{sea} , was taken as the time-averaged value of the scour depth readings below the mean bed level (MBL). The maximum and minimum (or smallest) recorded scour depths (d_{sem} and d_{ses} respectively) were also noted with respect to the MBL.
- (2) A photographic record of most of the runs was kept and notes made about each run.
- (3) Water temperature was monitored. Generally the water temperature variation was limited to $\pm 2^\circ\text{C}$ during each run.

- 25 -

Figure 3.10 : Profile of Bed Surface before and after a 4.54 hour run.
Left: Profile downstream of pier
Below: Profile upstream of pier



- 26 -

- (4) The flow-rate, depth of flow and water surface elevation were periodically checked to ensure that they were steady.
- (5) The sediment discharge rate into the collecting tank was measured and plotted cumulatively. A linear relationship between total accumulated sediment and time indicated steady sediment transport conditions (see Section 3.1).

At the commencement of the clear-water scour experiments, the tail-gate and the flow control valves were opened simultaneously. Each experiment was allowed to continue until at least 3-4 hours after an apparent equilibrium scour depth had been attained. The time-development of scour depths was recorded throughout the experiment and the final depth at equilibrium was noted.

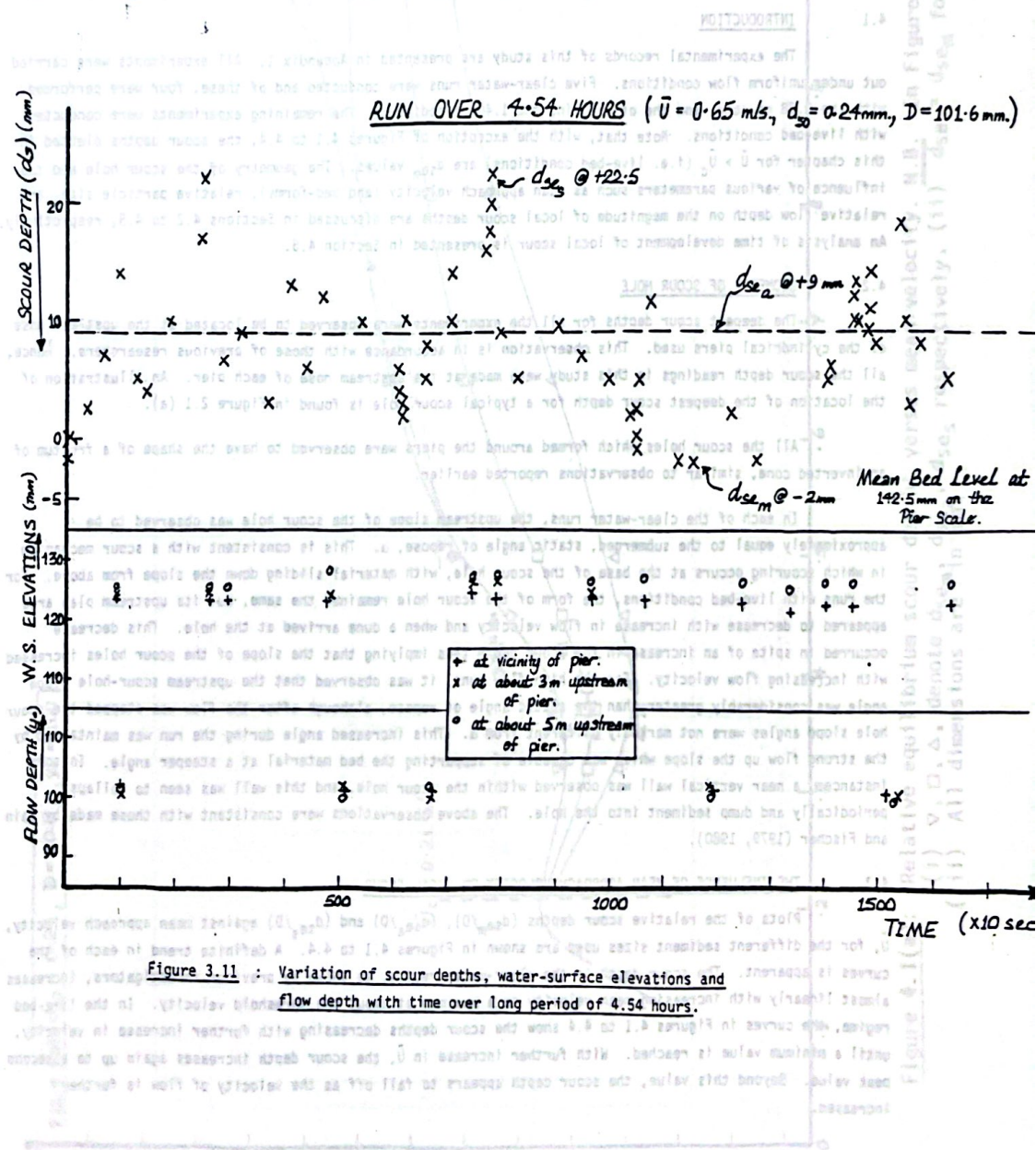


Figure 3.11 : Variation of scour depths, water-surface elevations and flow depth with time over long period of 4.54 hours.

- 27 -

CHAPTER 4

RESULTS AND DISCUSSION

4.1 INTRODUCTION

The experimental records of this study are presented in Appendix 1. All experiments were carried out under uniform flow conditions. Five clear-water runs were conducted and of these, four were performed with the 0.38 mm sand, and the other using the 1.40 mm sediment. The remaining experiments were conducted with live-bed conditions. Note that, with the exception of Figures 4.1 to 4.4, the scour depths plotted in this chapter for $\bar{U} > \bar{U}_c$ (i.e. live-bed conditions) are d_{sem} values. The geometry of the scour hole and the influence of various parameters such as mean approach velocity (and bed-forms), relative particle size, and relative flow depth on the magnitude of local scour depths are discussed in Sections 4.2 to 4.5, respectively. An analysis of time development of local scour is presented in Section 4.6.

4.2 GEOMETRY OF SCOUR HOLE

The deepest scour depths for all the experiments were observed to be located at the upstream nose of the cylindrical piers used. This observation is in accordance with those of previous researchers. Hence, all the scour depth readings in this study were made at the upstream nose of each pier. An illustration of the location of the deepest scour depth for a typical scour hole is found in Figure 2.1 (a).

All the scour holes which formed around the piers were observed to have the shape of a frustum of an inverted cone, similar to observations reported earlier.

In each of the clear-water runs, the upstream slope of the scour hole was observed to be approximately equal to the submerged, static angle of repose, α . This is consistent with a scour mechanism in which scouring occurs at the base of the scour hole, with material sliding down the slope from above. For the runs with live-bed conditions, the form of the scour hole remained the same, but its upstream plan area appeared to decrease with increase in flow velocity and when a dune arrived at the hole. This decrease occurred in spite of an increase in the scour depth thus implying that the slope of the scour holes increased with increasing flow velocity. For the high flow runs, it was observed that the upstream scour-hole slope angle was considerably greater than the static angle of repose, although after the flow was stopped the scour hole slope angles were not markedly different from α . This increased angle during the run was maintained by the strong flow up the slope which was capable of supporting the bed material at a steeper angle. In some instances, a near vertical wall was observed within the scour hole, and this wall was seen to collapse periodically and dump sediment into the hole. The above observations were consistent with those made by Jain and Fischer (1979, 1980).

4.3 THE INFLUENCE OF MEAN APPROACH VELOCITY ON LOCAL SCOUR

Plots of the relative scour depths (d_{sem}/D), (d_{sea}/D) and (d_{ses}/D) against mean approach velocity, \bar{U} , for the different sediment sizes used are shown in Figures 4.1 to 4.4. A definite trend in each of the curves is apparent. The scour depth in the clear-water regime, as shown by previous investigators, increases almost linearly with increasing mean velocity to a maximum at about the threshold velocity. In the live-bed regime, the curves in Figures 4.1 to 4.4 show the scour depths decreasing with further increase in velocity, until a minimum value is reached. With further increase in \bar{U} , the scour depth increases again up to a second peak value. Beyond this value, the scour depth appears to fall off as the velocity of flow is further increased.

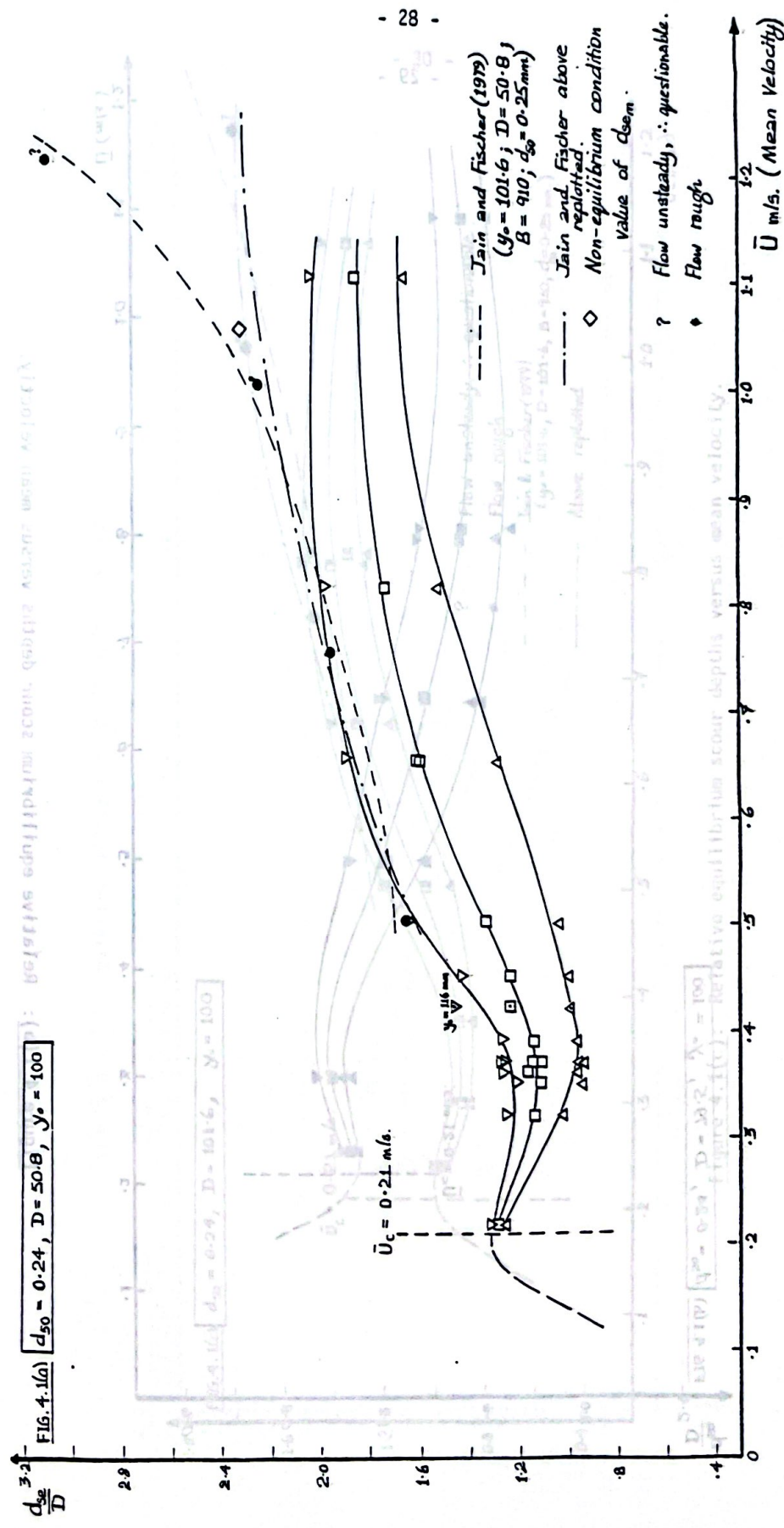


Figure 4.1(a): Relative equilibrium scour depths versus mean velocity. N.B.
 (i) ∇, \square, Δ , denote d_{se}, d_{se} , d_{se} respectively. (ii) $\frac{d_{se}}{D} = 100$
 (iii) All dimensions are in mm.

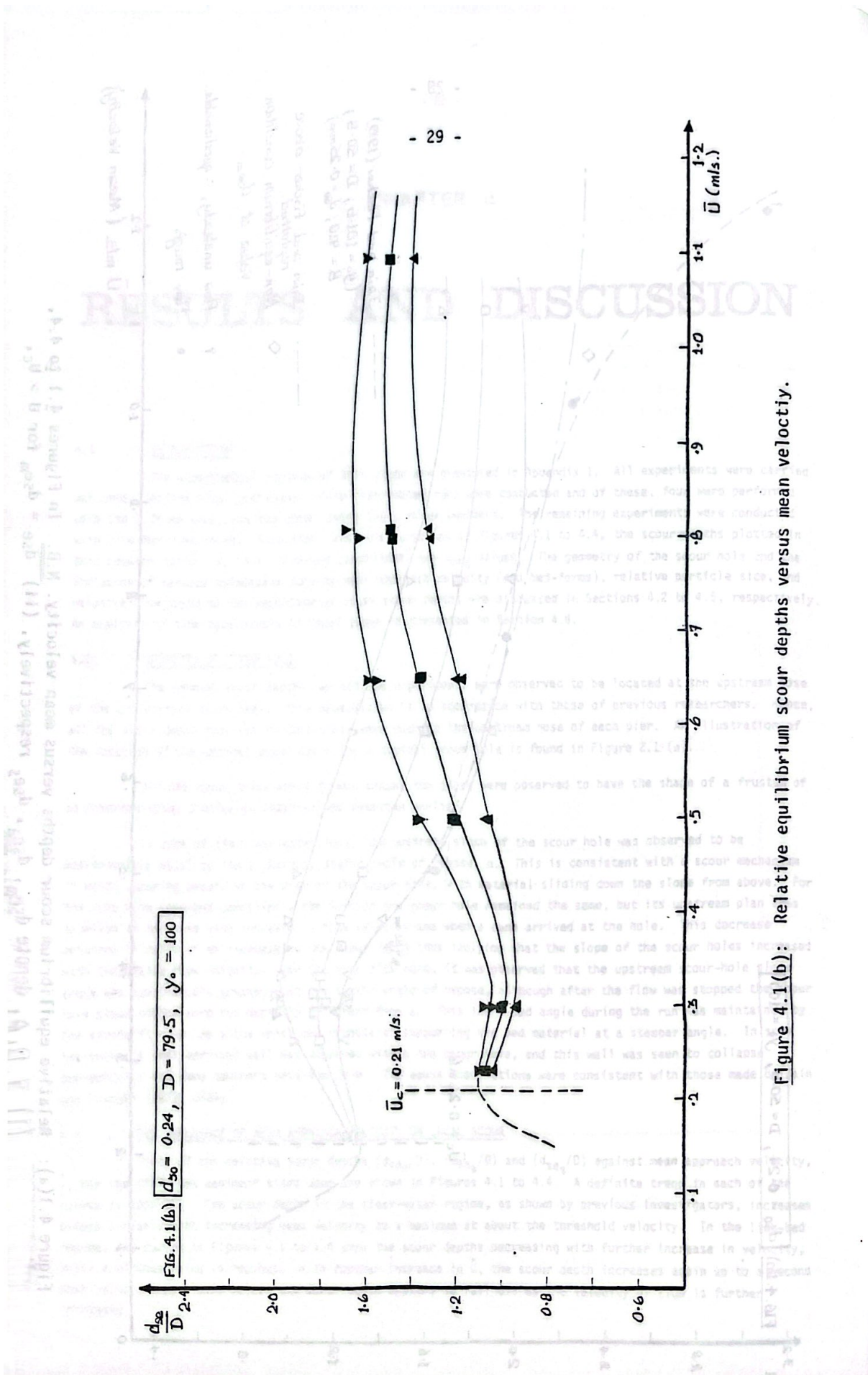


Figure 4.1(b): Relative equilibrium scour depths versus mean velocity.

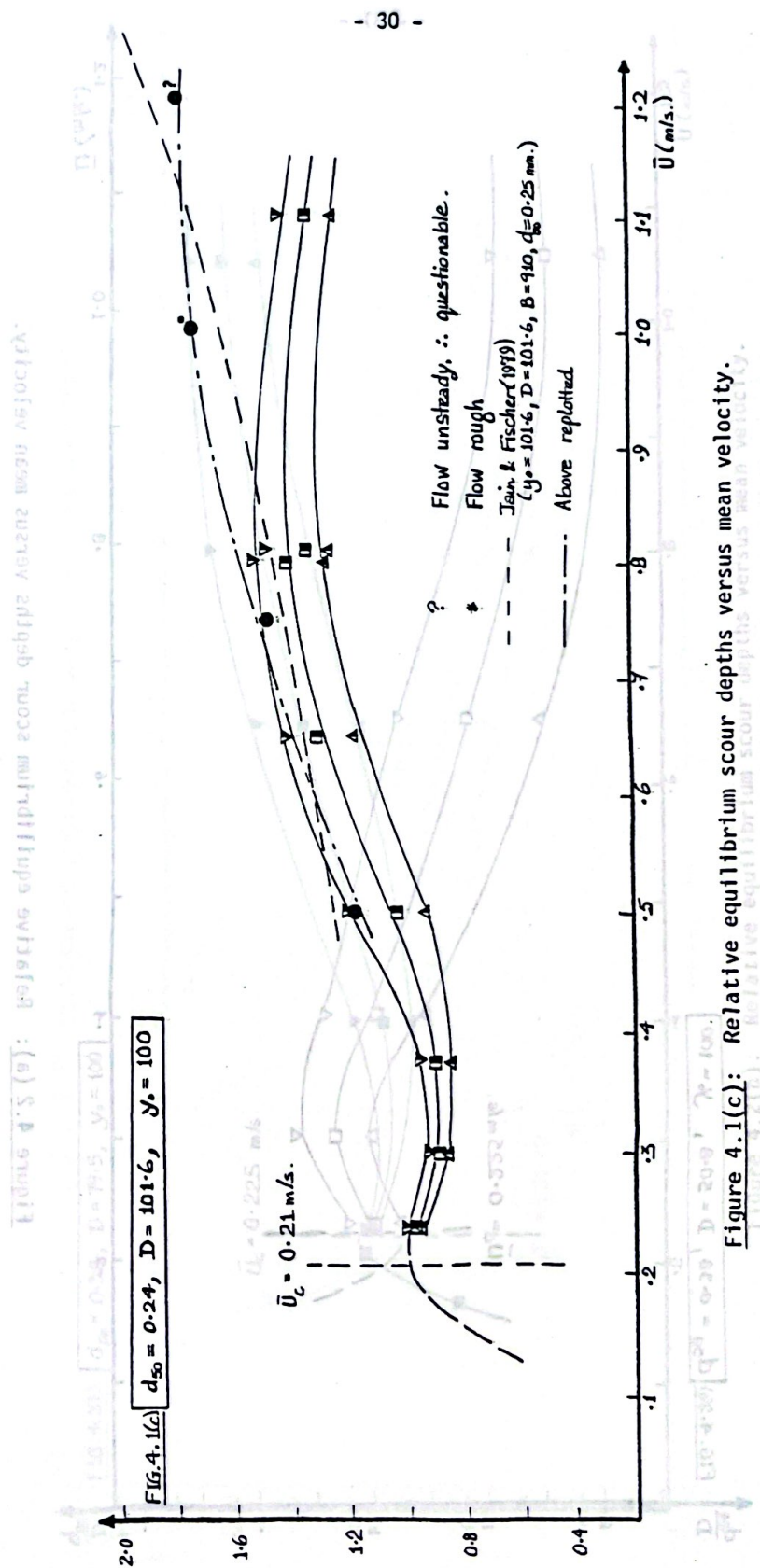


Figure 4.1(c): Relative equilibrium scour depths versus mean velocity.

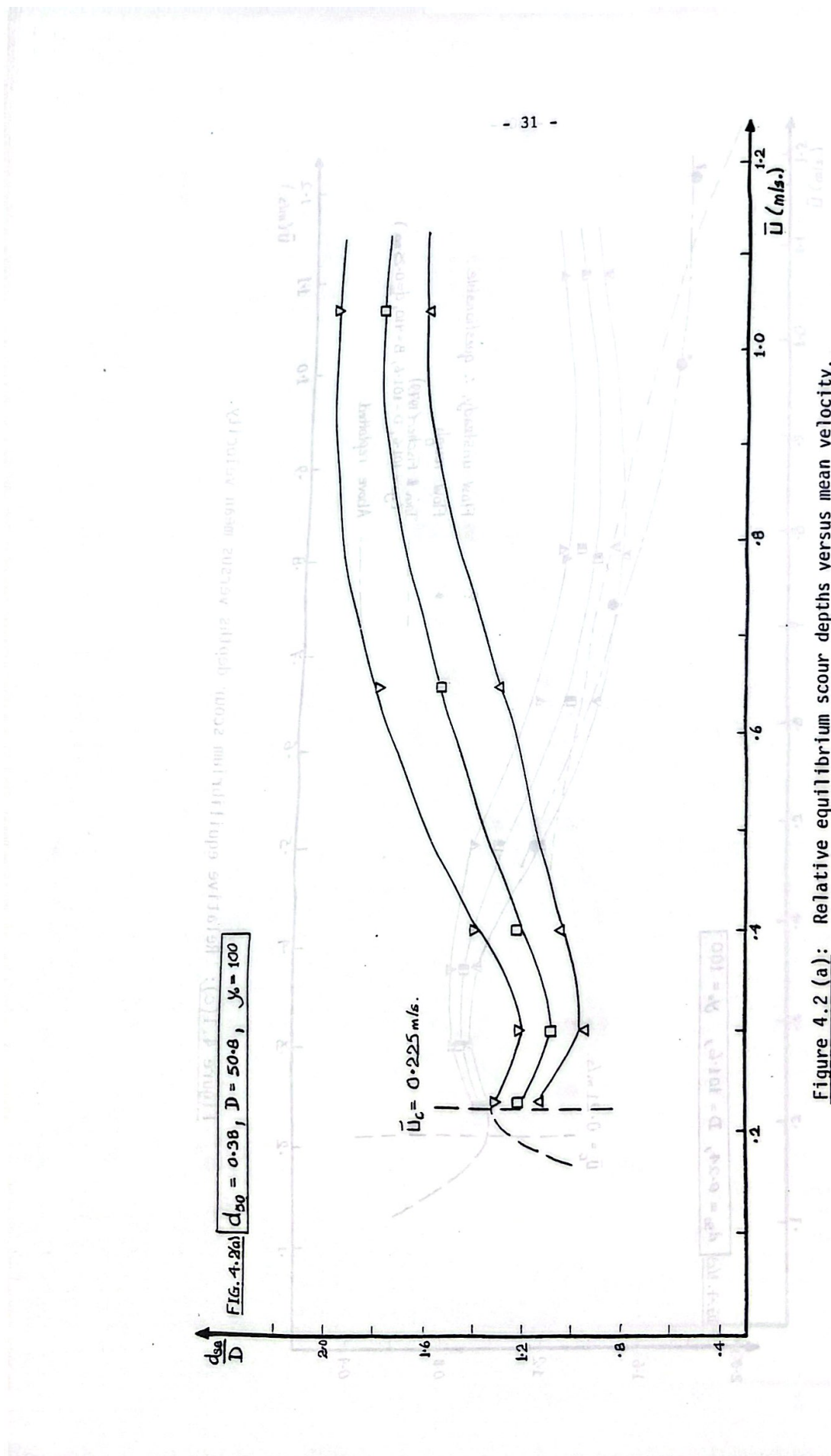


Figure 4.2 (a): Relative equilibrium scour depths versus mean velocity.

- 32 -

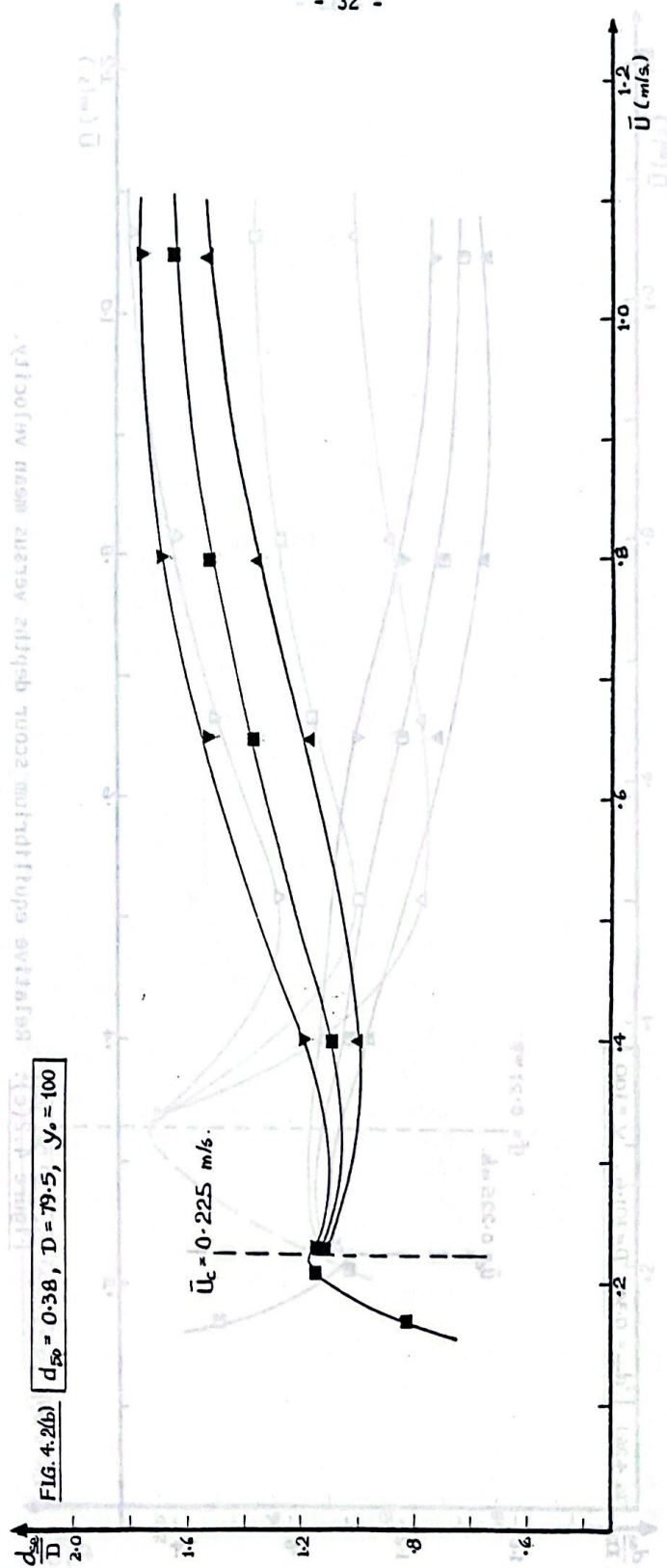
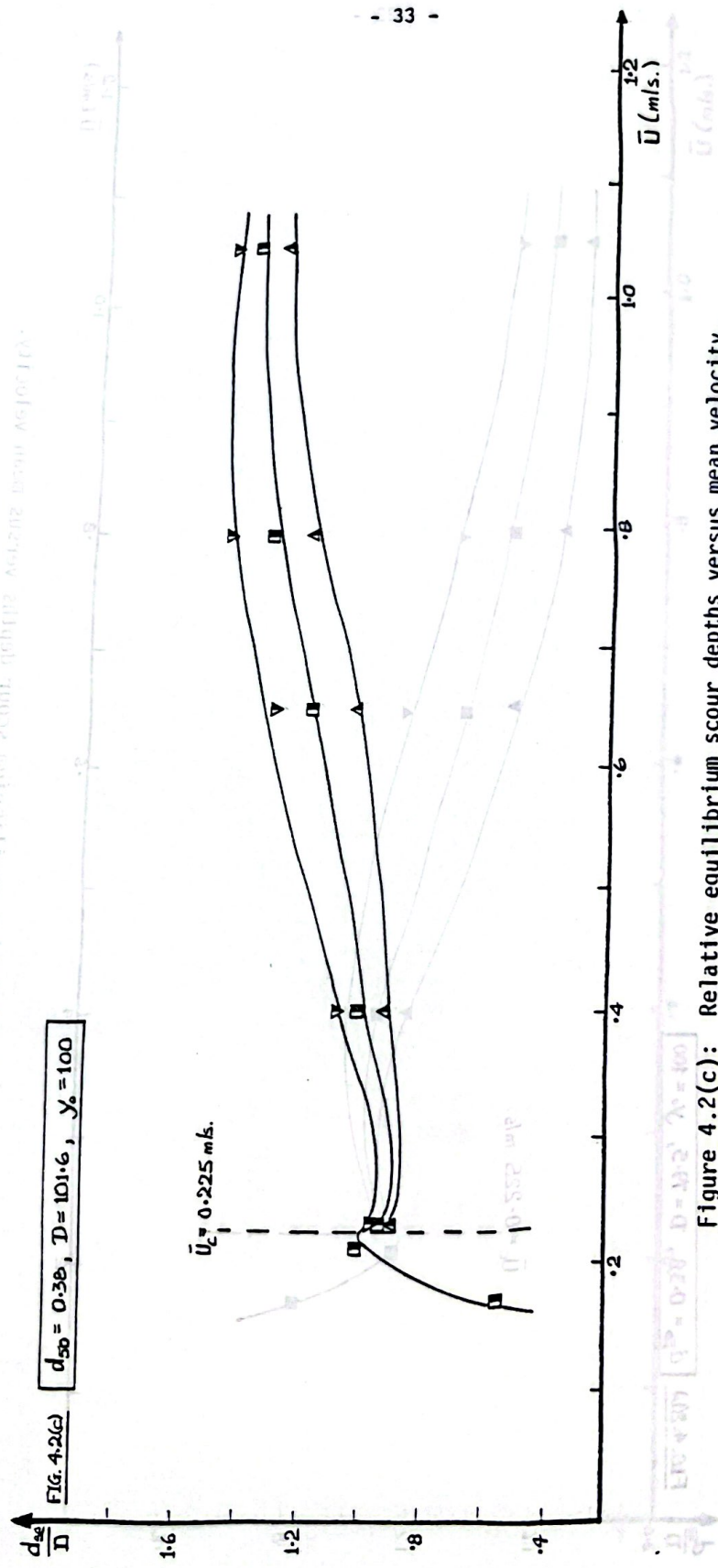


Figure 4.2(b): Relative equilibrium scour depths versus mean velocity.

- 33 -



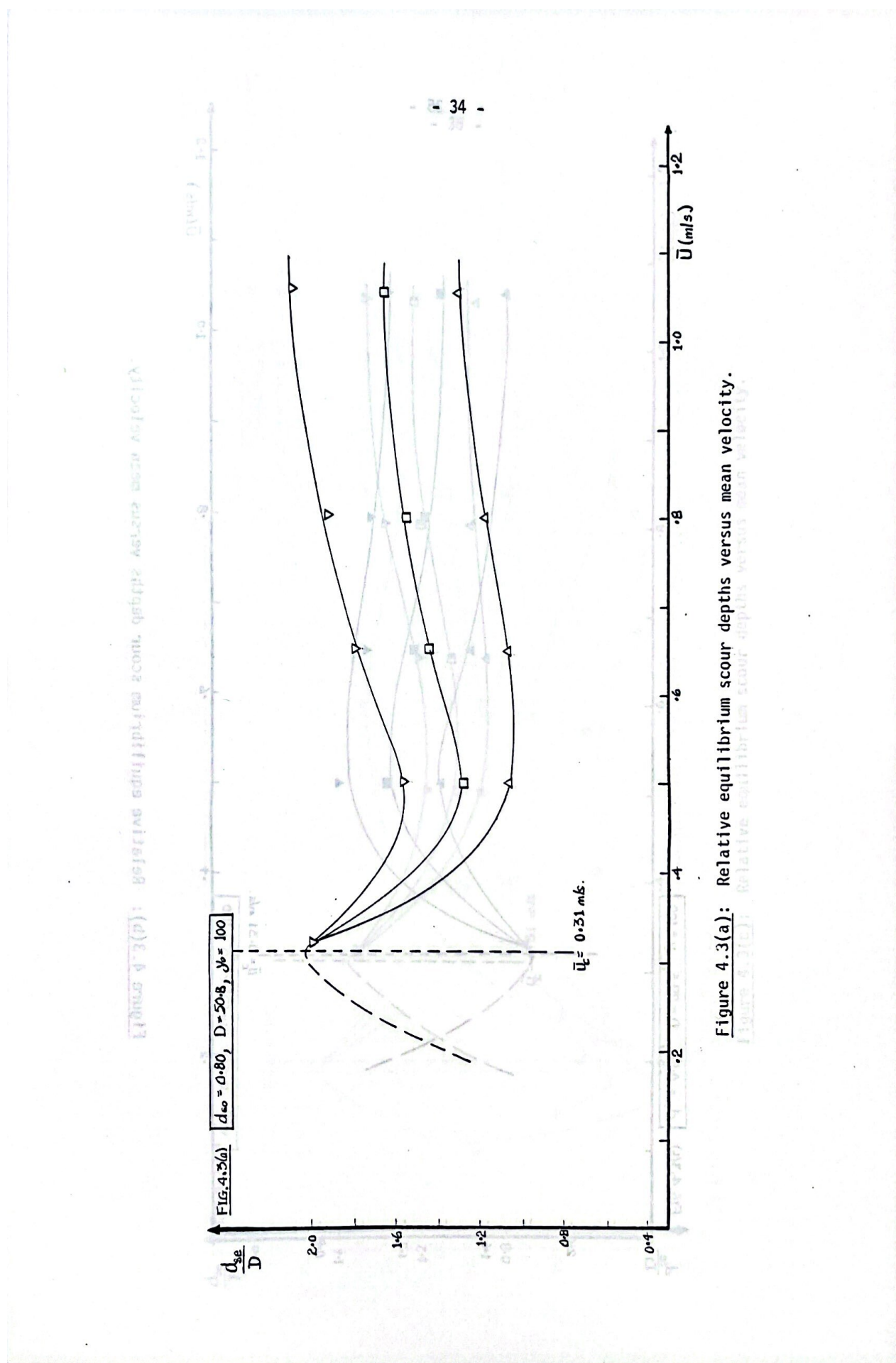


Figure 4.3(a): Relative equilibrium scour depths versus mean velocity.

Figure 4.3(b): Relative equilibrium scour depths versus mean velocity.

Figure 4.3(c): Relative equilibrium scour depths versus mean velocity.

Figure 4.3(d): Relative equilibrium scour depths versus mean velocity.

Figure 4.3(e): Relative equilibrium scour depths versus mean velocity.

Figure 4.3(f): Relative equilibrium scour depths versus mean velocity.

Figure 4.3(g): Relative equilibrium scour depths versus mean velocity.

Figure 4.3(h): Relative equilibrium scour depths versus mean velocity.

Figure 4.3(i): Relative equilibrium scour depths versus mean velocity.

Figure 4.3(j): Relative equilibrium scour depths versus mean velocity.

Figure 4.3(k): Relative equilibrium scour depths versus mean velocity.

Figure 4.3(l): Relative equilibrium scour depths versus mean velocity.

Figure 4.3(m): Relative equilibrium scour depths versus mean velocity.

Figure 4.3(n): Relative equilibrium scour depths versus mean velocity.

Figure 4.3(o): Relative equilibrium scour depths versus mean velocity.

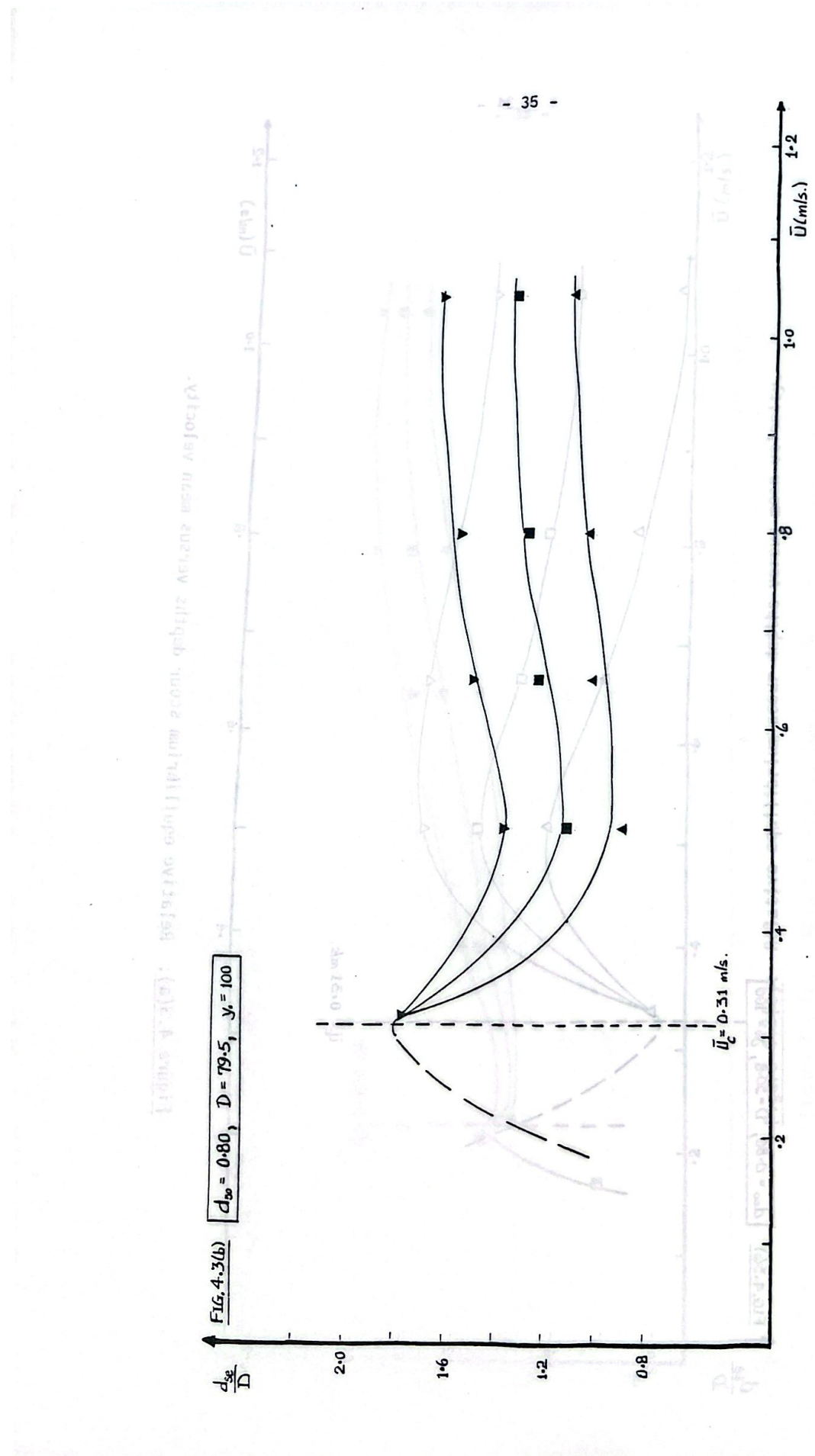


Figure 4.3(b): Relative equilibrium scour depths versus mean velocity.

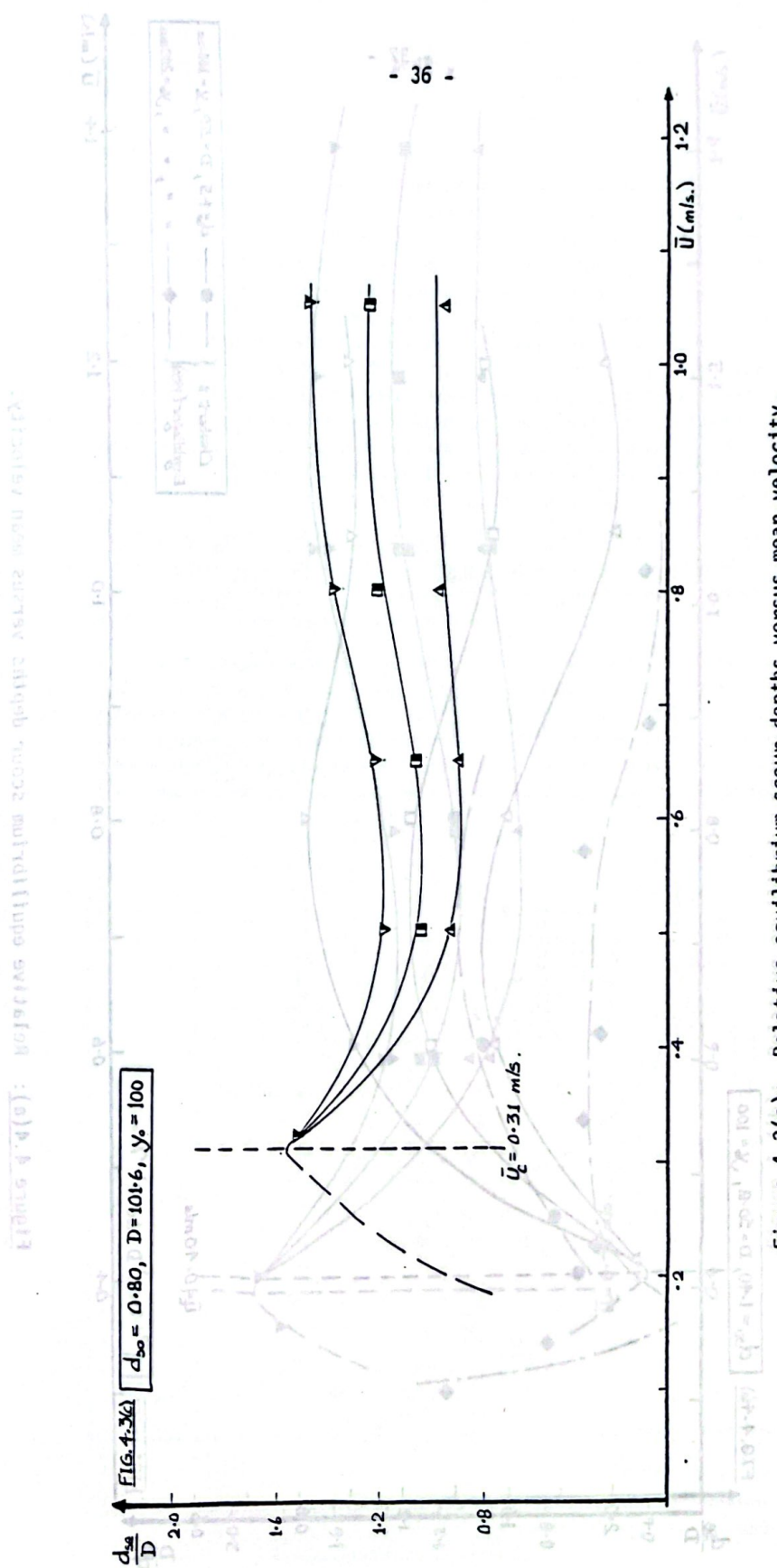


Figure 4.3(c): Relative equilibrium scour depths versus mean velocity.

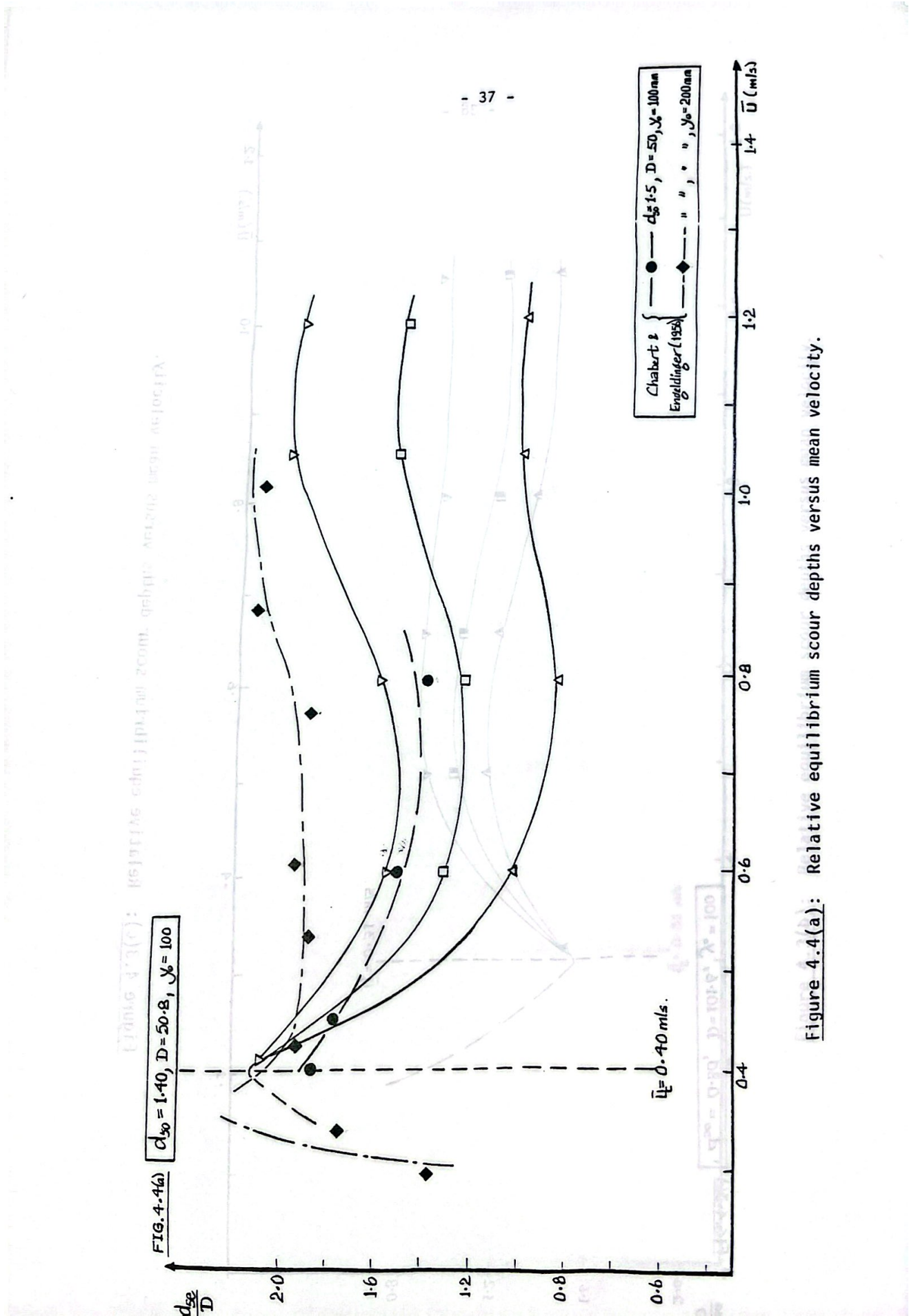
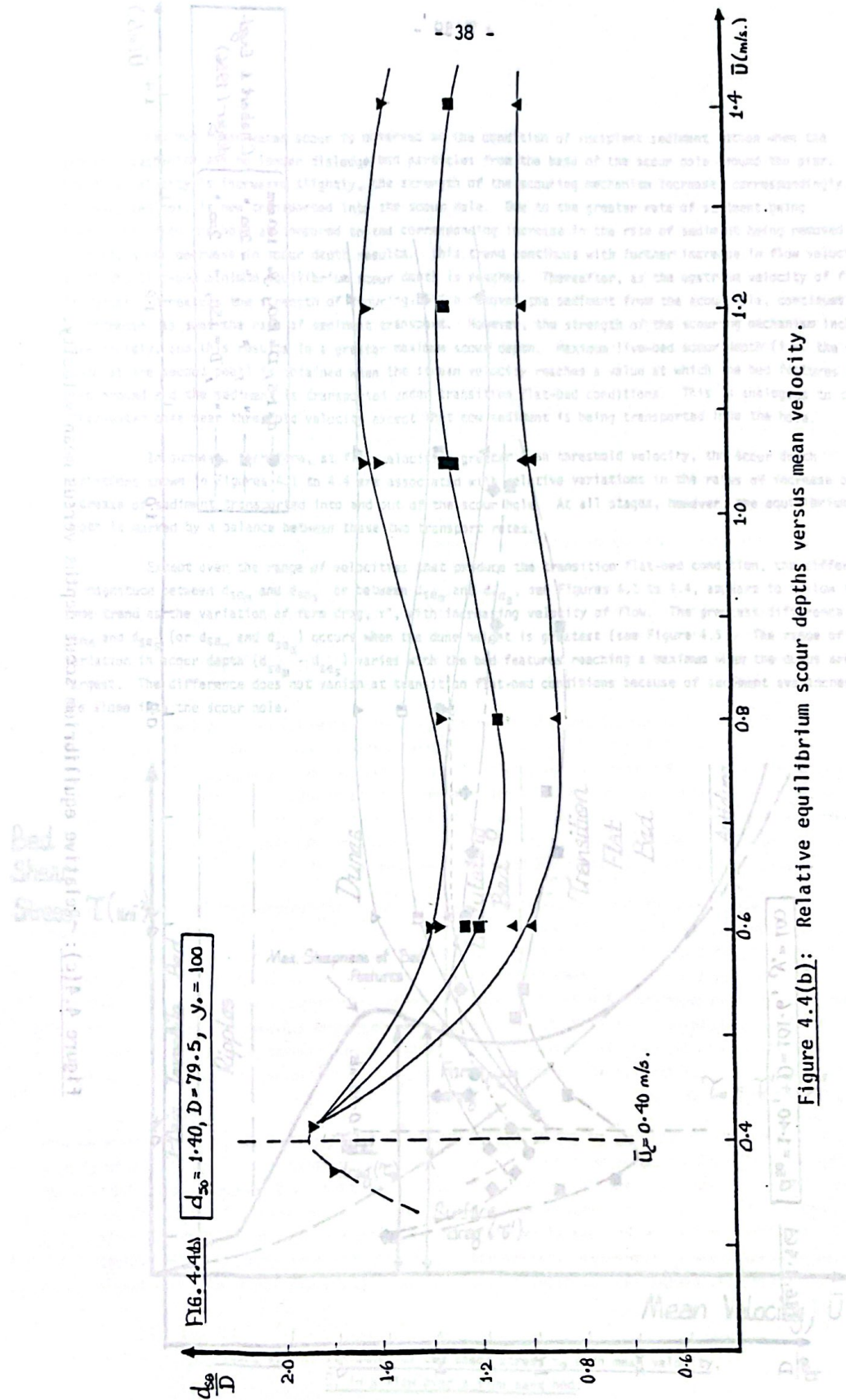


Figure 4.4(a): Relative equilibrium scour depths versus mean velocity.



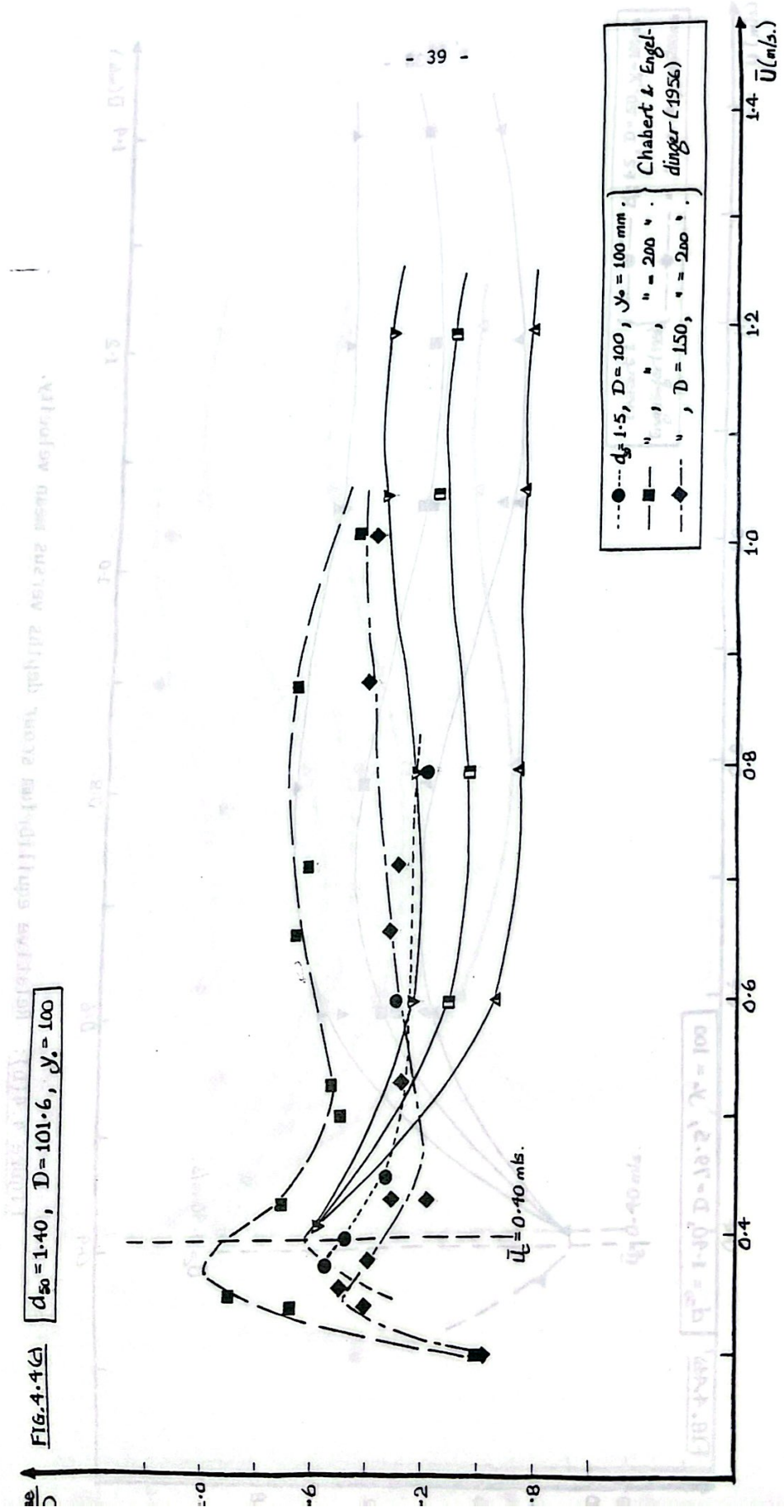


Figure 4.4(c): Relative equilibrium scour depths versus mean velocity.

- 40 -

Maximum clear-water scour is observed at the condition of incipient sediment motion when the scouring mechanism can no longer dislodge bed particles from the base of the scour hole around the pier. If the flow velocity is increased slightly, the strength of the scouring mechanism increases correspondingly. However, sediment is now transported into the scour hole. Due to the greater rate of sediment being transported into the hole as compared to the corresponding increase in the rate of sediment being removed from it, a net decrease in scour depth results. This trend continues with further increase in flow velocity until the live-bed minimum equilibrium scour depth is reached. Thereafter, as the upstream velocity of flow is further increased, the strength of scouring, which removes the sediment from the scour hole, continues to increase as does the rate of sediment transport. However, the strength of the scouring mechanism increases more rapidly, and this results in a greater maximum scour depth. Maximum live-bed scour depth (i.e. the scour depth at the second peak) is obtained when the stream velocity reaches a value at which the bed features have been eroded and the sediment is transported under transition flat-bed conditions. This is analogous to the clear-water case near threshold velocity except that now sediment is being transported into the hole.

In summary, therefore, at flow velocities greater than threshold velocity, the scour depth variations shown in Figures 4.1 to 4.4 are associated with relative variations in the rates of increase or decrease of sediment transported into and out of the scour hole. At all stages, however, the equilibrium depth is marked by a balance between these two transport rates.

Except over the range of velocities that produce the transition flat-bed condition, the difference in magnitude between d_{sem} and d_{ses} or between d_{sem} and d_{sea} , see Figures 4.1 to 4.4, appears to follow the same trend as the variation of form drag, τ'' , with increasing velocity of flow. The greatest difference in d_{sem} and d_{ses} (or d_{sem} and d_{sea}) occurs when the dune height is greatest (see Figure 4.5). The range of variation in scour depth ($d_{sem} - d_{ses}$) varies with the bed features reaching a maximum when the dunes are largest. The difference does not vanish at transition flat-bed conditions because of sediment avalanches from the slope into the scour hole.

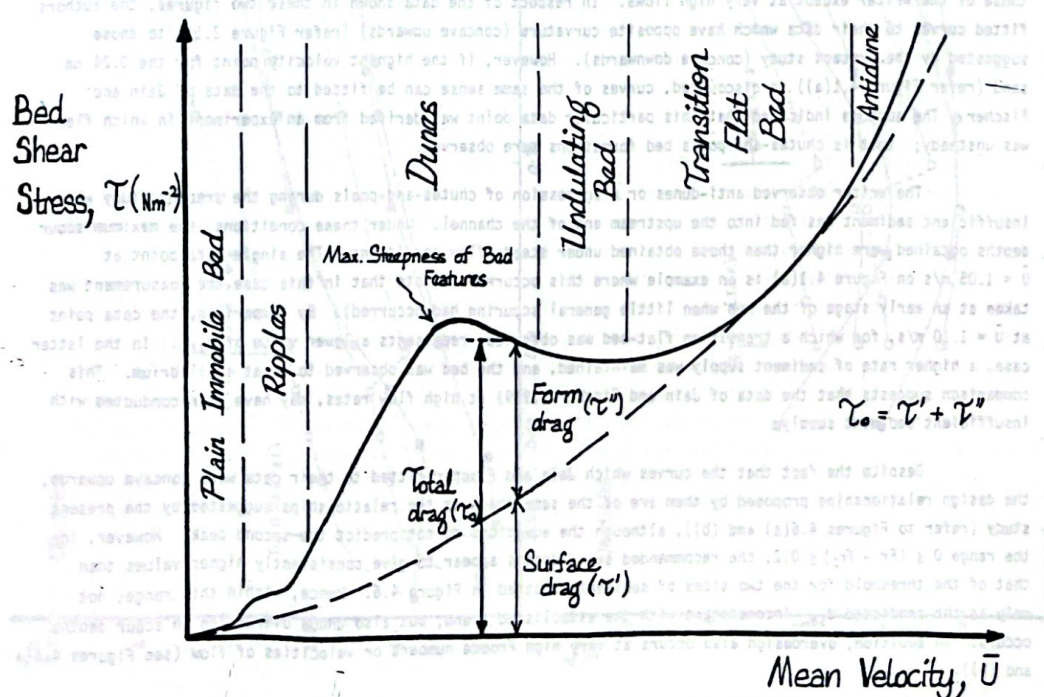


Figure 4.5 : Variation of bed shear stress τ_0 with mean velocity, U , in a flow over a fine sand bed.

- 41 -

Although Jain and Fischer (1979, 1980) compared the maximum scour depths with the maximum scour due to bed-forms alone and concluded that the contribution of the latter to the former in most cases became more significant as the velocity increased, they did not recognise the correlation between the effect of bed-forms on scour depths and the frictional resistance to flow due to the bed-forms. They did, however, measure a smaller scour depth due to bed-forms alone for the run (using 0.25 mm sediment) with a higher flow than the previous one when the bed condition was flat. In addition, they measured an increasing scour depth due to bed-form alone for both the 1.5 mm and 2.5 mm sediments with increasing velocity when the bed consisted of dunes. These observations agree with those made from this study. Jain and Fischer further stated that it is neither possible, nor necessary, to separate the component due to bed-forms and that due to the pier since the total or maximum scour depth, d_{se_m} , is required in the design of a bridge.

Observations suggest that the second peak in the $\frac{d_{se}}{D}$ versus \bar{U} curve occurs around the range of velocities which produce the transition flat-bed conditions. Accordingly, the occurrence of the peak may be partly explained by the fact that at the transition flat-bed the form drag vanishes (see Figure 4.5) so that more of the flow energy is available for scouring. Beyond the flat-bed condition, anti-dunes and chutes-and-pools formations, together with large energy losses due to surface waves, lead to a decrease in maximum scour depth with increase in \bar{U} .

The trend in the $\frac{d_{se}}{D}$ versus \bar{U} curves (Figures 4.1 to 4.4) which shows a reduction in the scour depths at velocities slightly higher than that of threshold velocity agrees with the findings of previous investigators, namely Chabert and Engeldinger (1956), Laursen et al. (1956), Shen et al. (1966), Nicollet (1971), Jain and Fischer (1979) and others, although the results of Hancu (1971) show the scour depth remaining constant at velocities greater than threshold. Several investigators have indicated an increase in scour depth with further increase in \bar{U} without a physical explanation or the limits of the increase; a broad outline of the physical behaviour of scour with increasing velocity was given by Raudkivi (1982).

Figures 4.1(a) and (c) show that the data of Jain and Fischer (1979) correspond very closely to those of the writer except at very high flows. In respect of the data shown in these two figures, the authors fitted curves to their data which have opposite curvature (concave upwards) (refer Figure 2.16) to those suggested by the present study (concave downwards). However, if the highest velocity point for the 0.24 mm sand (refer Figure 4.1(a)) is discounted, curves of the same sense can be fitted to the data of Jain and Fischer. The authors indicated that this particular data point was derived from an experiment in which flow was unsteady; that is chutes-and-pools bed formations were observed.

The writer observed anti-dunes or a succession of chutes-and-pools during the present study when insufficient sediment was fed into the upstream end of the channel. Under these conditions, the maximum scour depths obtained were higher than those obtained under steady flow conditions. The single data point at $\bar{U} = 1.05$ m/s on Figure 4.1(a) is an example where this occurred. (Note that in this case the measurement was taken at an early stage of the run when little general scouring had occurred). By comparison, the data point at $\bar{U} = 1.10$ m/s, for which a transition flat-bed was observed, represents a lower value of d_{se_m} . In the latter case, a higher rate of sediment supply was maintained, and the bed was observed to be at equilibrium. This comparison suggests that the data of Jain and Fischer (1979) at high flow rates, may have been conducted with insufficient sediment supply.

Despite the fact that the curves which Jain and Fischer fitted to their data were concave upwards, the design relationships proposed by them are of the same shape as the relationships suggested by the present study (refer to Figures 4.6(a) and (b)), although the equations do not predict the second peak. However, in the range $0 \leq (Fr - Fr_c) \leq 0.2$, the recommended scour depths appear to give consistently higher values than that of the threshold for the two sizes of sediments plotted in Figure 4.6. Hence, within this range, not only is the predicted d_{se_m} inconsistent with the established trend, but also undue overdesign in scour depths occurs. In addition, overdesign also occurs at very high Froude numbers or velocities of flow (see Figures 4.6(a) and (b)).

- 42 -

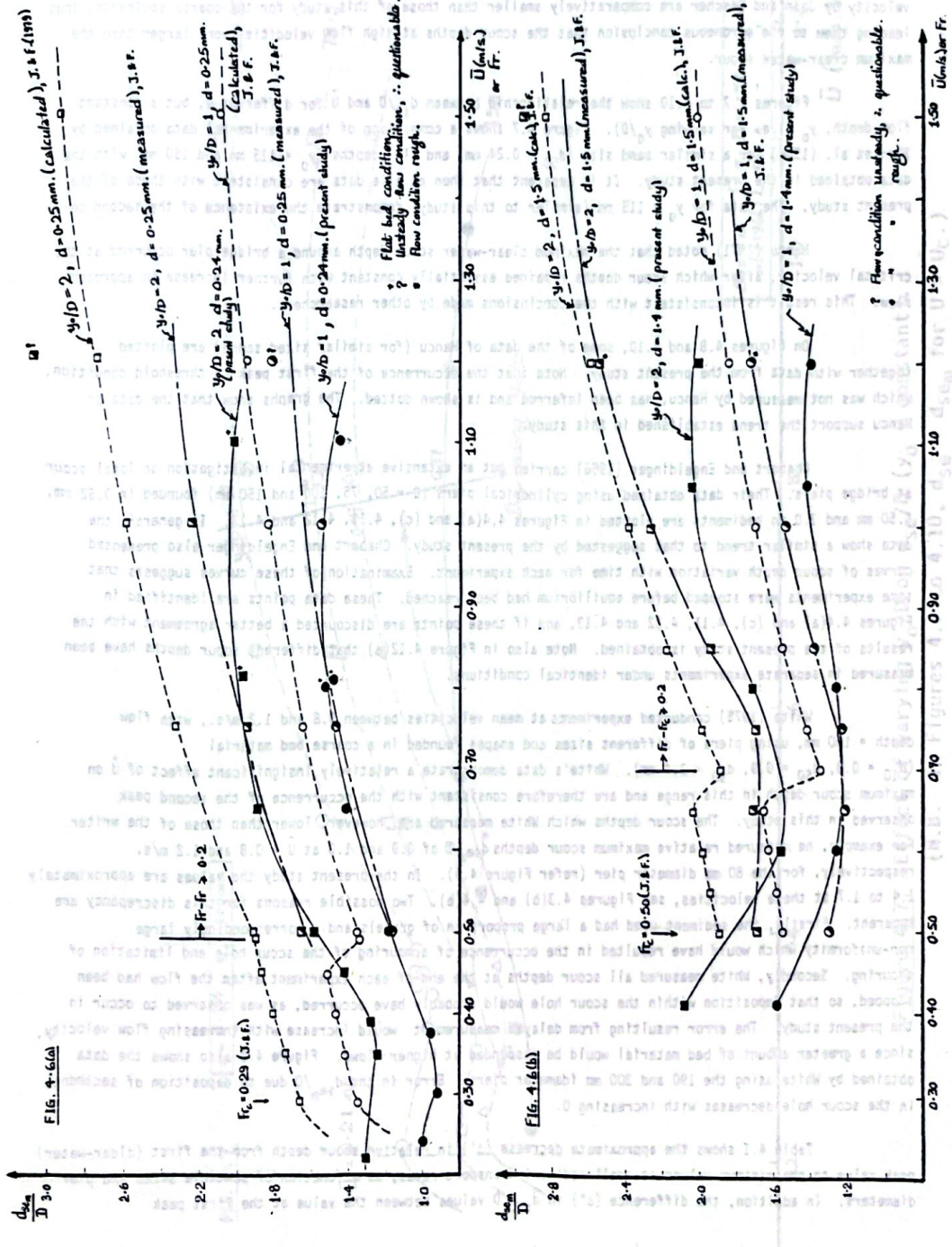


Figure 4.6: Comparison of data of present study with experimental and calculated data of Jain and Fischer (1980).

- 43 -

For the 2.50 mm sediment used in their study, Jain and Fischer observed smaller scour depths at threshold condition (i.e. at $\bar{U} = 0.62 \text{ m/s}$) than at lower flow velocity ($\bar{U} = 0.50 \text{ m/s}$). The trend of increasing scour depth with increasing flow velocity in the clear-water scour regime has been well documented. It is therefore likely that the data of Jain and Fischer at threshold velocity are incorrect, possibly because equilibrium had not been reached. It is probably for this reason that the scour depths obtained at threshold velocity by Jain and Fischer are comparatively smaller than those of this study for the coarse sediments, thus leading them to the erroneous conclusion that the scour depths at high flow velocities were larger than the maximum clear-water scour.

Figures 4.7 to 4.10 show the relationship between d_{se}/D and \bar{U} for different D , but a constant flow depth, y_0 (i.e. for varying y_0/D). Figure 4.7 shows a comparison of the experimental data obtained by Shen et al. (1966) for a similar sand size ($d_{50} = 0.24 \text{ mm}$) and flow depths ($y_0 = 115 \text{ mm}$ and 150 mm) with the data obtained in the present study. It is apparent that Shen et alia data are consistent with those of the present study. The data for $y_0 = 115 \text{ mm}$ (similar to this study) demonstrate the existence of the second peak.

Hancu (1971) noted that the maximum clear-water scour depth around a bridge pier occurred at the critical velocity, after which scour depths remained essentially constant with further increase in approach flow. This result is inconsistent with the conclusions made by other researchers.

On Figures 4.8 and 4.10, some of the data of Hancu (for similar sized sands) are plotted together with data from the present study. Note that the occurrence of the first peak at threshold condition, which was not measured by Hancu, has been inferred and is shown dotted. The graphs show that the data of Hancu support the trend established in this study.

Chabert and Engeldinger (1956) carried out an extensive experimental investigation on local scour at bridge piers. Their data obtained using cylindrical piers ($D = 50, 75, 100$ and 150 mm) founded in 0.52 mm , 1.50 mm and 3.0 mm sediments are plotted in Figures 4.4(a) and (c), 4.11, 4.12 and 4.13. In general, the data show a similar trend to that suggested by the present study. Chabert and Engeldinger also presented curves of scour depth variation with time for each experiment. Examination of these curves suggests that some experiments were stopped before equilibrium had been reached. These data points are identified in Figures 4.4(a) and (c), 4.11, 4.12 and 4.13, and if these points are discounted a better agreement with the results of the present study is obtained. Note also in Figure 4.12(a) that different scour depths have been measured in separate experiments under identical conditions.

White (1975) conducted experiments at mean velocities between 0.8 and 1.2 m/s , with flow depth = 100 mm , using piers of different sizes and shapes founded in a coarse bed material ($d_{10} = 0.3$, $d_{50} = 0.9$, $d_{90} = 3.4 \text{ mm}$). White's data demonstrate a relatively insignificant effect of \bar{U} on maximum scour depth in this range and are therefore consistent with the occurrence of the second peak observed in this study. The scour depths which White measured are, however, lower than those of the writer. For example, he measured relative maximum scour depths d_{sem}/D of 0.9 and 1.0 at $\bar{U} = 0.8$ and 1.2 m/s , respectively, for the 80 mm diameter pier (refer Figure 4.9). In the present study the values are approximately 1.4 to 1.7 at these velocities, see Figures 4.3(b) and 4.4(b). Two possible reasons for this discrepancy are apparent. Firstly, the sediment used had a large proportion of gravels and a correspondingly large non-uniformity which would have resulted in the occurrence of armouring of the scour hole and limitation of scouring. Secondly, White measured all scour depths at the end of each experiment after the flow had been stopped, so that deposition within the scour hole would probably have occurred, as was observed to occur in the present study. The error resulting from delayed measurement would increase with increasing flow velocity, since a greater amount of bed material would be suspended at higher flows. Figure 4.9 also shows the data obtained by White using the 190 and 300 mm diameter piers. Error in the d_{sem}/D due to deposition of sediments in the scour hole decreases with increasing D .

Table 4.1 shows the approximate decrease (Δ') in relative scour depth from the first (clear-water) peak value to the minimum values at small sediment transport rates, as a function of particle sizes and pier diameters. In addition, the difference (Δ'') in d_{sem}/D values between the value at the first peak and (2).

- 44 -

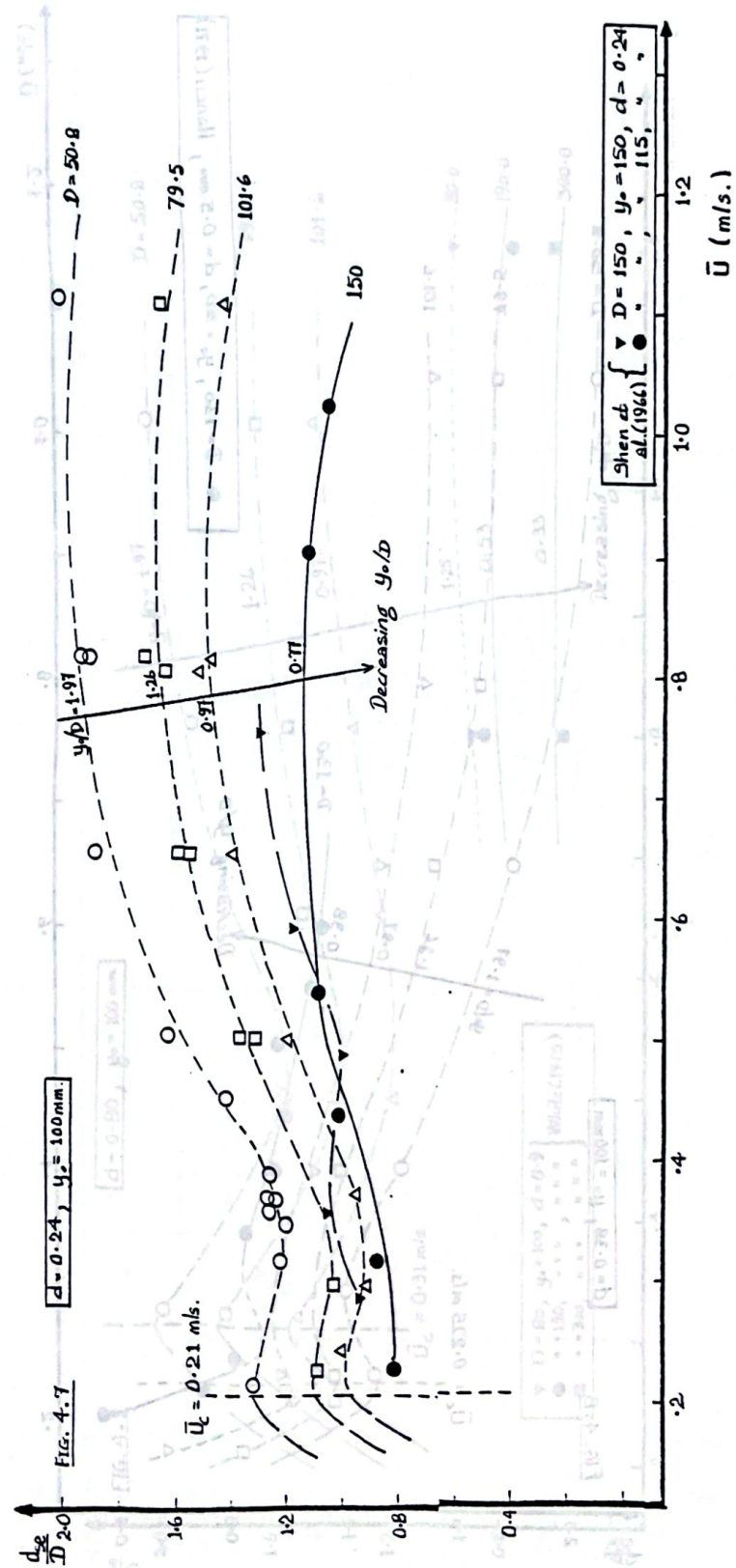
Figure 4.7: Effect of varying y_0/D on d_{se}/D ($y_0 = \text{constant}$)

Figure 4.7: Effect of varying y_0/D on d_{se}/D ($y_0 \approx \text{constant}$).
 (N.B. In Figures 4.7 to 4.10, $d_{se} \equiv d_{seIII}$ for $\bar{U} > U_c$.)

- 45 -

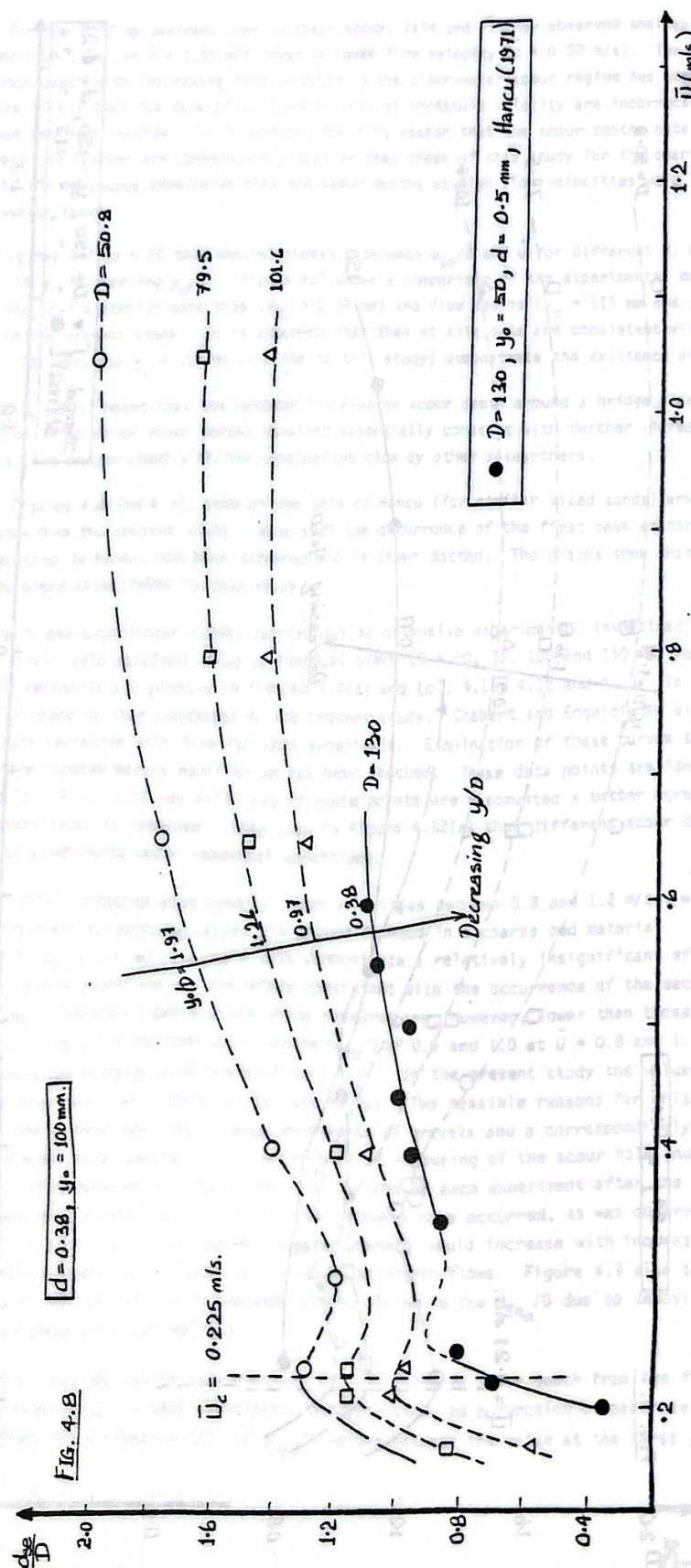


Figure 4.8: Effect of varying y_0/D on d_{se}/D ($y_0 = \text{constant}$).

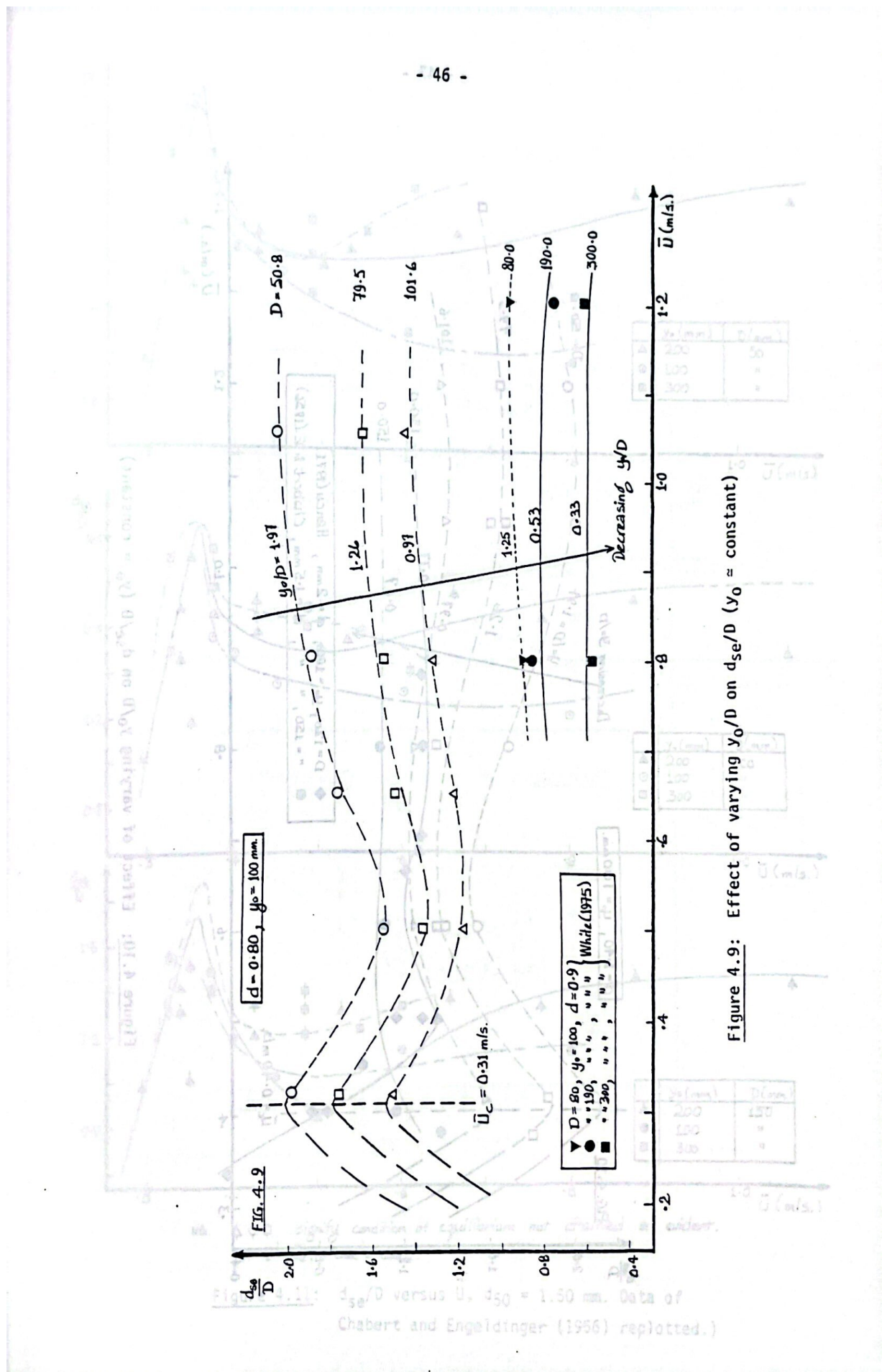


Figure 4.9: Effect of varying y_0/D on d_{se}/D ($y_0 \approx \text{constant}$)

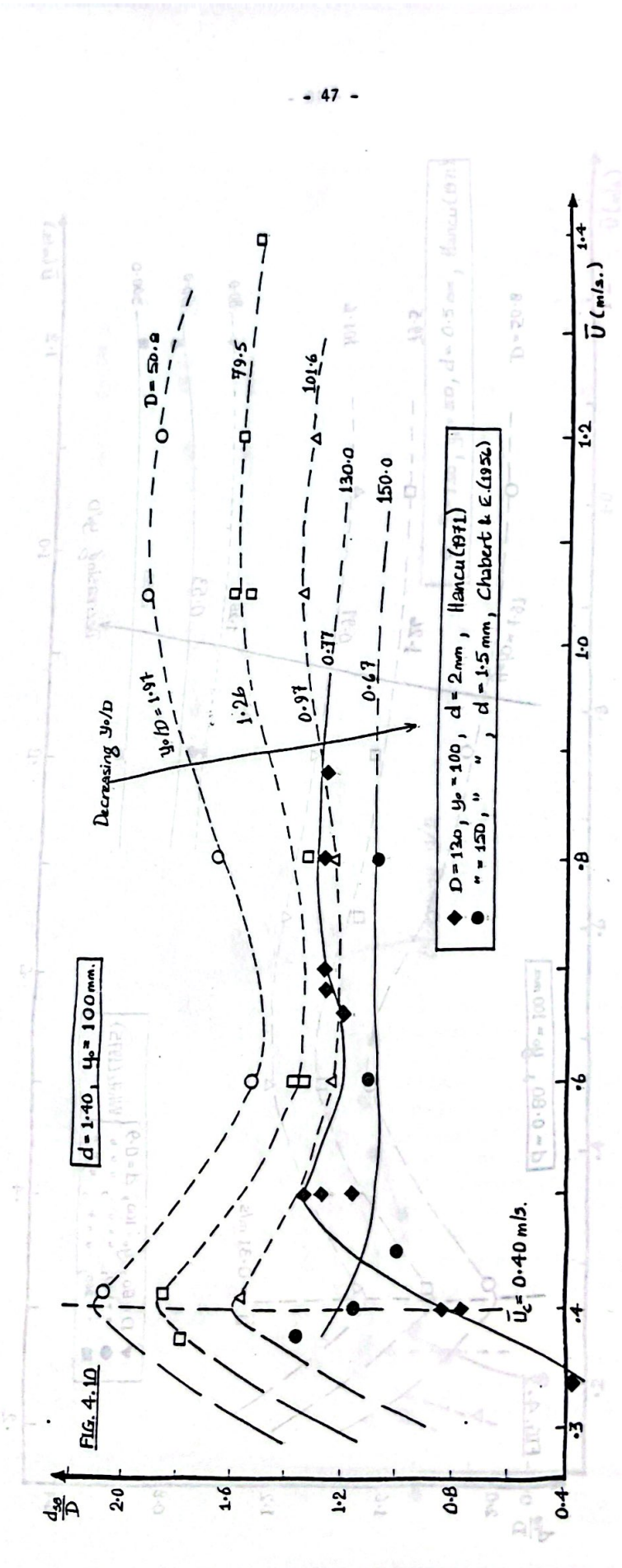
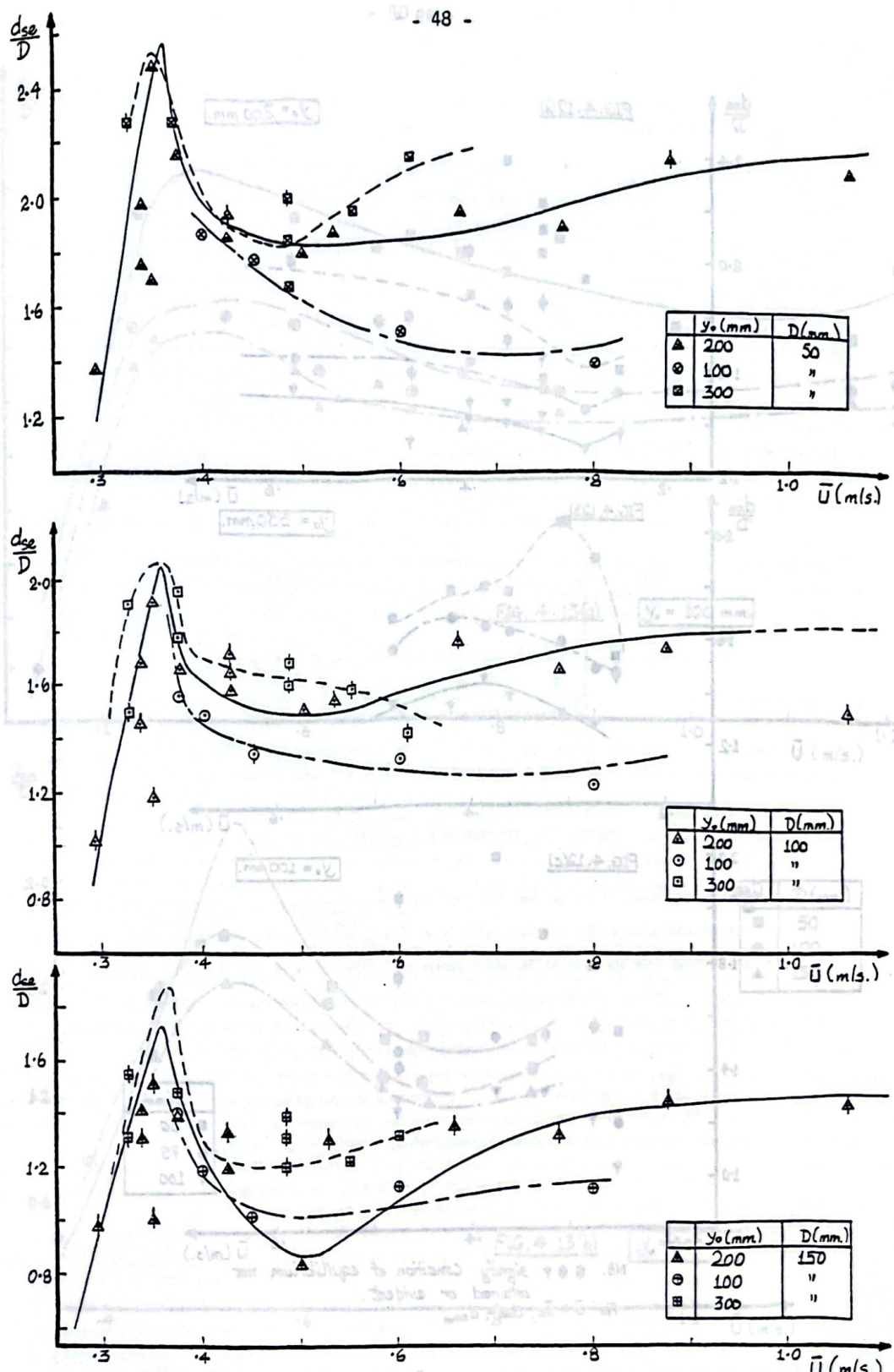


Figure 4.10: Effect of varying y_0/D on d_{se}/D ($y_0 \approx \text{constant}$)



N.B. $\Delta \circ \square$ signify condition of equilibrium not attained or evident.

For $\bar{U} > \bar{U}_c$, $d_{se} \approx d_{se,m}$.

(. betw. \bar{U}_c & \bar{U}_{se} replotting on \bar{U} vs d_{se})

Figure 4.11: d_{se}/D versus \bar{U} , $d_{50} = 1.50 \text{ mm}$. Data of Chabert and Engeldinger (1956) replotted.)

- 49 -

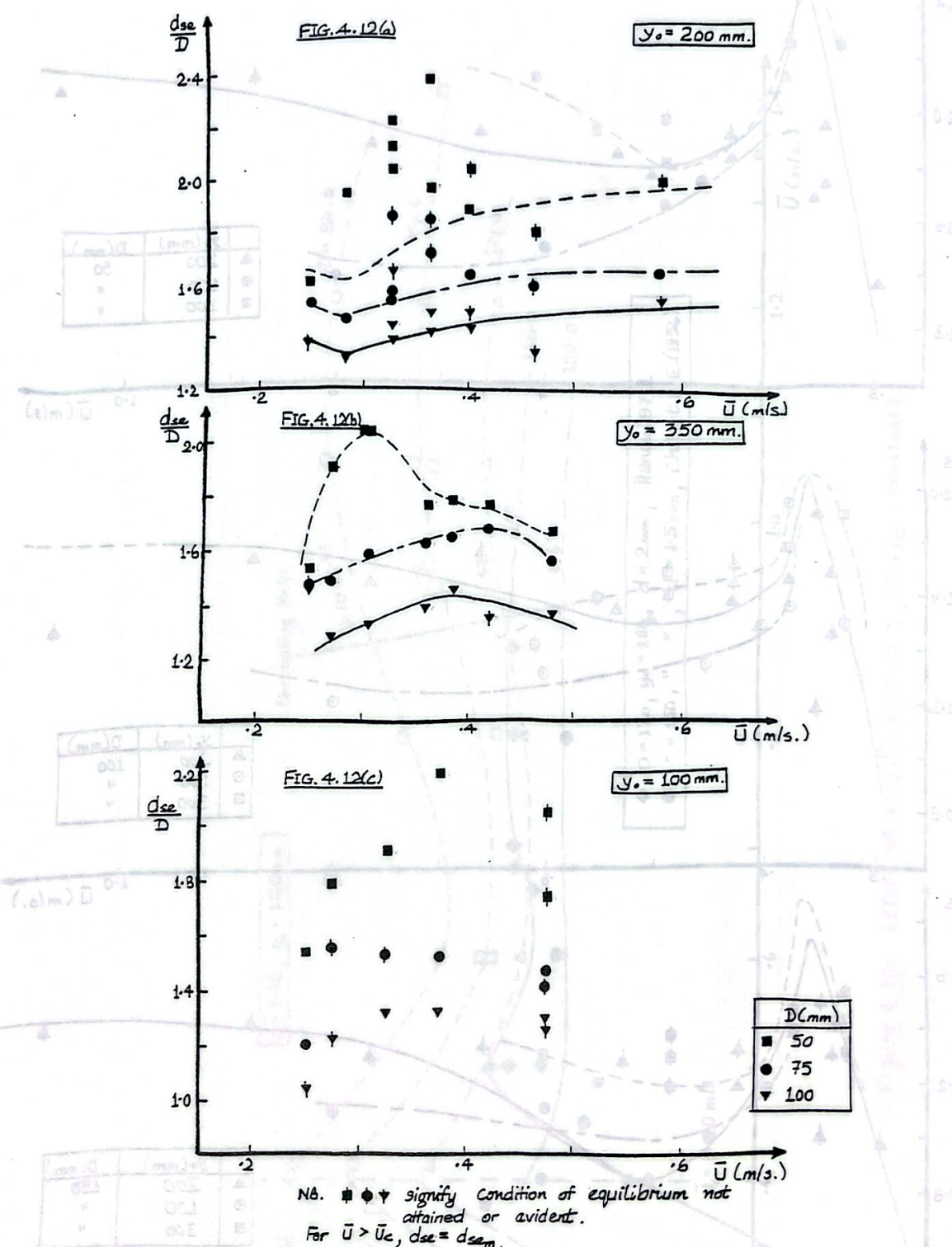


Figure 4.12: d_{se}/D versus \bar{U} , $d_{50} = 0.52 \text{ mm}$. (Data Chabert and Engeldinger (1956) replotted.)

- 50 -

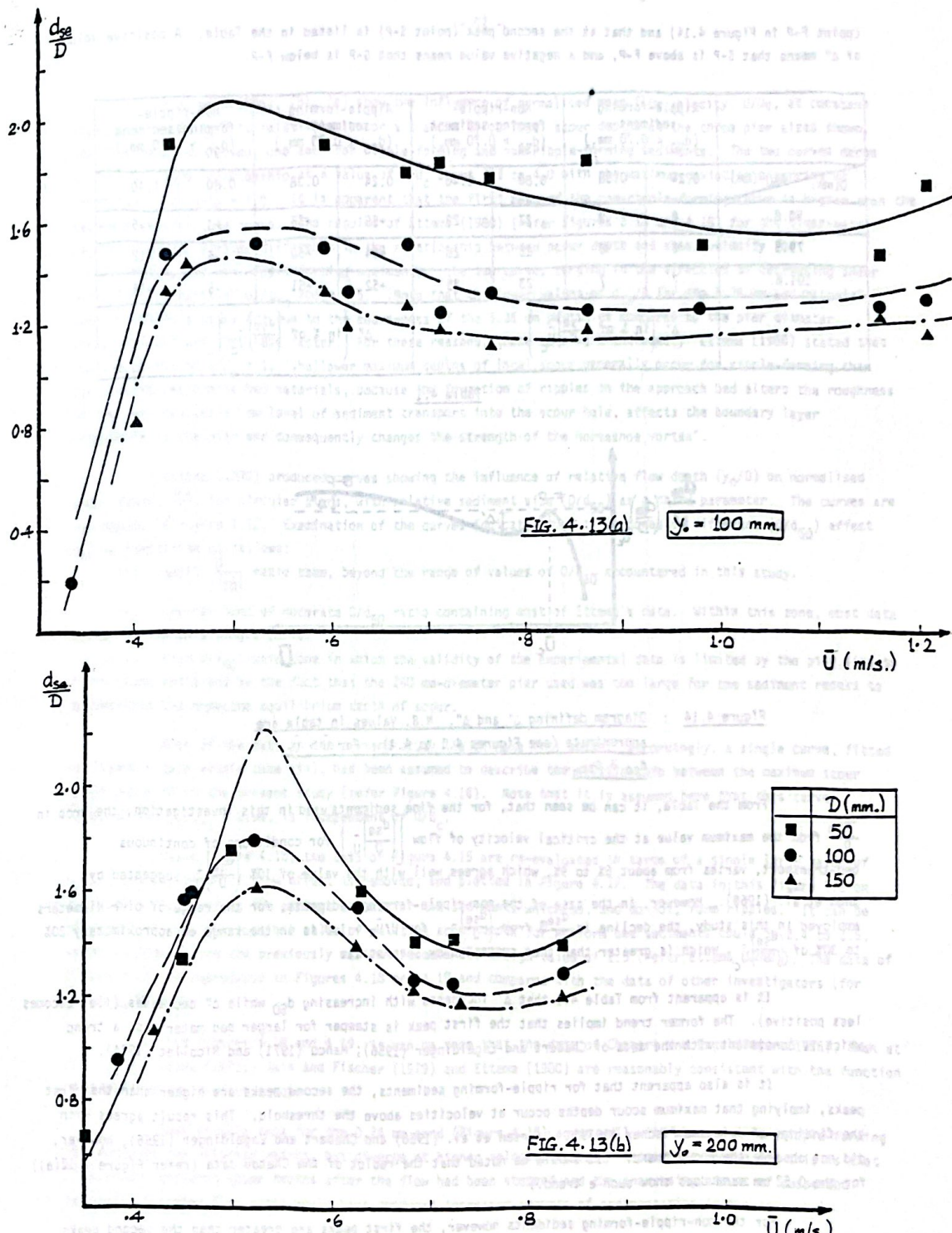


Figure 4.13: d_{se}/D versus \bar{U} , $d_{50} = 3.0 \text{ mm}$ (data of Chabert and Engeldinger (1956) replotted.) N.B. $d_{se} \equiv d_{se_m}$ for $\bar{U} > \bar{U}_c$.

- 51 -

(point F-P in Figure 4.14) and that at the second peak (point S-P) is listed in the Table. A positive value of Δ'' means that S-P is above F-P, and a negative value means that S-P is below F-P.

	Ripple-forming sediment ($d_{50} < 0.70$ mm.)	Non-ripple-forming sediment ($d_{50} > 0.70$ mm.)	Ripple-forming sediment ($d_{50} < 0.70$ mm.)	Non-ripple-forming sediment ($d_{50} > 0.70$ mm.)					
D (mm)	d_{50} (mm)	0.24	0.38	0.80	1.40	0.24	0.38	0.80	1.40
50.8	8	9	27	29	+55	+55	+3	-5	
79.5	6	8	25	28	+54	+50	-6	-12	
101.6	7	7	23	25	+52	+51	-6	-14	
		Δ' (in % of $\left(\frac{d_{se}}{D}\right)\bar{U}_c$)			Δ'' (in % of $\left(\frac{d_{se}}{D}\right)\bar{U}_c$)				

Table 4.1

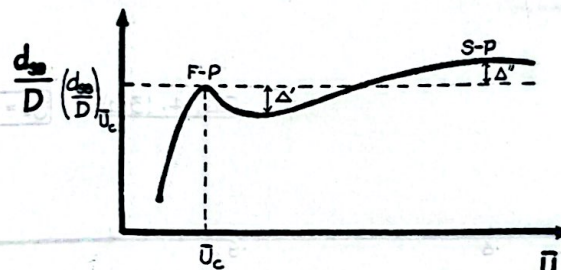


Figure 4.14 : Diagram defining Δ' and Δ'' . N.B. Values in table are approximate (see Figures 4.1 to 4.4). For $\bar{U} > \bar{U}_c$, $d_{se} \equiv d_{sem}$.

From the Table, it can be seen that, for the fine sediments used in this investigation, the drop in $\frac{d_{sem}}{D}$ from the maximum value at the critical velocity of flow $\left(\frac{d_{se}}{D}\right)\bar{U}_c$ for conditions of continuous bed-transport, varies from about 6% to 9%, which agrees well with the value of 10% $\left(\frac{d_{se}}{D}\right)\bar{U}_c$ suggested by Shen et al. (1969). However, in the case of the non-ripple-forming sediments, for the range of pier diameters employed in this study, the decline in $\frac{d_{sem}}{D}$ from $\left(\frac{d_{se}}{D}\right)\bar{U}_c$, for $\bar{U}/\bar{U}_c > 1.0$ is in the range of approximately 20% to 30% of $\left(\frac{d_{se}}{D}\right)\bar{U}_c$, which is greater than that suggested by Shen et al.

It is apparent from Table 4.1 that Δ' increases with increasing d_{50} while Δ'' decreases (i.e. becomes less positive). The former trend implies that the first peak is steeper for larger bed materials, a trend which is consistent with the data of Chabert and Engeldinger (1956), Hancu (1971) and Nicolle (1971).

It is also apparent that for ripple-forming sediments, the second peaks are higher than the first peaks, implying that maximum scour depths occur at velocities above the threshold. This result agrees with the findings of Jain and Fischer (1979). Laursen et al. (1956) and Chabert and Engeldinger (1956), however, did not observe the above trend. (It should be noted that the replot of the Chatou data (refer Figure 4.12(a)) for the 0.52 mm sand does show such a trend.)

For the non-ripple-forming sediments however, the first peaks are greater than the second peaks and maximum scour depths occur at the threshold condition. This result is inconsistent with the conclusion of Jain and Fischer (1979) (see section 2.1.4 and previous discussion in this section.)

- 52 -

Figures 4.15(a), (b), (c) show the influence of normalised mean flow velocity, \bar{U}/\bar{U}_c , at constant flow depth (i.e. y_0/D is relatively low or > 1 and < 2) on local scour depths at the three pier sizes shown. The data form two curves, one each for ripple-forming and non-ripple-forming sediments. The two curves merge to form a single relationship at a value of \bar{U}/\bar{U}_c about 3.5 to 4.0 with the maximum deviation occurring at threshold, i.e. $\bar{U}/\bar{U}_c = 1.0$. It is apparent that the first peak of the non-ripple-forming curve is higher than the second peak of either curve. The results of Ettema (1980) (refer Figures 2.13 and 4.18) for the clear-water regime, showed a similar difference in the relationship between scour depth and shear velocity for ripple-forming and non-ripple-forming sediments; the two curves merging in the direction of decreasing shear velocity at a value of u_s/u_{*c} about 0.5. (Note that the lower values of d_{se}/D for the 5.35 mm bed material used in Ettema's study are due to the coarseness of the 5.35 mm particles compared to the pier diameter ($D/d_{50} = 9.50$) and the shape factor. For these reasons, these data were excluded.) Ettema (1980) stated that for the condition $\bar{U}/\bar{U}_c = 1$, "shallower maximum depths of local scour generally occur for ripple-forming than for non-ripple-forming bed materials, because the formation of ripples on the approach bed alters the roughness of the bed, creates a low level of sediment transport into the scour hole, affects the boundary layer separation at the pier and consequently changes the strength of the horseshoe vortex".

Ettema (1980) produced curves showing the influence of relative flow depth (y_0/D) on normalised scour depth ($\frac{d_{se}}{D}$) for circular piers, with relative sediment size (D/d_{50}) as a third parameter. The curves are reproduced in Figure 2.12. Examination of the curves indicates that three zones of different (D/d_{50}) effect may be identified as follows:

- (i) Small $\left[\frac{D}{d_{50}}\right]$ ratio zone, beyond the range of values of D/d_{50} encountered in this study.
- (ii) Central band of moderate D/d_{50} ratio containing most of Ettema's data. Within this zone, most data appear to lie on a single curve.
- (iii) High D/d_{50} ratio zone in which the validity of the experimental data is limited by the pier size to flume width ratio and by the fact that the 240 mm-diameter pier used was too large for the sediment recess to accommodate the expected equilibrium depth of scour.

Most of the data in the present study lie in zone (ii) above. Accordingly, a single curve, fitted to Ettema's data within zone (ii), has been assumed to describe the relationship between the maximum scour depth and y_0/D in the present study (refer Figure 4.16). Note that it is assumed here that this curve, obtained for $u_s/u_{*c} = 0.90$, is independent of \bar{U}/\bar{U}_c .

Using Figure 4.16, the data of Figure 4.15 are re-evaluated in terms of a single large value of y_0/D , i.e., the depth of flow effect is removed, and plotted in Figure 4.17. The data in this figure lie on two curves representing the average values for the sediments which do, and do not, form ripples. It can be seen that the maximum possible value of relative scour depth for uniform bed sediments could be 2.4 to 2.5, which is higher than the previously maximum recommended design value of 2.3 (refer Ettema (1980)). The data of Figure 4.17 are reproduced in Figures 4.18 and 4.19 and compared with the data of other investigators (for large y_0/D ratios).

From Figures 4.18 and 4.19, it can be seen that the data of Chabert and Engeldinger (1956), Shen et al. (1966), Hancu (1971), Jain and Fischer (1979) and Ettema (1980) are reasonably consistent with the function suggested by the present study.

Shen et alia data for the 0.24 mm sand (Figure 4.18) agree well with the curve for ripple-forming sediments at low velocity ratios, but diverge at higher velocity ratios. A possible reason for this is that Shen et al. measured scour depths after the flow had been stopped and the increasing amount of suspended sediment at higher flow rates would have produced increased amounts of sedimentation in the scour hole.

The data of Jain and Fischer (1979), Figure 4.18, also correspond quite well with the data of this study at low velocity ratios. A possible reason for the discrepancy in scour depths at high flows, as discussed earlier in this section, lies in the unsteady flow conditions which existed in some of Jain and Fischer's experiments. All the data, however, with the exception of the highest velocity point for the 0.24 mm sand, do suggest the same trend as that obtained in the present study.

- 53 -

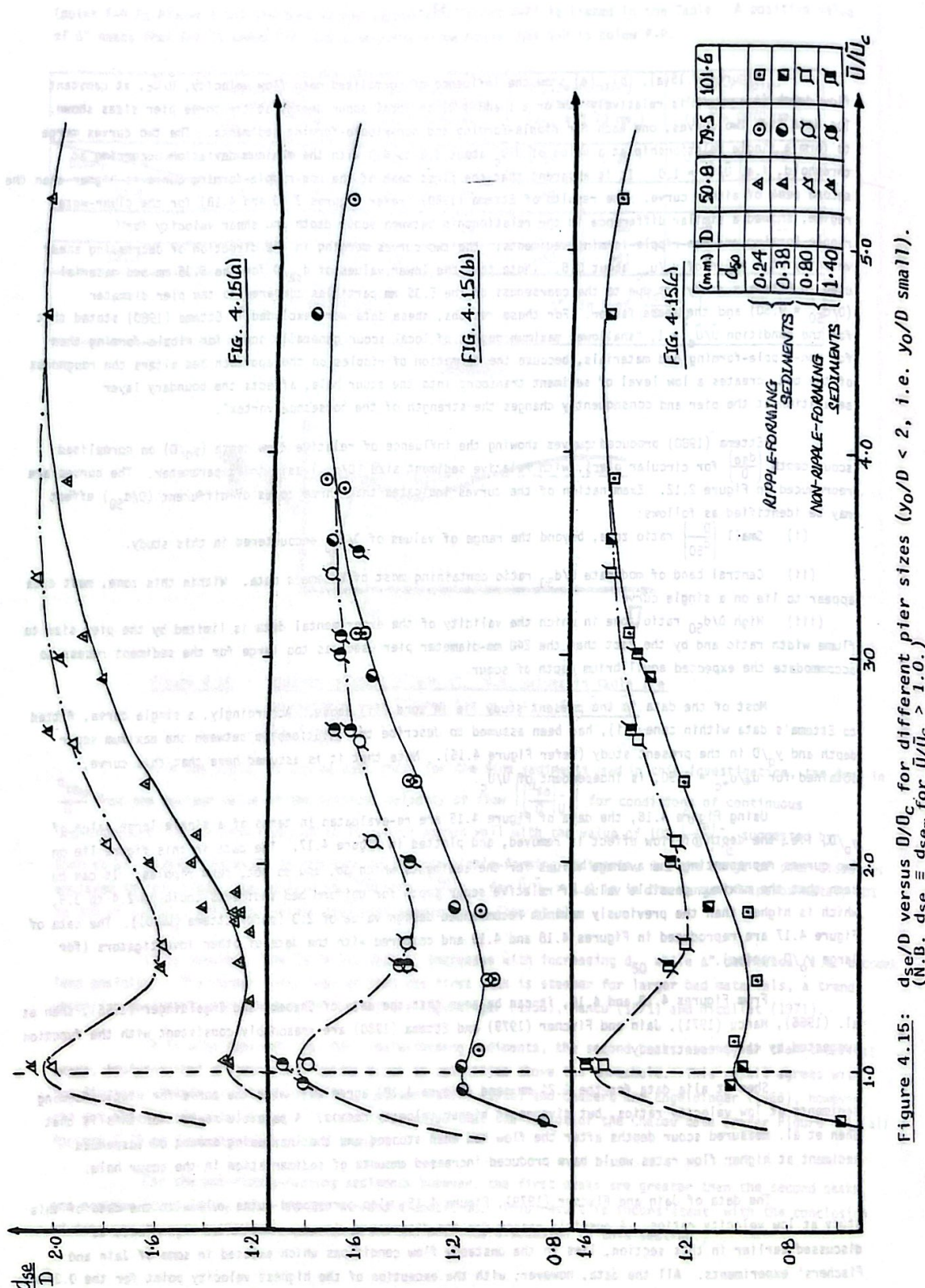


Figure 4.15: d_{se}/D versus D/D_0c for different pier sizes ($y_0/D < 2$, i.e. y_0/D small).
(N.B. $d_{se} \equiv d_{sem}$ for $\bar{U}/\bar{U}_c > 1.0$).

- 54 -

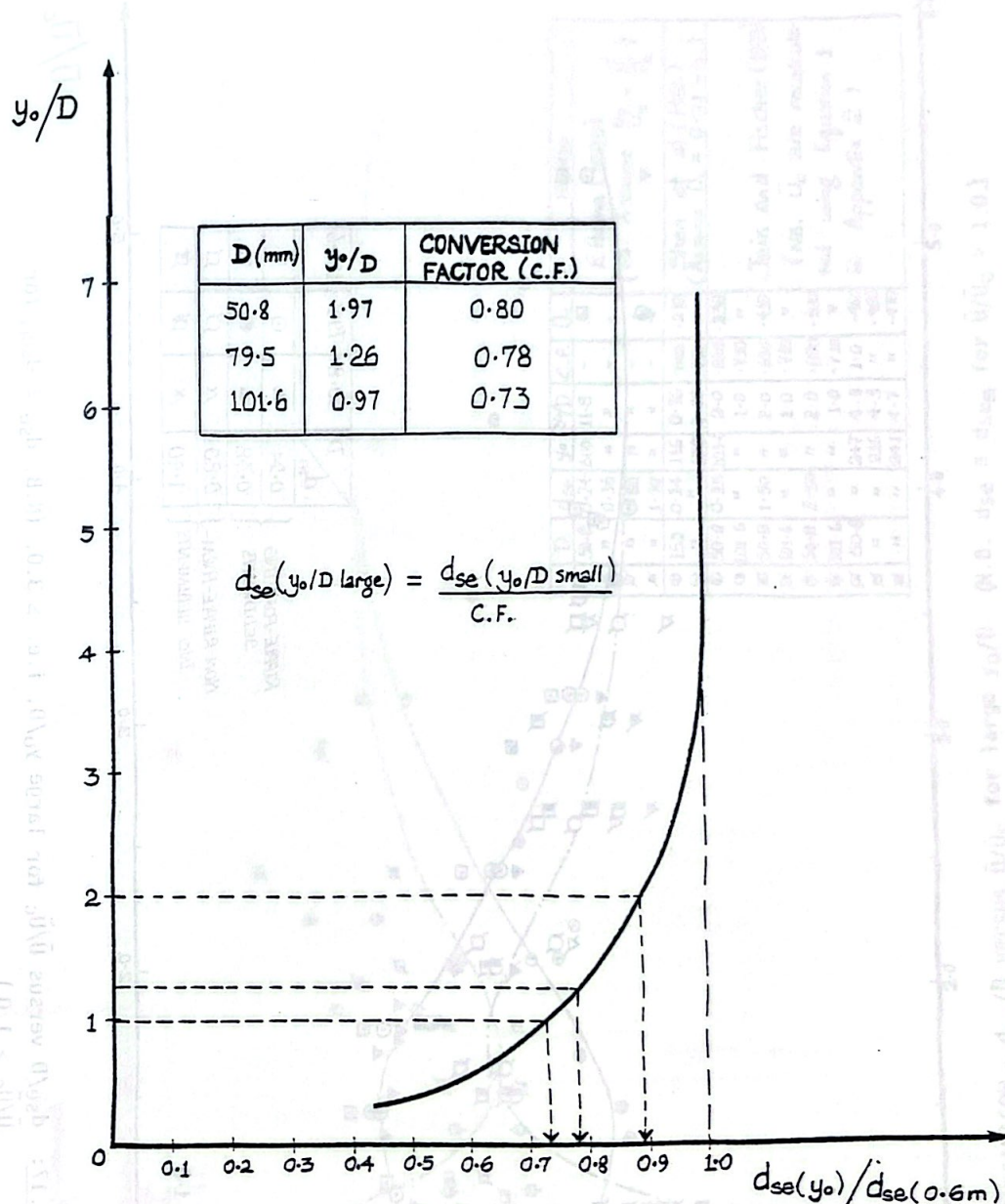


Figure 4.16: Idealised curve of equilibrium scour depth, d_{se}/D versus y_0/D for estimating d_{se} at large y_0/D ratios.

- 55 -

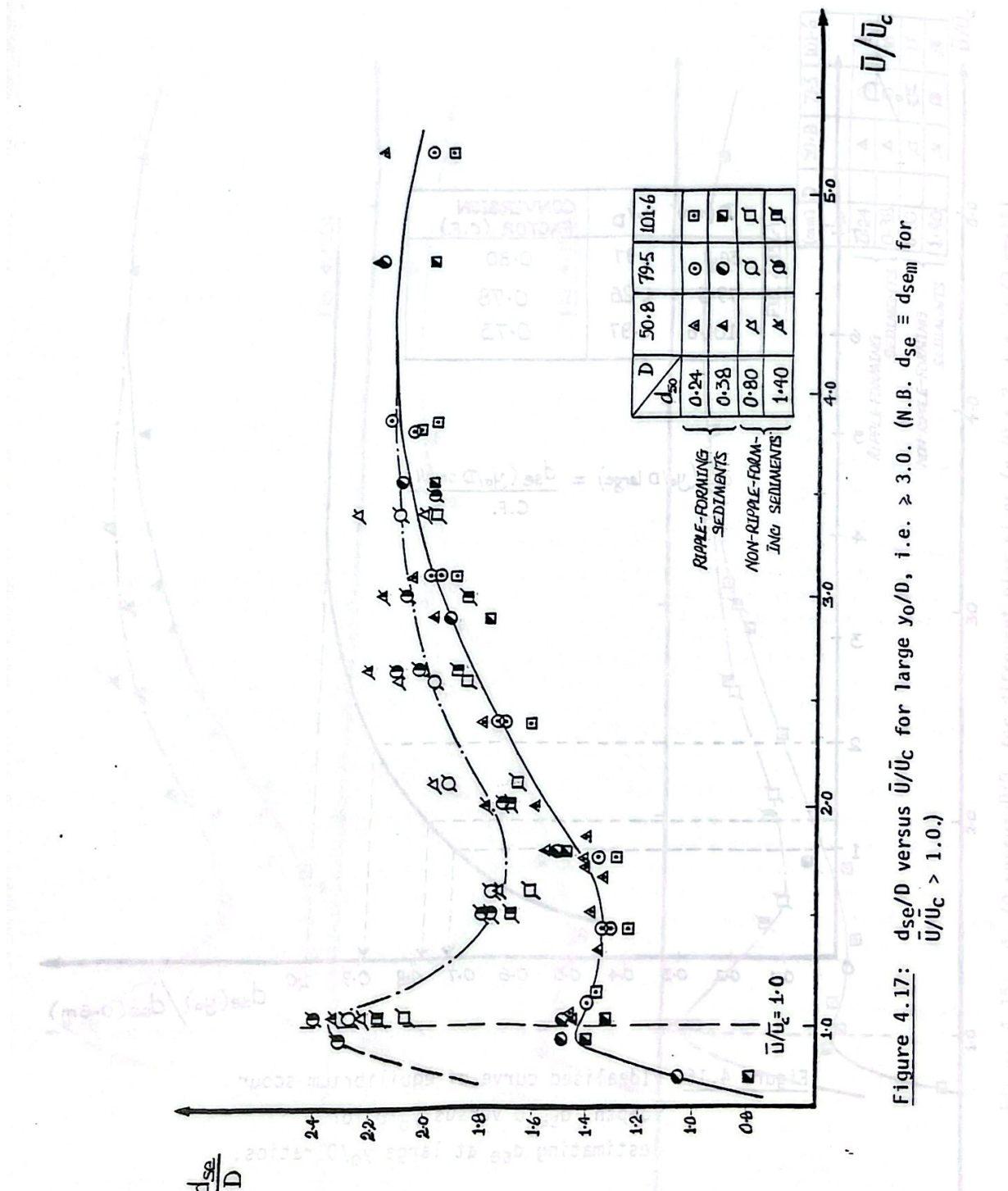


Figure 4.17: d_{se}/D versus U/U_c for large y_0/D , i.e. ≥ 3.0 . (N.B. $d_{se} \equiv d_{sem}$ for $U/U_c > 1.0$.)

- 56 -

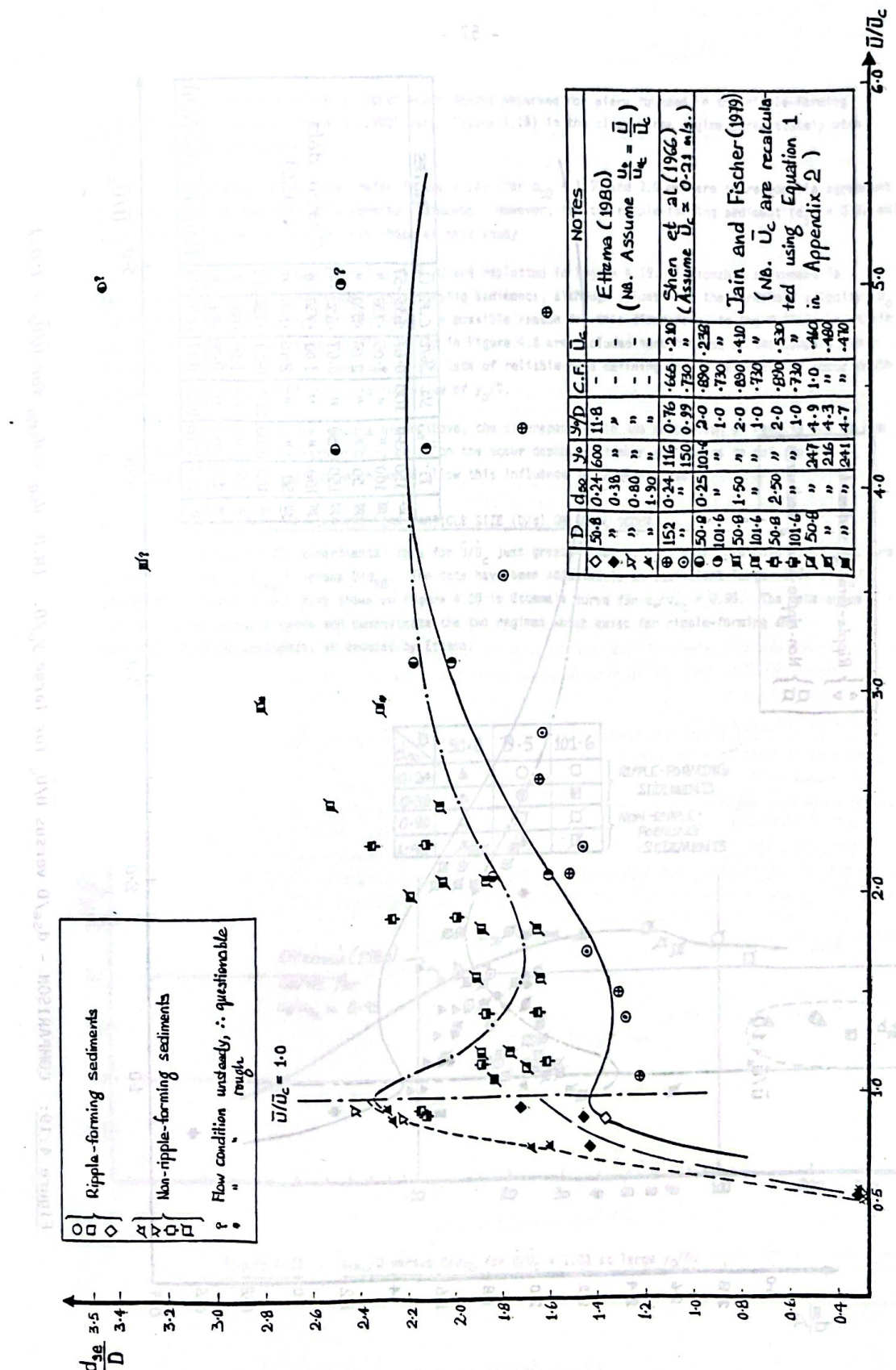


Figure 4.18: COMPARISON - d_{se}/D versus \bar{U}/\bar{U}_c for large y_0/D . (N.B. $d_{se} \equiv d_{sem}$ for $\bar{U}/\bar{U}_c > 1.0$)

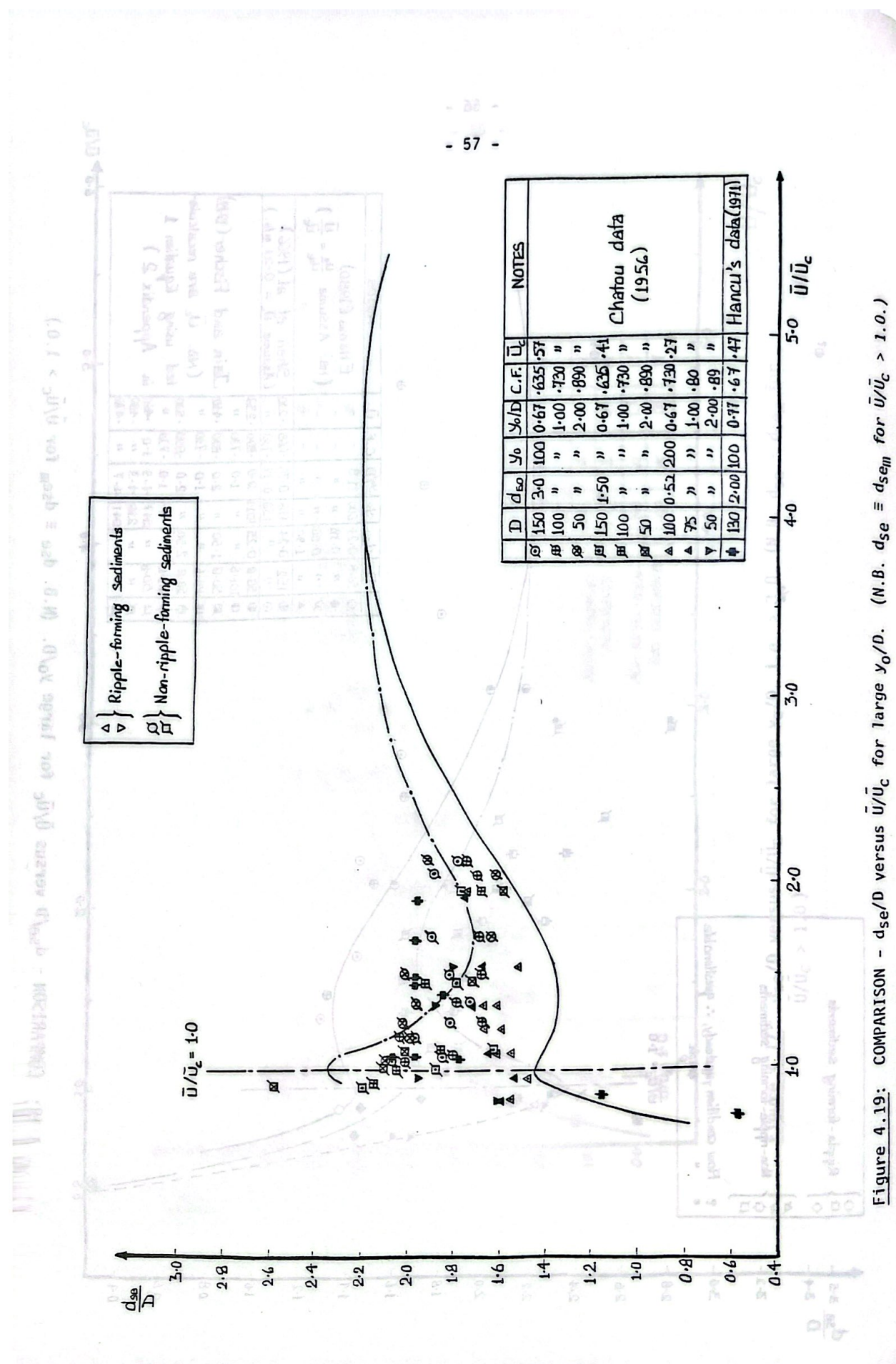


Figure 4.19: COMPARISON - d_{se}/D versus \bar{U}/\bar{U}_c for large y_0/D . (N.B. $d_{se} \equiv d_{seII}$ for $\bar{U}/\bar{U}_c > 1.0$.)

- 58 -

Except for the slightly higher scour depths observed for piers founded in the ripple-forming sediment ($d_{50} = 0.38 \text{ mm}$), Ettema's (1980) data (Figure 4.18) in the clear-water regime agree closely with those of this investigation.

The Chatou (1956) data (refer Figure 4.19) (for $d_{50} = 1.50 \text{ and } 3.0 \text{ mm}$) are in reasonable agreement with the curve for the non-ripple-forming sediments. However, for the ripple-forming sediment ($d_{50} = 0.52 \text{ mm}$), scour depths obtained are higher than those of this study.

Hancu's (1971) data from Figure 4.10 are replotted in Figure 4.19. Reasonable agreement is demonstrated with the curve for non-ripple-forming sediments, although values near the threshold velocity, U_c , are lower than those obtained in this study. A possible reason for this discrepancy is the failure to attain equilibrium. The data of Hancu (1971) plotted in Figure 4.8 are excluded here because of the comparatively low value of y_0/D ($= 0.38$) and because of the lack of reliable data defining the relationship of scour depth versus y_0/D of Ettema (1980) for this low value of y_0/D .

In addition to the reasons given above, the discrepancies in the comparison of results may be due to the influence of the variation of σ_I or σ_g on the scour depth. A number of reports do not contain information on sediment grading which would allow this influence to be determined.

4.4 THE INFLUENCE OF RELATIVE MEAN PARTICLE SIZE (D/d) ON LOCAL SCOUR

In Figure 4.20, experimental data for \bar{U}/\bar{U}_c just greater than 1, i.e. near threshold condition, are plotted in terms of d_{sem}/D versus D/d_{50} . The data have been adjusted to an equivalent large value of y_0/D , according to Figure 4.16. Also shown on Figure 4.20 is Ettema's curve for $u_*^*/u_* = 0.95$. The data agree very well with Ettema's curve and demonstrate the two regimes which exist for ripple-forming and non-ripple-forming sediments, as deduced by Ettema.

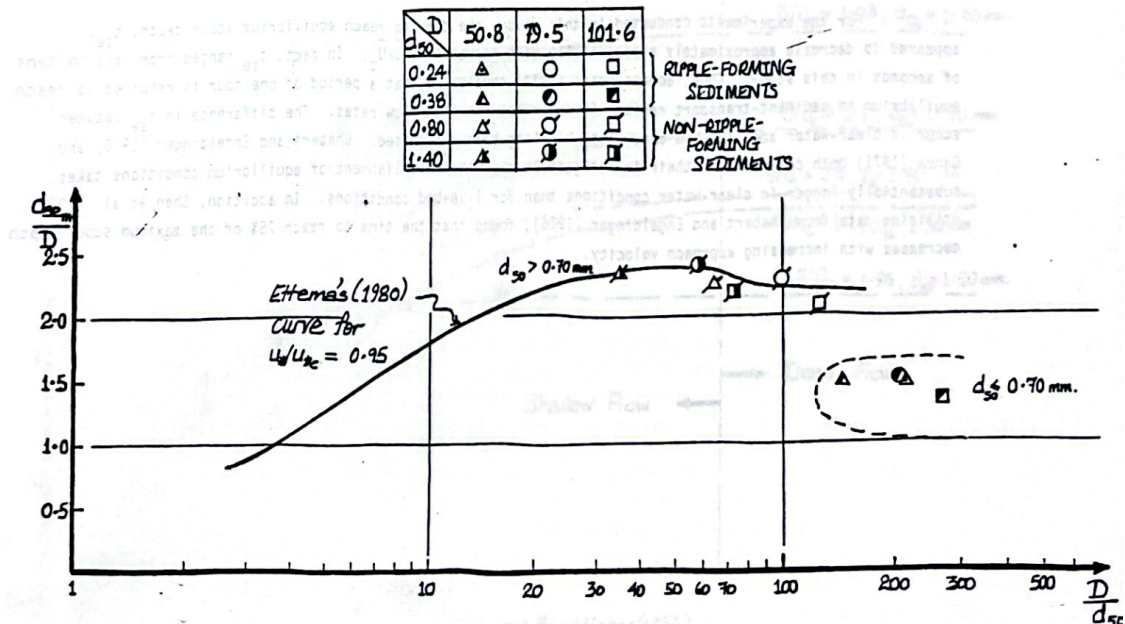


Figure 4.20 : d_{sem}/D versus D/d_{50} for $\bar{U}/\bar{U}_c = 1.03$ at large y_0/D .

- 59 -

A similar result would be obtained at higher values of \bar{U}/\bar{U}_c , although the difference between ripple-forming and non-ripple-forming sediments would decrease with increasing \bar{U}/\bar{U}_c . Figures 4.16 and 4.17 shows that at $\bar{U}/\bar{U}_c \approx 3.5$ to 4.0 no effect of ripple-formation would be apparent in the relationship between $\frac{d_{se}}{D}$ and $\frac{D}{d_{50}}$.

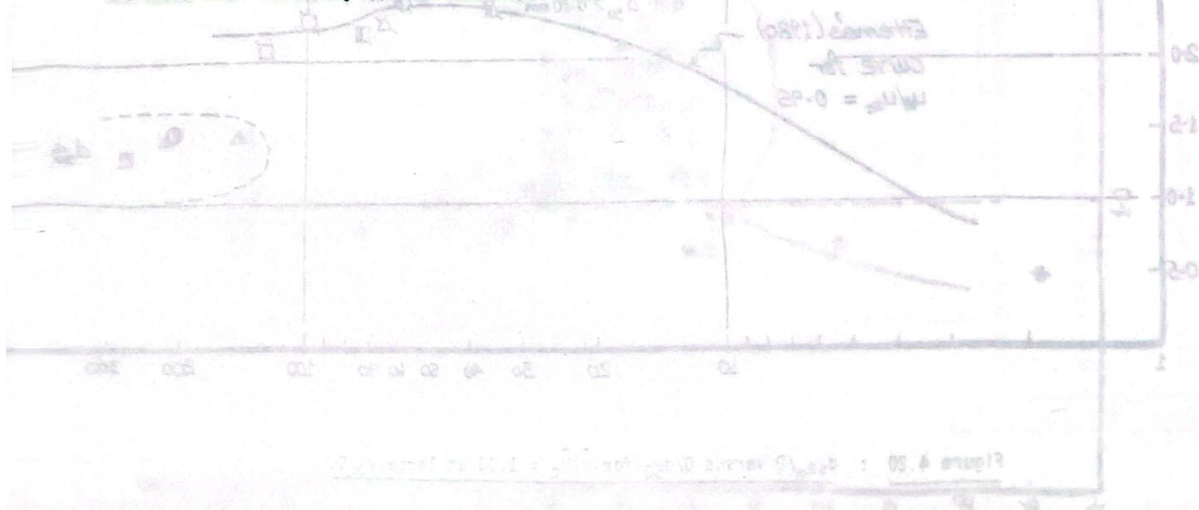
4.5 THE INFLUENCE OF RELATIVE FLOW DEPTH ON LOCAL SCOUR

Figures 4.21(a) and (b) show typical relationships of d_{se}/D versus y_0/D (with $y_0 = \text{constant}$) for the 0.24 mm (ripple-forming) and 1.40 mm (non-ripple-forming) sediments. The two curves in each figure represent the variation of d_{se}/D with y_0/D at constant \bar{U}/\bar{U}_c ratios. Curves of similar trend could also be drawn for other \bar{U}/\bar{U}_c ratios with the influence of \bar{U}/\bar{U}_c following the trend in the variation in $\frac{d_{se}}{D}$ when mean velocity, \bar{U} is varied. From Figures 4.21(a) and (b), it can be seen that relative scour depth for moderate $\frac{D}{d}$ ratios (refer page 52 and Figure 2.12) increases with relative flow depth $\left(\frac{y_0}{D}\right)$ up to a value of $y_0/D \approx 3$. (Thus, flows in which $y_0/D \leq 3$ are termed "shallow" while flows in which $y_0/D \geq 3$ are termed "deep". This, however, does not apply for small or large $\frac{D}{d}$ ratios.) From Figure 4.21(b), it can be noted that the data of Chabert and Engeldinger (1956) also show a similar trend in the curves with the variation in $\frac{d_{se}}{D}$ becoming negligible for $y_0/D > 2$ or 3. A similar trend was also shown by the data of Laursen and Toch (1956), Varzeliotis (1960), Bonasoundas (1973) and Basak et al. (1975). Shen et al. (1977) stated that depth of scour becomes independent of y_0/D for $y_0/D > 3$.

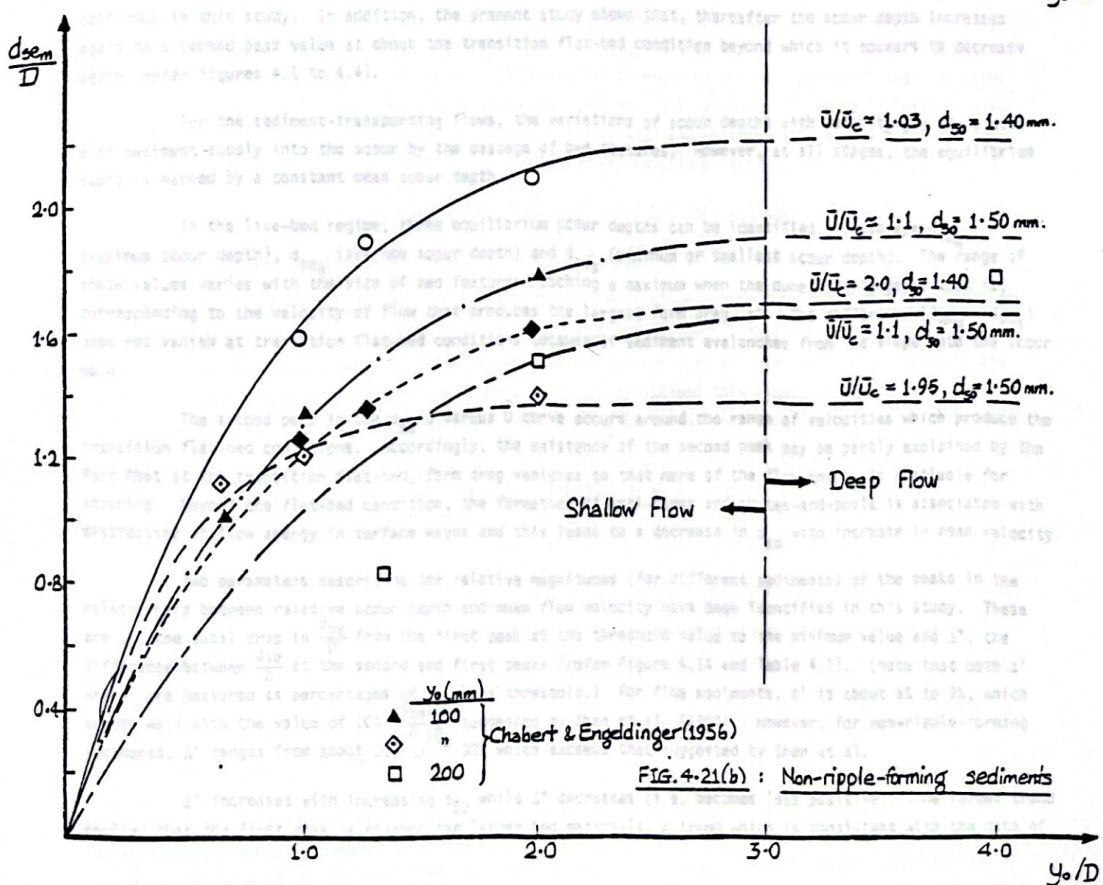
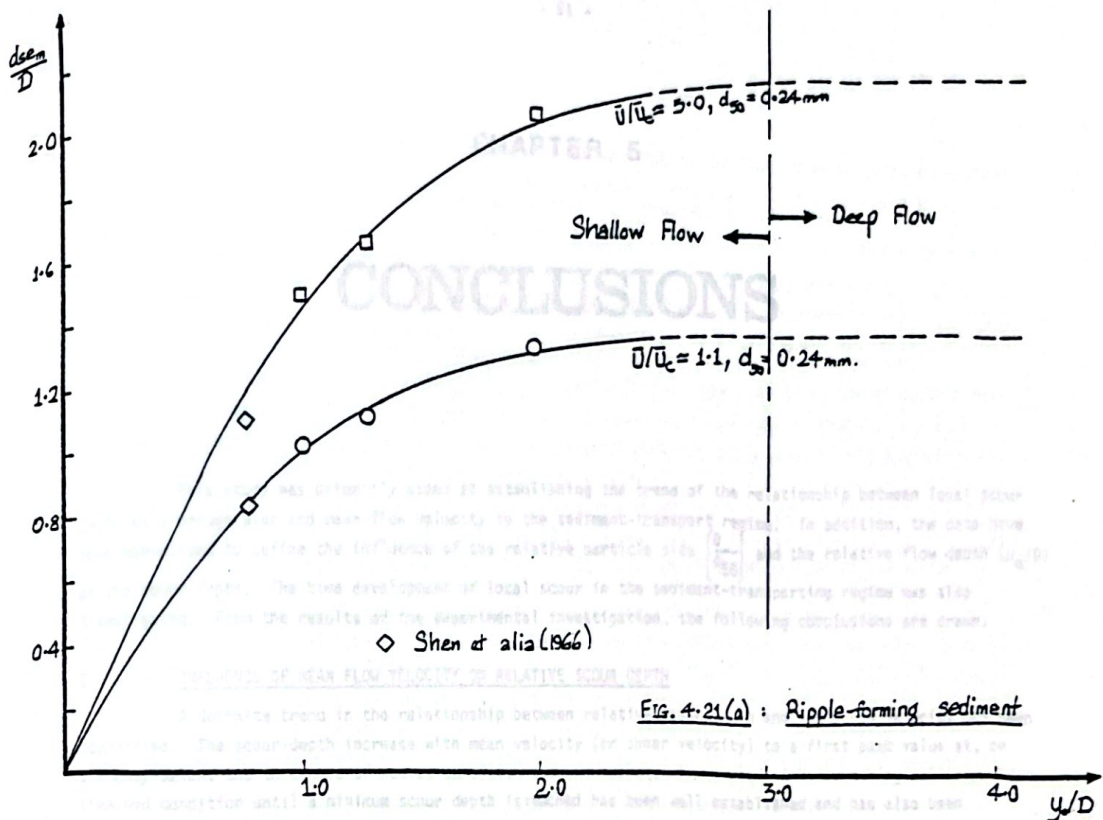
4.6 TIME DEVELOPMENT OF LOCAL SCOUR

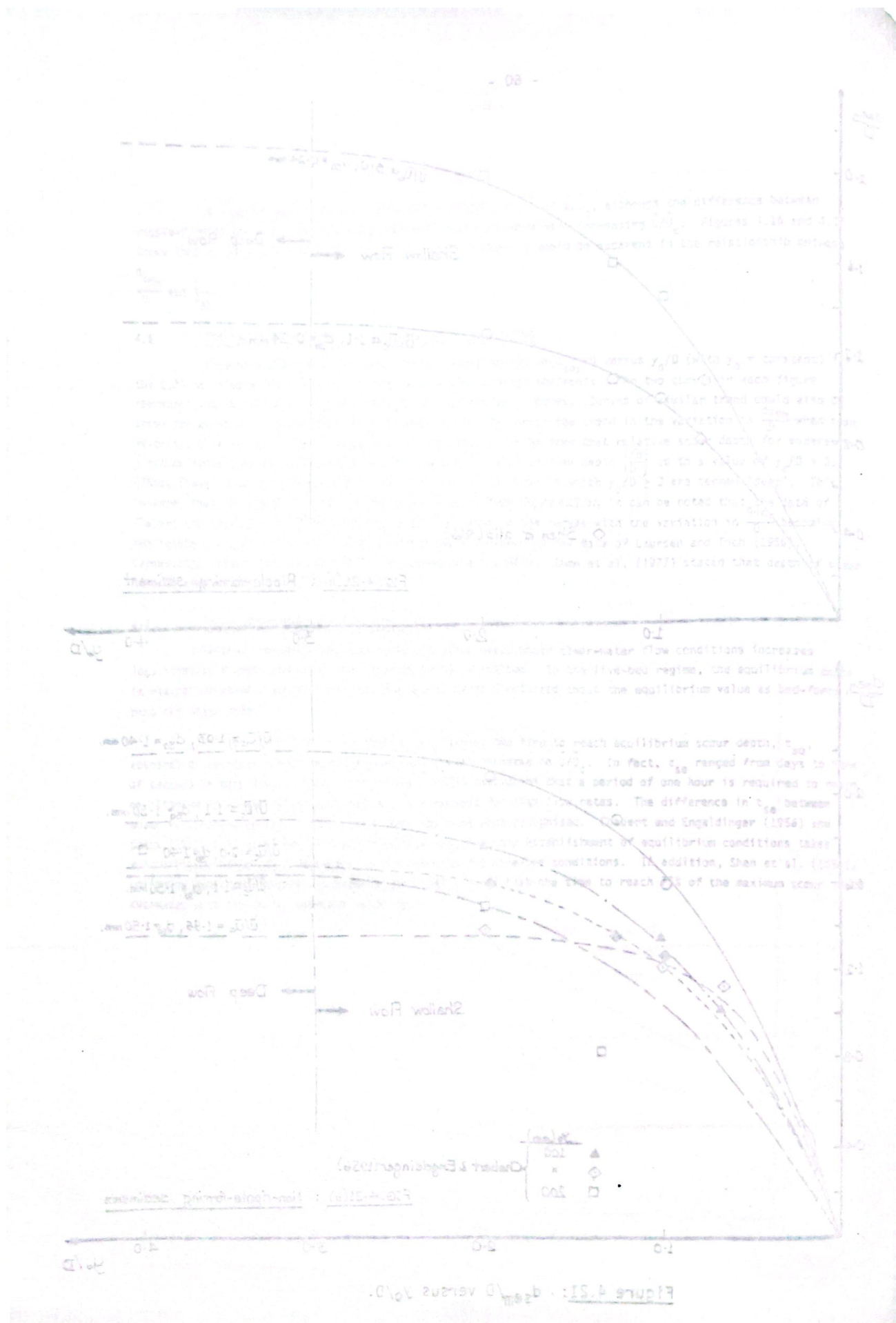
Previous research has shown that the scour depth under clear-water flow conditions increases logarithmically with time until the limiting depth is reached. In the live-bed regime, the equilibrium depth is reached relatively quickly and then the actual depth fluctuates about the equilibrium value as bed-forms pass the scour hole.

For the experiments conducted in this study, the time to reach equilibrium scour depth, t_{se} , appeared to decrease approximately exponentially with increase in \bar{U}/\bar{U}_c . In fact, t_{se} ranged from days to tens of seconds in this study. Thus, Bonasoundas' (1973) conclusion that a period of one hour is required to reach equilibrium in sediment-transport regime, is incorrect for high flow rates. The difference in t_{se} between scour in clear-water and live-bed conditions has long been recognised. Chabert and Engeldinger (1956) and Cunha (1971) both concluded in their investigations that the establishment of equilibrium conditions takes substantially longer in clear-water conditions than for live-bed conditions. In addition, Shen et al. (1966), utilising data from Chabert and Engeldinger (1956), found that the time to reach 75% of the maximum scour depth decreases with increasing approach velocity.



- 60 -

Figure 4.21: d_{semin}/D versus y_0/D .



CHAPTER 5

CONCLUSIONS

This study was primarily aimed at establishing the trend of the relationship between local scour depth at a bridge pier and mean flow velocity in the sediment-transport regime. In addition, the data have been normalised to define the influence of the relative particle size $\frac{D}{d_{50}}$ and the relative flow depth (y_0/D) on the scour depth. The time development of local scour in the sediment-transporting regime was also investigated. From the results of the experimental investigation, the following conclusions are drawn:

5.1 INFLUENCE OF MEAN FLOW VELOCITY ON RELATIVE SCOUR DEPTH

A definite trend in the relationship between relative scour depth and mean flow velocity has been identified. The scour-depth increase with mean velocity (or shear velocity) to a first peak value at, or slightly below, the threshold of motion condition and the subsequent decrease with increasing velocity under live-bed condition until a minimum scour depth is reached has been well established and has also been confirmed in this study. In addition, the present study shows that, thereafter the scour depth increases again to a second peak value at about the transition flat-bed condition beyond which it appears to decrease again (refer Figures 4.1 to 4.4).

For the sediment-transporting flows, the variations of scour depths with velocity are associated with sediment supply into the scour by the passage of bed features. However, at all stages, the equilibrium depth is marked by a constant mean scour depth.

In the live-bed regime, three equilibrium scour depths can be identified. These are d_{se_m} (maximum scour depth), d_{se_a} (average scour depth) and d_{se_s} (minimum or smallest scour depth). The range of these values varies with the size of bed features reaching a maximum when the dunes are largest, that is, corresponding to the velocity of flow that produces the largest form drag, τ^* . The difference $(d_{se_m} - d_{se_s})$ does not vanish at transition flat-bed conditions because of sediment avalanches from the slope into the scour hole.

The second peak in the d_{se}/D versus U curve occurs around the range of velocities which produce the transition flat-bed conditions. Accordingly, the existence of the second peak may be partly explained by the fact that at the transition flat-bed, form drag vanishes so that more of the flow energy is available for scouring. Beyond the flat-bed condition, the formation of anti-dunes and chutes-and-pools is associated with dissipation of flow energy in surface waves and this leads to a decrease in d_{se} with increase in mean velocity.

Two parameters describing the relative magnitudes (for different sediments) of the peaks in the relationship between relative scour depth and mean flow velocity have been identified in this study. These are Δ' , the total drop in $\frac{d_{se}}{D}$ from the first peak at the threshold value to the minimum value and Δ'' , the difference between $\frac{d_{se}}{D}$ at the second and first peaks (refer Figure 4.14 and Table 4.1). (Note that both Δ' and Δ'' are measured as percentages of d_{se}/D at threshold.) For fine sediments, Δ' is about 6% to 9%, which agrees well with the value of 10% $\frac{d_{se}}{D} U_c$ suggested by Shen et al. (1969). However, for non-ripple-forming sediments, Δ' ranges from about 20% to 30% which exceeds that suggested by Shen et al.

Δ' increases with increasing d_{50} while Δ'' decreases (i.e. becomes less positive). The former trend implies that the first peak is steeper for larger bed materials, a trend which is consistent with the data of non-rippled bed to assess the role of shear stresses in the initiation of shear-induced shear stress and shear

- 62 -

Chabert and Engeldinger (1956), Hancu (1971) and Nicollet (1971).

For the ripple-forming sediments, Δ'' is positive implying that the second peak is higher than the first peak and that maximum scour depths, $\left(\frac{d_{sem}}{D}\right)_{max}$, occur at $\bar{U} > \bar{U}_c$. The maximum scour depths are about 50-55% greater than the threshold value. For the non-ripple-forming sediments, however, Δ'' is negative and $\left(\frac{d_{sem}}{D}\right)_{max}$ occur at threshold condition.

The relative maximum scour depths $\left(\frac{d_{sem}}{D}\right)$ at the three different pier sizes employed in this study were plotted against normalised mean flow velocity, \bar{U}/\bar{U}_c (for y_0 constant and $\frac{y_0}{D}$ relatively low, i.e. $1.0 \leq \frac{y_0}{D} \leq 2.0$) (refer Figures 4.15(a), (b), (c)). For each pier, the data form two curves (one for ripple-forming and the other for non-ripple-forming sediments) which merge to form a single relationship at a value of \bar{U}/\bar{U}_c about 3.5 to 4.0 with the maximum deviation occurring at threshold velocity, i.e. at $\bar{U}/\bar{U}_c = 1.0$. A similar difference in the relationship between scour depth and shear velocity for ripple-forming and non-ripple-forming sediments was observed by Ettema (1980) at threshold condition (refer Figures 2.13 and 4.18) with the two curves merging in the direction of decreasing shear velocity at $\frac{U}{U_{*c}} = 0.5$.

All the data collected in this study were re-evaluated in terms of a single large value of y_0/D using a single idealized curve fitted to Ettema's (1980) data (refer Figure 4.16), and these are plotted in Figure 4.17. The data in this figure lie on two curves representing the average values for the sediments which do, and do not, form ripples. Exactly the same trend in the two curves, as compared with Figures 4.15(a), (b), (c), is apparent in this single-valued function for all data. The curves in Figure 4.17 were reproduced and compared with the data of other investigators (for large y_0/D ratios) (refer Figures 4.18 and 4.19).

The comparison of experimental data obtained under similar conditions reveals that the majority of the live-bed scour data of Chabert and Engeldinger (1956), Shen et al. (1966), Hancu (1971), White (1971) and Jain and Fischer (1979), when replotted, suggest a similar trend in the relationship between relative scour depth and mean flow velocity to that observed in this study. In addition, the data of these investigators when adjusted to large y_0/D ratios ($y_0/D \geq 3$) are reasonably consistent with those of the present study (refer Figures 4.18 and 4.19). Scatter in the data in these figures is mainly due to differences in measurement techniques, non-equilibrium flow conditions and variations in σ_1 and σ_g between the sediments.

5.2 INFLUENCE OF RELATIVE PARTICLE SIZE $\left(\frac{D}{d_{50}}\right)$ ON RELATIVE SCOUR DEPTH

The data of this study for \bar{U} just greater than 1.0 when adjusted to an equivalent large value of y_0/D (i.e. no y_0/D effect) and plotted in the form of $\frac{d_{sem}}{D}$ versus $\frac{D}{d_{50}}$, show a similar trend to that obtained by Ettema (1980) (see Figure 4.20). Two regimes which exist for ripple-forming and non-ripple-forming sediments are apparent in this figure. The data for non-ripple-forming sediments form a single curve. At low values of D/d_{50} (≤ 30), $\frac{d_{sem}}{D}$ increases with increasing $\frac{D}{d_{50}}$ up to a maximum value of about 2.3 to 2.5 in the intermediate range ($30 \leq \frac{D}{d_{50}} \leq 130$). At higher values of $\frac{D}{d_{50}}$ (≥ 130) the curve asymptotes to a constant value of $\frac{d_{sem}}{D}$ of about 2.2. The data for ripple-forming sediments lie in a cluster below this curve. At higher values of the ratio \bar{U}/\bar{U}_c the above trend would also be apparent. However, the difference between the two sediment types would decrease with increasing \bar{U}/\bar{U}_c until $\bar{U}/\bar{U}_c = 3.5$ to 4.0, after which no effect of ripple-formation would be apparent and all data would plot on a single curve.

5.3 INFLUENCE OF RELATIVE FLOW DEPTH ON RELATIVE SCOUR DEPTH

For a constant value of $\frac{U}{U_c}$, the relative scour depth, $\frac{d_{sem}}{D}$ increases with increasing y_0/D for shallow flows. The variation in relative scour depth for moderate D/d_{50} ratios (refer page 52 and Figure 2.12) for $y_0/D \geq 3$ (refer Figure 4.21). Thus, flows in which $y_0/D \leq 3$ are termed "shallow" while flows in which $y_0/D \geq 3$ are termed "deep". This, however, does not apply for small or large D/d_{50} ratios.

5.4 TIME DEVELOPMENT OF LOCAL SCOUR

The scour depth in the clear-water regime increases logarithmically with time up to the limiting depth at equilibrium. In the live-bed regime, the equilibrium depth is reached relatively quickly after which the actual scour depth fluctuates with time about this average value with the passage of bed-forms past the pier.

- 63 -

An approximately exponential decrease in time to reach equilibrium scour depth, t_{se} , was measured over a small range of velocities just greater than the threshold velocity. At higher velocities equilibrium was attained very rapidly.

5.5 SUGGESTIONS FOR FUTURE RESEARCH

- (a) Experimental data are required for very shallow flows ($\frac{y_0}{D} < 1.0$) and deep flows ($\frac{y_0}{D} \geq 3$) in the sediment-transport regime. Such data should be obtained by varying both flow depth and pier size and include pier sizes greater than 200 mm.
 - (b) Experimental data are also required for relatively large sediments ($\frac{D}{d_{50}} \leq 30$) in the sediment-transport regime. Such data should include particle sizes greater than 3 mm.
 - (c) The influence of particle shape factor and bed material gradation on the relative scour depth in the live-bed regime requires investigation.
 - (d) The local scour of layered bed sediments in the sediment-transport regime has not previously been investigated. Many natural channels consist of layered beds and an investigation into the way in which local scour develops in such beds would be valuable.

BIBLIOGRAPHY

- AHMAD, M. (1962), Discussion of "Scour of Bridge Crossings" by E. M. Laursen, Trans. A.S.C.E., Vol. 127, pt. 1.
- ARUNACHALAM, K. (1965), "Scour around Bridge Piers", Journal of Indian Roads Congress, Paper No. 251.
- A.S.C.E. Committee on Sedimentation (1975), Manual No. 154, "Sedimentation Engineering".
- BASAK, V. et al. (1975), "Scour at Square Piers", Devlet su isteri genel müdürlüğü, Report No. 583, Ankara.
- BATA, C. (1960), "Erozija oko novosadskog mostorskog stuba", (Serbian), (Scour around Bridge Piers), Institut za Vodoprivreda, Jaroslav Cerai Beozrod Yugoslavia, English translation by Markovic filed at Colorado State University, Ft. Collins.
- BLENCH, T. (1965), "Mobile Bed Fluviology", University of Alberta Press.
- BONASOUNDAS, Dr. Ing. (1973), "Non-stationary Hydromorphological Phenomena and Modelling of Scour Processes", Proc. 16th Congress I.A.H.R. São Paulo, Brazil, Vol. 2, pp. 9-16.
- BREUSERS, H.N.C. (1965), "Scour Around Drilling Platforms", Bulletin, Hydraulic Research 1964 and 1965, I.A.H.R., Vol. 19, pp. 276.
- BREUSERS, H.N.C., NICOLLET, G. and SHEN, H. W. (1977), "Local Scour around Cylindrical Piers", Journal of Hydr. Research, 15, No. 3 pp. 211-252.
- CARSTENS, T. and SHARMA, H. R. (1975), "Local Scour around Large Obstructions", Proc. 16th Congress I.A.H.R., São Paulo, Brazil, Vol. 832, pp. 251-262.
- CHABERT, J. and ENGELDINGER, P. (1958), "Etude des Affouillements autour des Piles des Ponts", Laboratoire National d'Hydraulique, Chatou, France.
- CHITALE, S. V. (1962), Discussion of "Scour at Bridge Crossings" by E. M. Laursen, Trans. A.S.C.E., Vol. 127, pt. 1.
- COLEMAN, N. L. (1971), "Analysing Laboratory Measurements of Scour at Cylindrical Piers in Sand Beds", Proc. I.A.H.R., 14th Congress, Paris, Vol. 3.
- CUNHA, L. Viega Da (1975), Discussion on "Local Scour around Bridge Piers", by Shen, Schneider and Karaki, Proc. A.S.C.E., Journal Hydraulics Division, Vol. 96, HY 8.
- EINSTEIN, H. A. (1942), "Formulas for the Transportation of Bed-load", Trans. Amer. Soc. Civil Eng., Vol. 117, pp. 561-597.
- ENGELUND, F. and HANSEN, E. (1967), "A monograph on Sediment Transport in Alluvial Streams", Technical Univ. of Denmark, Hydraulic Laboratory, Teknisk Forlag, Skelbaeksgade 4, Copenhagen V, Denmark.
- ETTEMA, R. (1976), "Influence of Bed Material Gradation on Local Scour", M. Engr. Thesis, Univ. of Auckland, School of Engineering, Report No. 124, Auckland, New Zealand.

- 65 -

- ETTEMA, R. (1980), "Scour at Bridge Piers" Ph.D. Thesis, Sch. of Engr., Rep. No. 216, Univ. of Auckland, Auckland, N.Z.
- FIELD, W. G. (1971), "Flood Protection at Highway Bridge", Engr. Bulletin CE3, Univ. of Newcastle, Australia.
- GARDE, R. J. (1961), "Local Bed Variation at Bridge Piers in Alluvial Channels", Univ. of Roorkee Research Journal, Vol. IV, No. 1.
- HANCU, S. (1971), "Sur le calcul des affouillements locaux dans la zone des piles de ponts", Proc. 14th I.A.H.R. Congress, Paris, 3, pp. 299-313.
- HANNAH, C. R. (1978), "Scour at Pile Groups", M.E. Thesis, Univ. of Canterbury, Christchurch, N.Z.
- HARWOOD, N. J. (1977), "Local Scour at Bridge Pier caused by Flood Waves", M.E. Thesis, Univ. of Canterbury, Christchurch, N.Z.
- HJORTH, P. (1972), "Lokal Erosion och Erosionsverken vid Aroppsledning i Kustriära Områden", Institute för Vattenbyggnad, Tekniska Högskolan i Lund, Bulletin Serie 8, nr. 21.
- HJORTH, P. (1975), "Studies on the Nature of Local Scour", Department of Water Resources Eng., Lund Institute of Technology, Bulletin Series A, No. 46.
- INGLIS, Sir Claude (1949), "The Behaviour and Control of Rivers and Canals", Research Publications No. 13, Pt. 2, Central Power, Irrigation and Navigation Report, Poona Research Station, India.
- INGLIS, C. C., THOMAS, A. R., and JOGLEKAR, D. V. (1939), "The Protection of Bridge Piers against Scour. Annual Report of work done during 1938-39. Central Irrigation and Hydrodynamics Research Station, Poona, Research Publication, No. 2.
- JAIN, S. C. and FISCHER, E. E. (1979), "Scour around Bridge Piers at High Froude Numbers", Report No. FH-WA-RD-79-104, Federal Highway Administration, Washington, D. C., Apr., 1979.
- JAIN, S. C. and FISCHER, E. E. (1980), "Scour at Bridge Piers at High Flow Velocities", Journal of the Hydraulics Div., A.S.C.E., Vol. 106, HY 11, Nov. 1980, pp. 1827-1842.
- KAIN, D. H. (1961), "Scour Effects at the Chirna Bridge", Public Works Department, Zomba, Nyasaland.
- KEUTNER, Chr. (1932), "Stromungsvorgänge an Strompfeilern von verschiedenen Grundriss formen und ihre Einwirkung auf die Flussohle" (German), (The Flow around Bridge Piers of Different Shapes and Its Effect on the River Bed) Die Bautechnik, Vol. 10, No. 12, March 15, 1932, (Translated from the German by E. F. Wilsey, April 22, 1937. U. S. Bureau of Reclamation Report HYD-19, Translation No. 40).
- KNEZEVIC, B. (1960), "Prilog proucavanju erozije oko mostovskih stubova", (Serbian), (Contributions to Research Work of Erosion around Bridge Piers), Institut za Vodoprivrednu Jaroslav Ceri Beograd, Yugoslavia, Translated by Markovic, filed at Colorado State Univ., Civil Eng. Dept.
- LARRAS, J. (1963), "Profondeurs Maximales d'Erosion des Fonds Mobiles autour des Piles en Rivière", Annales des Ponts et Chaussées, Vol. 133, No. 4, pp. 411-424.
- LAURSEN, E. M. (1958), "Scour at Bridge Crossings", Iowa Highway Research Bd., Bulletin No. 8.
- LAURSEN, E. M. (1962), "Scour at Bridge Crossings", Trans. A.S.C.E., Vol. 127, pt. 1, pp. 166-179.
- LAURSEN, E. M. (1963), "Analysis of Relief Bridge Scour" Proc. A.S.C.E., Journal Hydraulics Div., Vol. 89, HY3.
- LAURSEN, E. M. and TOCH, A. (1956), "Scour Around Bridge Piers and Abutments", Bulletin No. 4, Iowa Road Research Bd.

- 66 -

- LECLERC, J. P. (1971), "Recherche des Lois Régissant Les Phénomènes d'Affouillement au Pied des Piles de Pont, Premiers Resultats", Proc. 14th Congress, I.A.H.R., Paris, Vol.3, pp. 323-330.
- MARIN, J.N.M. (1962), "An Investigation of Local Scour Around Bridge Piers", M. Tech. Thesis, Univ. of New South Wales, Water Resources Lab., Manley Vale, N.S.W., Australia.
- MAZA ALVAREZ, J. A. and SANCHEZ BRIBIESCA, J. L. (1964), "Contribution al Estudio de la Socavacion Local en Pilas de Puente", Universidae Federal do Rio Grande do Sul, Mexico.
- MAZA ALVAREZ, J. A. and SANCHEZ BRIBIESCA, J. L. (1966), "Socavación y protección al pie de pilas de puentes; Segundo Congr. Latin-americo de Hidraulica, Caracas.
- MAZA ALVAREZ, J. A. (1967), "Erosión del cause de un río por el cruce de un puente. Ing. Hidr. en Mexico, 20(2), pp. 93-106.
- MAZA ALVAREZ, J. A. (1968), "Socavación en cauces naturales; Inst. de Eng., Univ. Nac. de Mexicó, Publ. No. 177.
- MELVILLE, B. W. (1975), "Local Scour at Bridge Sites", Ph.D. Thesis, Univ. of Auckland, Rep. No. 117, Auckland, N.Z.
- NEILL, C. R. (1964), "River Bed Scour", A Review for Engineers, Canadian Good Roads Assn., Tech, Publ. No. 23.
- NEILL, C. R. (1970), Discussion on "Local Scour Around Bridge Piers" by Shen, Schneider, and Karaki, Proc. A.S.C.E. Journal Hydraulics Div., Vol. 96, HYS.
- NEILL, C. R. (1973), "Guide to Bridge Hydraulics", Edited by C. R. Neill, published for Roads and Transportation Assn. of Canada for Univ. of Toronto Press.
- NICOLLET, G. (1971), "Déformation des Lits Alluvionaires Affouillements Autour des Piles de Ponts Cylindriques", Rep. No. HC 043 684, Laboratoire National d'Hydraulique, Chatou, France.
- NICOLLET, G. and RAMETTE, M. (1971), "Affouillements au Voisinage de Piles des Ponts Cylindriques Circulaires", Proc. 14th Congress I.A.H.R., Paris, Vol. 3, pp. 315-322.
- POSEY, C. J. (1949), "Why Bridge Fail in Floods", Civ. Eng. 19, pp. 42-90.
- RAUDKIVI, A. J. (1976), "Loose Boundary Hydraulics", published by Pergamon Press.
- RAUDKIVI, A. J. (1981), "Grundlagen des Sedimenttransports", Sonderforschungsbereich 79, Wasserforschung Im Küstenbereich, Universität Hannover.
- RAUDKIVI, A. J. and SUTHERLAND, A. J. (1981), "Scour at Bridge Crossings", Road Research Unit, National Roads Board, Wellington, N.Z.
- RAUDKIVI, A. J. and ETTEMA, R. (1982), "Scour at Bridge Piers", 3rd Congress of the Asian and Pacific Regional Division (A.P.D.) of the International Association for Hydraulic Research (I.A.H.R.).
- ROPER, A. T., SCHNEIDER, V. R., SHEN, H. W. (1967), "Analytical Approach to Local Scour", Proc. 12th Congress I.A.H.R., Ft. Collins, Vol. 3, pp. 151-161.
- SCHWARTZ, K. (1929), "Comparative Experiments on the Influence of the Size of Particles on a River Bottom on the Depth of Excavation occurring in the Vicinity of Bridge Piers", Hydraulic Laboratory Practice, edited by J. R. Freeman, p. 201.
- SHEN, W. H. (1971), "Scour Near Piers", Ch. 23, River Mechanics, Vol. II.
- SHEN, H. W., SCHNEIDER, V. R., KARAKI, S. S. (1966), "Mechanics of Local Scour", U. S. Dept. of Commerce, National Bureau of Standards, Institute for Applied Technology.

- SHEN, H. W., SCHNEIDER, V. R., KARAKI, S. S. (1969), "Local Scour Around Bridge Piers", Proc. A.S.C.E., Journal Hydraulics Div., Vol. 95, HY6.
- SHEN, H. W. (1973), General Report of Technical Session 3, Proc. Symposium on River Mechanics, Bangkok, Vol. 4, pp. 69-81.
- SHELDIS, A. (1936), "Application of Similarity Principles and Turbulence Research to Bed-Load Movement", Translated Version.
- SMITHS, D. W. (1976), "Bridge Failures", Paper 7921, Proc. The Institution of Civil Engineers, Pt. 1, Aug. 1976, Vol. 60.
- TARARE, Z. S. (1962), "A Theoretical and Experimental Determination of the Erosion Pattern around Obstructions placed in an Alluvial channel with particular reference to Vertical Circular Cylinders and Piers", Ph.D. Dissertation, Univ. of Minnesota.
- THOMAS, A. R. (1962), Discussion on "Local Scour around Bridge Crossings", Trans. A.S.C.E., Vol. 127, pt. 1.
- TIMONOFF, V. E. (1929), "Experiments on the Spacing of Bridge Piers in the Case of Parallel Bridges", Hydraulic Laboratory Practice, edited by J. R. Freeman, Am. Soc. of Mech. Engrs., New York.
- TISON, L. J. (1940), "Erosion autour de Piles de Ponts en Riviere", Annales des Travaux Publics de Belgique, Vol. 41, No. 6.
- VARZELIOTIS, A. N. (1960), "Model Studies of Scour around Bridge Piers", M.Sc. Thesis, Dept. of Civil Engr., Univ. of Alberta.
- WALKER, B.F.G. (1975), "Scour at Cylindrical Pier by Translation Waves", M.E. Thesis, Univ. of Canterbury, Christchurch, N.Z.
- WHITE, W. R. (1975), "Scour around Bridge Piers in Steep Streams", Proc. 16th I.A.H.R. Congress, São Paulo, 2, pp. 279-284.
- YALIN, M. S. (1977), "Mechanics of Sediment Transport", published by Pergamon Press.
- YARNELL, D. L. and NAGLER, F. A. (1931), A report upon a hydraulic investigation of North Carolina standard reinforced concrete bridge pier number P-401-R and modifications thereof. Iowa Institute of Hydraulic Research, Univ. of Iowa, Iowa City, December 1931.
- YAROSLAVTIEV, J. A. (1954), "Protection of Bridge Supports from Scour", Moscow, Mintranssfoj, U.S.S.R.
- ZHURABOV, V. V. (1961), "The Problem of Protection of Bridge Foundations from Scour", Proc. of the 1st International Conference on Soil Mechanics and Foundation Engineering, Moscow, 1961, Vol. 1, Ch. 1, Sections 10, 11, 12, 13, 14, 15, 16, 17, 18, 19, 20, 21, 22, 23, 24, 25, 26, 27, 28, 29, 30, 31, 32, 33, 34, 35, 36, 37, 38, 39, 40, 41, 42, 43, 44, 45, 46, 47, 48, 49, 50, 51, 52, 53, 54, 55, 56, 57, 58, 59, 60, 61, 62, 63, 64, 65, 66, 67, 68, 69, 70, 71, 72, 73, 74, 75, 76, 77, 78, 79, 80, 81, 82, 83, 84, 85, 86, 87, 88, 89, 90, 91, 92, 93, 94, 95, 96, 97, 98, 99, 100, 101, 102, 103, 104, 105, 106, 107, 108, 109, 110, 111, 112, 113, 114, 115, 116, 117, 118, 119, 120, 121, 122, 123, 124, 125, 126, 127, 128, 129, 130, 131, 132, 133, 134, 135, 136, 137, 138, 139, 140, 141, 142, 143, 144, 145, 146, 147, 148, 149, 150, 151, 152, 153, 154, 155, 156, 157, 158, 159, 160, 161, 162, 163, 164, 165, 166, 167, 168, 169, 170, 171, 172, 173, 174, 175, 176, 177, 178, 179, 180, 181, 182, 183, 184, 185, 186, 187, 188, 189, 190, 191, 192, 193, 194, 195, 196, 197, 198, 199, 200, 201, 202, 203, 204, 205, 206, 207, 208, 209, 210, 211, 212, 213, 214, 215, 216, 217, 218, 219, 220, 221, 222, 223, 224, 225, 226, 227, 228, 229, 230, 231, 232, 233, 234, 235, 236, 237, 238, 239, 240, 241, 242, 243, 244, 245, 246, 247, 248, 249, 250, 251, 252, 253, 254, 255, 256, 257, 258, 259, 260, 261, 262, 263, 264, 265, 266, 267, 268, 269, 270, 271, 272, 273, 274, 275, 276, 277, 278, 279, 280, 281, 282, 283, 284, 285, 286, 287, 288, 289, 290, 291, 292, 293, 294, 295, 296, 297, 298, 299, 300, 301, 302, 303, 304, 305, 306, 307, 308, 309, 310, 311, 312, 313, 314, 315, 316, 317, 318, 319, 320, 321, 322, 323, 324, 325, 326, 327, 328, 329, 330, 331, 332, 333, 334, 335, 336, 337, 338, 339, 340, 341, 342, 343, 344, 345, 346, 347, 348, 349, 350, 351, 352, 353, 354, 355, 356, 357, 358, 359, 360, 361, 362, 363, 364, 365, 366, 367, 368, 369, 370, 371, 372, 373, 374, 375, 376, 377, 378, 379, 380, 381, 382, 383, 384, 385, 386, 387, 388, 389, 390, 391, 392, 393, 394, 395, 396, 397, 398, 399, 400, 401, 402, 403, 404, 405, 406, 407, 408, 409, 410, 411, 412, 413, 414, 415, 416, 417, 418, 419, 420, 421, 422, 423, 424, 425, 426, 427, 428, 429, 430, 431, 432, 433, 434, 435, 436, 437, 438, 439, 440, 441, 442, 443, 444, 445, 446, 447, 448, 449, 450, 451, 452, 453, 454, 455, 456, 457, 458, 459, 460, 461, 462, 463, 464, 465, 466, 467, 468, 469, 470, 471, 472, 473, 474, 475, 476, 477, 478, 479, 480, 481, 482, 483, 484, 485, 486, 487, 488, 489, 490, 491, 492, 493, 494, 495, 496, 497, 498, 499, 500, 501, 502, 503, 504, 505, 506, 507, 508, 509, 510, 511, 512, 513, 514, 515, 516, 517, 518, 519, 520, 521, 522, 523, 524, 525, 526, 527, 528, 529, 530, 531, 532, 533, 534, 535, 536, 537, 538, 539, 540, 541, 542, 543, 544, 545, 546, 547, 548, 549, 550, 551, 552, 553, 554, 555, 556, 557, 558, 559, 550, 551, 552, 553, 554, 555, 556, 557, 558, 559, 560, 561, 562, 563, 564, 565, 566, 567, 568, 569, 570, 571, 572, 573, 574, 575, 576, 577, 578, 579, 580, 581, 582, 583, 584, 585, 586, 587, 588, 589, 580, 581, 582, 583, 584, 585, 586, 587, 588, 589, 590, 591, 592, 593, 594, 595, 596, 597, 598, 599, 590, 591, 592, 593, 594, 595, 596, 597, 598, 599, 600, 601, 602, 603, 604, 605, 606, 607, 608, 609, 600, 601, 602, 603, 604, 605, 606, 607, 608, 609, 610, 611, 612, 613, 614, 615, 616, 617, 618, 619, 610, 611, 612, 613, 614, 615, 616, 617, 618, 619, 620, 621, 622, 623, 624, 625, 626, 627, 628, 629, 620, 621, 622, 623, 624, 625, 626, 627, 628, 629, 630, 631, 632, 633, 634, 635, 636, 637, 638, 639, 630, 631, 632, 633, 634, 635, 636, 637, 638, 639, 640, 641, 642, 643, 644, 645, 646, 647, 648, 649, 640, 641, 642, 643, 644, 645, 646, 647, 648, 649, 650, 651, 652, 653, 654, 655, 656, 657, 658, 659, 650, 651, 652, 653, 654, 655, 656, 657, 658, 659, 660, 661, 662, 663, 664, 665, 666, 667, 668, 669, 660, 661, 662, 663, 664, 665, 666, 667, 668, 669, 670, 671, 672, 673, 674, 675, 676, 677, 678, 679, 680, 681, 682, 683, 684, 685, 686, 687, 688, 689, 680, 681, 682, 683, 684, 685, 686, 687, 688, 689, 690, 691, 692, 693, 694, 695, 696, 697, 698, 699, 690, 691, 692, 693, 694, 695, 696, 697, 698, 699, 700, 701, 702, 703, 704, 705, 706, 707, 708, 709, 700, 701, 702, 703, 704, 705, 706, 707, 708, 709, 710, 711, 712, 713, 714, 715, 716, 717, 718, 719, 710, 711, 712, 713, 714, 715, 716, 717, 718, 719, 720, 721, 722, 723, 724, 725, 726, 727, 728, 729, 720, 721, 722, 723, 724, 725, 726, 727, 728, 729, 730, 731, 732, 733, 734, 735, 736, 737, 738, 739, 730, 731, 732, 733, 734, 735, 736, 737, 738, 739, 740, 741, 742, 743, 744, 745, 746, 747, 748, 749, 740, 741, 742, 743, 744, 745, 746, 747, 748, 749, 750, 751, 752, 753, 754, 755, 756, 757, 758, 759, 750, 751, 752, 753, 754, 755, 756, 757, 758, 759, 760, 761, 762, 763, 764, 765, 766, 767, 768, 769, 760, 761, 762, 763, 764, 765, 766, 767, 768, 769, 770, 771, 772, 773, 774, 775, 776, 777, 778, 779, 770, 771, 772, 773, 774, 775, 776, 777, 778, 779, 780, 781, 782, 783, 784, 785, 786, 787, 788, 789, 780, 781, 782, 783, 784, 785, 786, 787, 788, 789, 790, 791, 792, 793, 794, 795, 796, 797, 798, 799, 790, 791, 792, 793, 794, 795, 796, 797, 798, 799, 800, 801, 802, 803, 804, 805, 806, 807, 808, 809, 800, 801, 802, 803, 804, 805, 806, 807, 808, 809, 810, 811, 812, 813, 814, 815, 816, 817, 818, 819, 810, 811, 812, 813, 814, 815, 816, 817, 818, 819, 820, 821, 822, 823, 824, 825, 826, 827, 828, 829, 820, 821, 822, 823, 824, 825, 826, 827, 828, 829, 830, 831, 832, 833, 834, 835, 836, 837, 838, 839, 830, 831, 832, 833, 834, 835, 836, 837, 838, 839, 840, 841, 842, 843, 844, 845, 846, 847, 848, 849, 840, 841, 842, 843, 844, 845, 846, 847, 848, 849, 850, 851, 852, 853, 854, 855, 856, 857, 858, 859, 850, 851, 852, 853, 854, 855, 856, 857, 858, 859, 860, 861, 862, 863, 864, 865, 866, 867, 868, 869, 860, 861, 862, 863, 864, 865, 866, 867, 868, 869, 870, 871, 872, 873, 874, 875, 876, 877, 878, 879, 870, 871, 872, 873, 874, 875, 876, 877, 878, 879, 880, 881, 882, 883, 884, 885, 886, 887, 888, 889, 880, 881, 882, 883, 884, 885, 886, 887, 888, 889, 890, 891, 892, 893, 894, 895, 896, 897, 898, 899, 890, 891, 892, 893, 894, 895, 896, 897, 898, 899, 900, 901, 902, 903, 904, 905, 906, 907, 908, 909, 900, 901, 902, 903, 904, 905, 906, 907, 908, 909, 910, 911, 912, 913, 914, 915, 916, 917, 918, 919, 910, 911, 912, 913, 914, 915, 916, 917, 918, 919, 920, 921, 922, 923, 924, 925, 926, 927, 928, 929, 920, 921, 922, 923, 924, 925, 926, 927, 928, 929, 930, 931, 932, 933, 934, 935, 936, 937, 938, 939, 930, 931, 932, 933, 934, 935, 936, 937, 938, 939, 940, 941, 942, 943, 944, 945, 946, 947, 948, 949, 940, 941, 942, 943, 944, 945, 946, 947, 948, 949, 950, 951, 952, 953, 954, 955, 956, 957, 958, 959, 950, 951, 952, 953, 954, 955, 956, 957, 958, 959, 960, 961, 962, 963, 964, 965, 966, 967, 968, 969, 960, 961, 962, 963, 964, 965, 966, 967, 968, 969, 970, 971, 972, 973, 974, 975, 976, 977, 978, 979, 970, 971, 972, 973, 974, 975, 976, 977, 978, 979, 980, 981, 982, 983, 984, 985, 986, 987, 988, 989, 980, 981, 982, 983, 984, 985, 986, 987, 988, 989, 990, 991, 992, 993, 994, 995, 996, 997, 998, 999, 990, 991, 992, 993, 994, 995, 996, 997, 998, 999, 1000, 1001, 1002, 1003, 1004, 1005, 1006, 1007, 1008, 1009, 1000, 1001, 1002, 1003, 1004, 1005, 1006, 1007, 1008, 1009, 1010, 1011, 1012, 1013, 1014, 1015, 1016, 1017, 1018, 1019, 1010, 1011, 1012, 1013, 1014, 1015, 1016, 1017, 1018, 1019, 1020, 1021, 1022, 1023, 1024, 1025, 1026, 1027, 1028, 1029, 1020, 1021, 1022, 1023, 1024, 1025, 1026, 1027, 1028, 1029, 1030, 1031, 1032, 1033, 1034, 1035, 1036, 1037, 1038, 1039, 1030, 1031, 1032, 1033, 1034, 1035, 1036, 1037, 1038, 1039, 1040, 1041, 1042, 1043, 1044, 1045, 1046, 1047, 1048, 1049, 1040, 1041, 1042, 1043, 1044, 1045, 1046, 1047, 1048, 1049, 1050, 1051, 1052, 1053, 1054, 1055, 1056, 1057, 1058, 1059, 1050, 1051, 1052, 1053, 1054, 1055, 1056, 1057, 1058, 1059, 1060, 1061, 1062, 1063, 1064, 1065, 1066, 1067, 1068, 1069, 1060, 1061, 1062, 1063, 1064, 1065, 1066, 1067, 1068, 1069, 1070, 1071, 1072, 1073, 1074, 1075, 1076, 1077, 1078, 1079, 1070, 1071, 1072, 1073, 1074, 1075, 1076, 1077, 1078, 1079, 1080, 1081, 1082, 1083, 1084, 1085, 1086, 1087, 1088, 1089, 1080, 1081, 1082, 1083, 1084, 1085, 1086, 1087, 1088, 1089, 1090, 1091, 1092, 1093, 1094, 1095, 1096, 1097, 1098, 1099, 1090, 1091, 1092, 1093, 1094, 1095, 1096, 1097, 1098, 1099, 1100, 1101, 1102, 1103, 1104, 1105, 1106, 1107, 1108, 1109, 1100, 1101, 1102, 1103, 1104, 1105, 1106, 1107, 1108, 1109, 1110, 1111, 1112, 1113, 1114, 1115, 1116, 1117, 1118, 1119, 1110, 1111, 1112, 1113, 1114, 1115, 1116, 1117, 1118, 1119, 1120, 1121, 1122, 1123, 1124, 1125, 1126, 1127, 1128, 1129, 1120, 1121, 1122, 1123, 1124, 1125, 1126, 1127, 1128, 1129, 1130, 1131, 1132, 1133, 1134, 1135, 1136, 1137, 1138, 1139, 1130, 1131, 1132, 1133, 1134, 1135, 1136, 1137, 1138, 1139, 1140, 1141, 1142, 1143, 1144, 1145, 1146, 1147, 1148, 1149, 1140, 1141, 1142, 1143, 1144, 1145, 1146, 1147, 1148, 1149, 1150, 1151, 1152, 1153, 1154, 1155, 1156, 1157, 1158, 1159, 1150, 1151, 1152, 1153, 1154, 1155, 1156, 1157, 1158, 1159, 1160, 1161, 1162, 1163, 1164, 1165, 1166, 1167, 1168, 1169, 1160, 1161, 1162, 1163, 1164, 1165, 1166, 1167, 1168, 1169, 1170, 1171, 1172, 1173, 1174, 1175, 1176, 1177, 1178, 1179, 1170, 1171, 1172, 1173, 1174, 1175, 1176, 1177, 1178, 1179, 1180, 1181, 1182, 1183, 1184, 1185, 1186, 1187, 1188, 1189, 1180, 1181, 1182, 1183, 1184, 1185, 1186, 1187, 1188, 1189, 1190, 1191, 1192, 1193, 1194, 1195, 1196, 1197, 1198, 1199, 1190, 1191, 1192, 1193, 1194, 1195, 1196, 1197, 1198, 1199, 1200, 1201, 1202, 1203, 1204, 1205, 1206, 1207, 1208, 1209, 1200, 1201, 1202, 1203, 1204, 1205, 1206, 1207, 1208, 1209, 1210, 1211, 1212, 1213, 1214, 1215, 1216, 1217, 1218, 1219, 1210, 1211, 1212, 1213, 1214, 1215, 1216, 1217, 1218, 1219, 1220, 1221, 1222, 1223, 1224, 1225, 1226, 1227, 1228, 1229, 1220, 1221, 1222, 1223, 1224, 1225, 1226, 1227, 1228, 1229, 1230, 1231, 1232, 1233, 1234, 1235, 1236, 1237, 1238, 1239, 1230, 1231, 1232, 1233, 1234, 1235, 1236, 1237, 1238, 1239, 1240, 1241, 1242, 1243, 1244, 1245, 1246, 1247, 1248, 1249, 1240, 1241, 1242, 1243, 1244, 1245, 1246, 1247, 1248, 1249, 1250, 1251, 1252, 1253, 1254, 1255, 1256, 1257, 1258, 1259, 1250, 1251, 1252, 1253, 1254, 1255, 1256, 1257, 1258, 1259, 1260, 1261, 1262, 1263, 1264, 1265, 1266, 1267, 1268, 1269, 1260, 1261, 1262, 1263, 1264, 1265, 1266, 1267, 1268, 1269, 1270, 1271, 1272, 1273, 127

- 68 -

NOTATION

b	pier width or diameter	geometric moments
d	mean particle size (i.e. 50% passing)	volume to volume
d_{50}	particle size (90% passing)	equivalent to channel width
d_0	deepest depth of scour around a cylindrical pier (at time t) below the upstream mean bed level or undisturbed bed level; i.e. scour depth at upstream nose of cylindrical pier	
d_s	scour depth at equilibrium, i.e. d_s at conditions of equilibrium	
d_{se}	time-averaged value of d_s after equilibrium live-bed condition has been reached	
d_{se1}	maximum and minimum (or smallest) recorded values of d_s , respectively, over duration of each experimental run at equilibrium live-bed condition	
d_{se2}, d_{se3}	d_{se} at condition of critical/threshold flow velocity	
$(d_{se})_{lc}$		particular
Fr	Froude Number $\left[= \frac{\bar{U}}{\sqrt{gY_0}} \right]$	particular
Fr_c	Froude Number at critical velocity $\left[= \frac{\bar{U}_c}{\sqrt{gY_0}} \right]$	particular
f	Weisbach frictional factor	
g	gravitational constant ($= 9.81 \text{ m/s}^2$)	
K_s	coefficient	
L	length of pier (longitudinal, i.e. in direction of flow)	
Q	flowrate	
q_s	rate of local scour in volume per unit time	
q'_s	capacity of the flow to transport sediment out of scour hole in volume per unit time	
q''_s	rate at which sediment is fed into the scour hole in volume per unit time	
s_s	specific gravity	
t	time	
t_{se}	time taken for scour to reach equilibrium	
\bar{U}	mean velocity of approach flow in a channel	

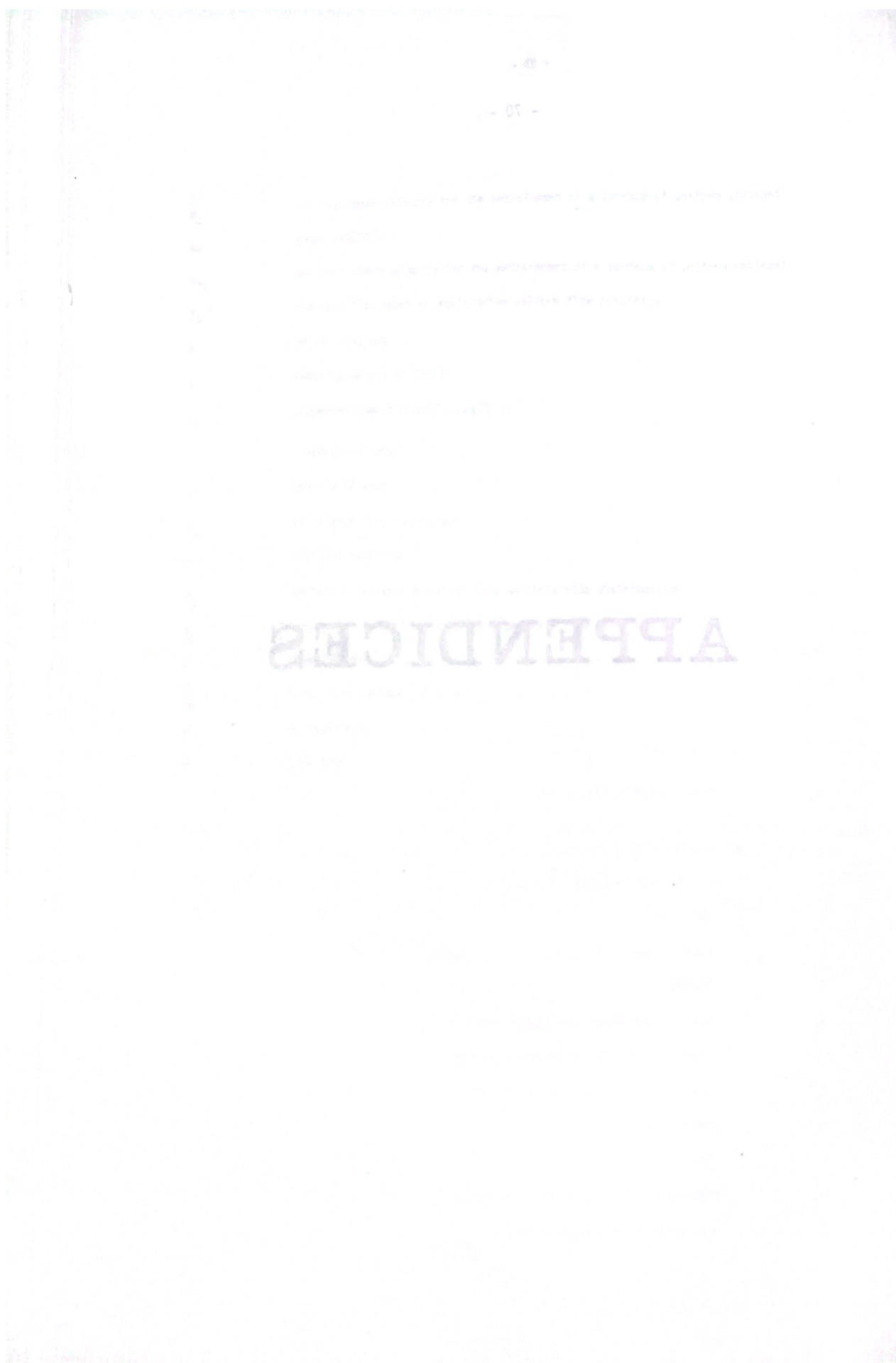
- 69 -

\bar{U}_c	critical mean velocity for the entrainment of a surface of uniform sediment
u_*	shear velocity
u_{*c}	critical shear velocity for the entrainment of a surface of uniform sediment
y_0	approach flow depth at equilibrium uniform flow condition
α	angle, constant
γ	specific weight of fluid
γ'_s	submerged specific weight, $\rho g(S_s-1)$
ν	kinematic viscosity
ρ	density of water
ρ_s	solid density of particles
σ	standard deviation
σ_g	geometric standard deviation of a particle size distribution
σ_I	inclusive standard deviation of a particle size distribution
τ	shear stress
τ_0	total shear stress ($= \tau' + \tau''$)
τ'	surface drag
τ''	form drag

- 70 -

APPENDICES

SUMMARY OF EXPERIMENTAL RESULTS



- 71 -

APPENDIX 1

SUMMARY OF EXPERIMENTAL RESULTS

RUNS WITH SEDIMENT TRANSPORT $d_{50} = 0.24 \text{ mm}$, $y_0 = 100 \text{ mm}$ unless otherwise stated.

Test No.	Pier Diam., D (mm)	Mean Vel., \bar{U} (m/s)	d_{se_a} (mm)	d_{se_a}/D	d_{se_m} (mm)	d_{se_m}/D	d_{se_s} (mm)	d_{se_s}/D	t_{se} (x10s)	Temp. (°C.)	u_* / u_{*c}
1	50.8	0.22	65.0	1.28	66.5	1.31	64.0	1.26	-	19-22	1.5
2	79.5	0.23	84.5	1.06	87.0	1.09	82.0	1.03	-	19-22	-
3	101.6	0.24	99.0	0.97	101.5	1.00	97.0	0.95	-	19-22	1.5
4	79.5	0.30	77.0	0.97	82.0	1.03	73.0	0.92	1 600	19	2.62
5	79.5	0.30	79.0	0.99	83.5	1.05	74.0	0.93	-	19	2.62
6	101.6	0.30	89.5	0.88	92.5	0.91	86.5	0.85	-	19	2.62
7	50.8	0.32	58.0	1.14	63.5	1.25	52.0	1.02	-	20	-
8	50.8	0.35	56.0	1.10	61.0	1.20	47.5	0.94	66	20	-
9	50.8	0.36	59.0	1.16	64.0	1.26	49.0	0.96	180	23	-
10	50.8	0.37	56.0	1.10	63.0	1.24	47.0	0.93	175	22	3.4
11	50.8	0.37	58.0	1.14	64.5	1.24	48.5	0.95	80	23	3.4
12	101.6	0.37	91.5	0.90	96.5	0.95	88.0	0.87	250	24	3.4
13	50.8	0.39	57.5	1.13	64.0	1.26	49.0	0.96	310	24	3.7
14	50.8	0.42 ($y_0 = 116$)	62.5	1.23	73.0	1.44	50.5	0.99	125	26	-
15	50.8	0.45	62.5	1.23	72.0	1.42	50.5	0.99	-	24	-
16	50.8	0.50	67.0	1.32	83.0	1.63	52.5	1.03	-	25	4.5
17	79.5	0.50	96.0	1.21	110.0	1.38	84	1.06	-	26	4.5

c/...

Test No.	Pier Diam., D (mm)	Mean Vel., U (m/s)	d _{sea} (mm)	d _{sea} /D	d _{se_m} (mm)	d _{se_m} /D	d _{se_S} (mm)	d _{se_S} /D	t _{se} (x10s)	Temp. (°C.)	u _* /u _{*c}
18	79.5	0.50	97.0	1.22	108.0	1.36	86.0	1.08	-	26	4.5
19	101.6	0.50	104.5	1.03	121.5	1.20	94.5	0.93	59	25	4.5
20	50.8	0.65	80.0	1.57	96.0	1.89	64.5	1.27	-	25	-
21	79.5	0.65	110.0	1.38	127.0	1.60	96.0	1.21	7	25	-
22	79.5	0.65	110.0	1.38	124.5	1.57	93.0	1.17	-	24	-
23	101.6	0.65	133.5	1.31	144.5	1.42	120.0	1.18	11	25	-
24	79.5	0.80	120.5	1.52	132.0	1.66	106.5	1.34	-	25	-
25	101.6	0.80	144.0	1.42	156.5	1.54	130.0	1.28	-	23	-
26	50.8	0.81	89.0	1.75	104.0	1.97	76.5	1.51	-	24	-
27	79.5	0.81	122.0	1.53	137.5	1.73	108.0	1.36	-	23	-
28	101.6	0.81	137.5	1.35	151.5	1.49	129.0	1.27	-	24	-
29	50.8	1.10	94.0	1.85	103.0	2.03	84.0	1.65	-	23	-
30	79.5	1.10	122.0	1.53	129.0	1.62	112.0	1.41	-	23	-
31	101.6	1.10	137.5	1.35	148.5	1.46	129.0	1.27	-	23	-
32	79.5	1.05	110.0	1.35	130.0	1.70	90.0	1.13	-	24	-
33	101.6	1.05	126.5	1.25	151.5	1.40	97.5	0.96	-	24	-

c/...

Test No.	Pier Diam., D (mm)	Mean Vel., \bar{U} (m/s)	d_{se_a} (mm)	d_{se_a}/D	d_{se_m} (mm)	d_{se_m}/D	d_{se_s} (mm)	d_{se_s}/D	t_{se} (x10s.)	Temp. (°C.)	u_*/u_{*c}
10	50.8	0.23	61.5	1.21	66.0	1.30	59.0	1.12	-	22	1.95
32	50.8	0.23	70.5	1.41	76.5	1.16	89.0	1.12	-	22	1.95
33	79.5	0.23	95.0	0.94	98.5	0.97	92.5	0.91	-	22	1.95
34	101.6	0.23	55.0	1.08	61.5	1.21	48.0	0.94	130	23	3.0
35	50.8	0.30	62.0	1.22	71.0	1.40	50.5	0.99	70	21	3.4
36	50.8	0.40	87.0	1.09	94.5	1.19	81.0	1.02	85	22	3.4
37	79.5	0.40	104.5	1.03	111.5	1.10	94.5	0.93	-	22	3.4
38	101.6	0.40	80.5	1.58	92.0	1.81	68.0	1.34	11	21	5.3
39	50.8	0.65	109.0	1.37	122.0	1.53	92.0	1.16	12	22	5.3
40	79.5	0.65	121.5	1.20	135.5	1.33	107.5	1.06	-	20	5.3
41	101.6	0.65	122.0	1.53	135.0	1.70	107.0	1.35	-	20	6.8
42	79.5	0.8	138.0	1.36	152.5	1.50	123.0	1.21	-	19-20	6.8
43	101.6	0.8	95.5	1.85	104.0	2.05	84.0	1.65	-	19	-
44	50.8	1.05	132.0	1.66	141.0	1.77	122.0	1.53	-	20	-
45	79.5	1.05	144.5	1.42	153.0	1.51	135.5	1.33	-	20	-
46	101.6	1.05	-	-	-	-	-	-	-	-	-
16	50.8	0.50	67.0	1.32	70.0	1.32	60.0	1.20	-	-	-
17	79.5	0.50	96.0	1.21	110.0	1.30	88.0	1.06	-	-	-

- 75 -

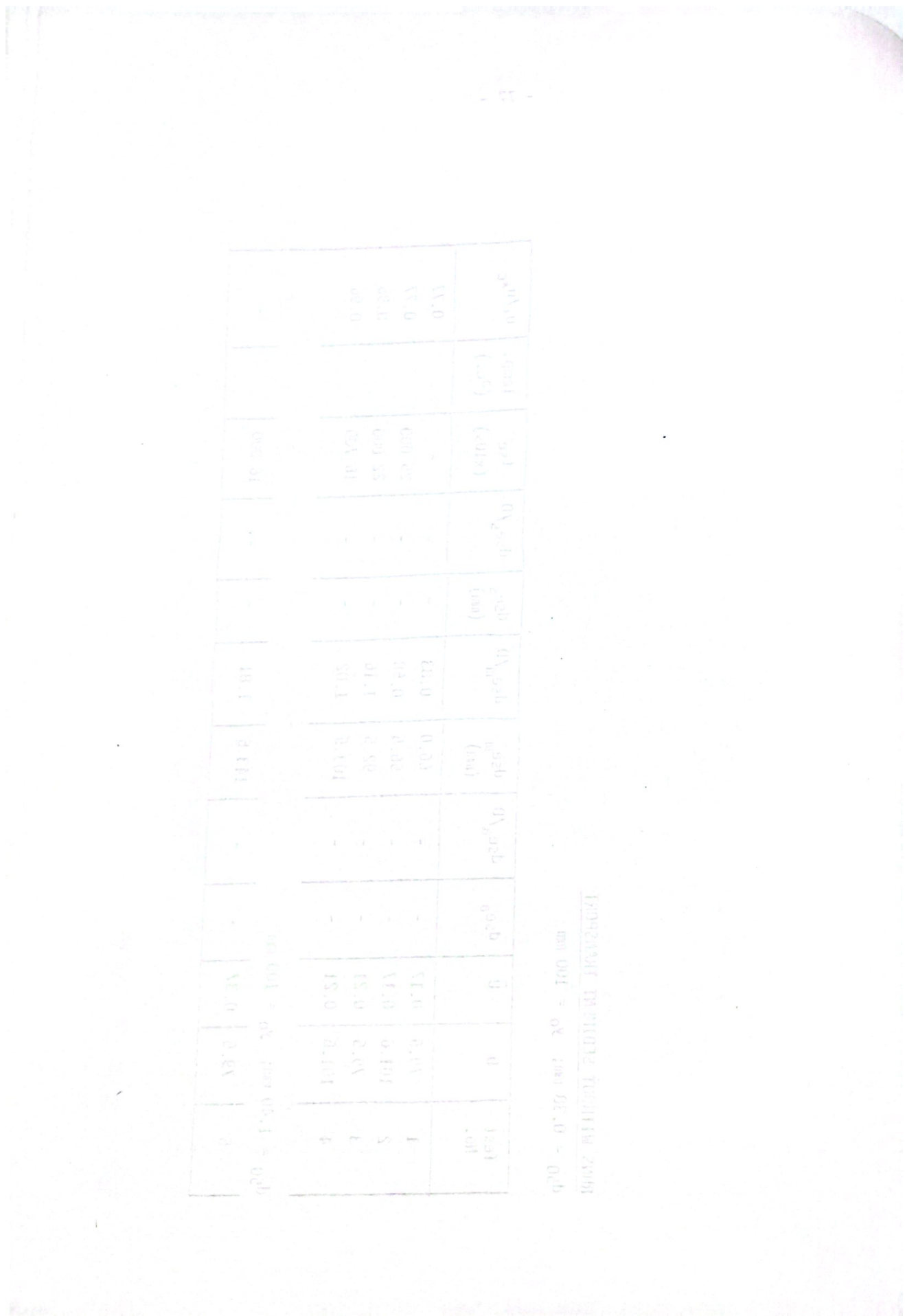
Test No.	D (mm)	\bar{U} (m/s)	d_{sea} (mm)	d_{sea}/D	d_{se_m}	d_{se_m}/D	d_{se_s}	d_{se_s}/D	t_{se} (x10sec.)	Temp. (°C.)	u_*/u_{*c}
47	50.8	0.32	-	-	101.5	2.00	-	-	12.500	23	1.14
48	79.5	0.32	-	-	141.5	1.78	-	-	21.500	23	1.14
49	101.6	0.32	-	-	154.5	1.52	-	-	13.800	24	1.14
50	50.8	0.50	65.0	1.28	79.5	1.56	54.0	1.06	48	23	2.34
51	79.5	0.50	89.0	1.12	110.0	1.38	70.5	0.89	44	23	2.34
52	101.6	0.50	105.5	1.04	120.5	1.19	94.5	0.93	-	23	2.34
53	50.8	0.65	73.0	1.44	91.0	1.79	54.0	1.06	20	23	4.5
54	79.5	0.65	99.0	1.25	121.0	1.52	81.0	1.02	-	23	4.5
55	101.6	0.65	108.5	1.07	125.0	1.23	91.5	0.90	20	24	4.5
56	50.8	0.80	80.0	1.57	97.5	1.92	59.5	1.17	5	23	6.5
57	79.5	0.80	103.0	1.30	125.5	1.58	83.0	1.04	3	24	6.5
58	101.6	0.80	124.0	1.22	141.5	1.39	100.0	0.98	-	24	6.5
59	50.8	1.05	84.0	1.65	106.0	2.09	66.0	1.30	-	25	-
60	79.5	1.05	110.0	1.38	130.0	1.70	90.0	1.13	1	24	-
61	101.6	1.05	126.5	1.25	151.5	1.49	97.5	0.96	-	24	-

c/...

Test No.	D (mm)	\bar{U} (m/s)	d_{se_a} (mm)	d_{se_a}/D	d_{se_m} (mm)	d_{se_m}/D	d_{se_s} (mm)	d_{se_s}/D	t_{se} (x10s)	Temp. (°C.)	u_*/u_{*c}
62	50.8	0.41	-	-	106.0	2.09	-	-	12 800	28	1.18
63	79.5	0.41	-	-	150.5	1.89	-	-	13 000	27	1.18
64	101.6	0.41	-	-	161.5	1.59	-	-	14 100	27	1.18
65	50.8	0.60	67.0	1.32	79.5	1.56	52.0	1.02	-	28	-
66	79.5	0.60	96.5	1.21	110.0	1.38	79.0	0.99	-	28	-
67	79.5	0.60	100.0	1.26	112.0	1.41	85.0	1.07	-	28	-
68	101.6	0.60	114.5	1.13	128.0	1.26	96.5	0.95	52	28	-
69	50.8	0.80	63.0	1.24	82.0	1.61	42.0	0.83	2	28	-
70	79.5	0.80	90.0	1.13	108.5	1.36	71.0	0.89	2	26	-
71	101.6	0.80	108.5	1.07	128.0	1.26	89.5	0.88	2	26	-
72	50.8	1.05	77.0	1.52	103.0	2.03	51.0	1.00	-	27	-
73	79.5	1.05	107.0	1.35	133.0	1.69	82.0	1.03	1	27	-
74	79.5	1.05	105.0	1.32	129.0	1.62	79.0	0.99	-	27	-
75	101.6	1.05	123.0	1.21	143.0	1.41	89.5	0.88	1	27	-
76	50.8	1.20	77.0	1.52	101.0	1.99	51.0	1.00	-	28	-
77	79.5	1.20	107.0	1.35	133.0	1.67	77.0	1.03	-	27	-
78	101.6	1.20	117.0	1.15	141.0	1.39	86.5	0.85	-	26	-
79	79.5	1.40	105.0	1.32	127.0	1.60	83.0	1.04	-	28	-

RUNS WITHOUT SEDIMENT TRANSPORT $d_{50} = 0.38 \text{ mm}; y_0 = 100 \text{ mm}$

Test No.	D	\bar{U}	d_{se_a}	d_{se_a}/D	d_{se_m} (mm)	d_{se_m}/D	d_{se_s} (mm)	d_{se_s}/D	t_{se} (x10s)	Temp. (°C.)	u_*/u_{*c}
1	79.5	0.17	-	-	66.0	0.83	-	-	-		0.77
2	101.6	0.17	-	-	56.5	0.58	-	-	25 000		0.77
3	79.5	0.21	-	-	92.5	1.16	-	-	22 000		0.96
4	101.6	0.21	-	-	103.5	1.02	-	-	16 700		0.96
$d_{50} = 1.40 \text{ mm}; y_0 = 100 \text{ mm}$											
5	79.5	0.37	-	-	143.5	1.81	-	-	16 000		-



- 78 -

$\frac{Q}{Q_{max}}$	u_{*c}	\bar{u}_c	$(\bar{u}_c - u_{*c}) \times 10^3$	$Q_{max} = 1000$
0.34	0.40	0.38	-0.20	0.38
0.38	0.40	0.39	-0.10	0.38
0.40	0.40	0.39	-0.10	0.38
0.42	0.40	0.39	-0.10	0.38
0.44	0.40	0.39	-0.10	0.38
0.46	0.40	0.39	-0.10	0.38
0.48	0.40	0.39	-0.10	0.38
0.50	0.40	0.39	-0.10	0.38
0.52	0.40	0.39	-0.10	0.38
0.54	0.40	0.39	-0.10	0.38
0.56	0.40	0.39	-0.10	0.38
0.58	0.40	0.39	-0.10	0.38
0.60	0.40	0.39	-0.10	0.38
0.62	0.40	0.39	-0.10	0.38
0.64	0.40	0.39	-0.10	0.38
0.66	0.40	0.39	-0.10	0.38
0.68	0.40	0.39	-0.10	0.38
0.70	0.40	0.39	-0.10	0.38
0.72	0.40	0.39	-0.10	0.38
0.74	0.40	0.39	-0.10	0.38
0.76	0.40	0.39	-0.10	0.38
0.78	0.40	0.39	-0.10	0.38
0.80	0.40	0.39	-0.10	0.38
0.82	0.40	0.39	-0.10	0.38
0.84	0.40	0.39	-0.10	0.38
0.86	0.40	0.39	-0.10	0.38
0.88	0.40	0.39	-0.10	0.38
0.90	0.40	0.39	-0.10	0.38
0.92	0.40	0.39	-0.10	0.38
0.94	0.40	0.39	-0.10	0.38
0.96	0.40	0.39	-0.10	0.38
0.98	0.40	0.39	-0.10	0.38
1.00	0.40	0.39	-0.10	0.38

APPENDIX 2

- 79 -

d_{50}	0.24	0.38	0.80	1.40	0.25	0.50	0.52	1.50	2.00	2.50	3.00
u_{*c}	0.0125	0.0143	0.0203	0.0279	0.0128	0.0162	0.0164	0.0293	0.0360	0.042	0.0467
$\bar{U}_c (y_0 = 50)$					0.24						
$\bar{U}_c (y_0 = 100)$	0.23	0.247	0.31	0.39	0.238		0.270	0.41	0.47	0.53	0.57
$\bar{U}_c (y_0 = 200)$							0.30				

The Shields function was used to calculate the critical shear velocity, u_{*c} for the d_{50} particle size of each sediment. The threshold mean velocity, \bar{U}_c was calculated using the following equation:

$$\frac{\bar{U}_c}{u_{*c}} = 7.66 \left(\frac{y_0}{k_s} \right)^{1/6},$$

where k_s was assumed to be equal to $2d_{50}$. (Note that \bar{U}_c values calculated for the four sediments used in this study correspond very well to those estimated from observed data. (refer Figures 4.1 to 4.4)

